EXPERIMENTAL PERFORMANCE INVESTIGATION AND VARIABLE SPEED COMPRESSOR IMPLEMENTATION OF A HOUSEHOLD REFRIGERATOR

A Thesis Submitted to
the Graduate School of Engineering and Science of
İzmir Institute of Technology
in Partial Fulfillment of the Requirements for the Degree of

MASTER OF SCIENCE

in Energy Engineering

by
Veysel Egemen AĞAKAY

July, 2013
İZMİR

We approve the thesis of **Veysel Egemen AĞAKAY**

Examining Committee Members:

_____
Assist. Prof. Dr. Ünver ÖZKOL
Department of Mechanical Engineering, İzmir Institute of Technology

_____
Prof. Dr. Gülden GÖKÇEN AKKURT
Department of Mechanical Engineering, İzmir Institute of Technology

_____
Assoc. Prof. Dr. Tahsin BAŞARAN
Department of Architecture, İzmir Institute of Technology

4 July 2013

_____
Assist. Prof. Dr. Ünver ÖZKOL
Supervisor
Department of Mechanical Engineering
İzmir Institute of Technology

_____
Assoc. Prof. Dr. Moghtada MOBEDİ
Co-Supervisor
Department of Mechanical Engineering
İzmir Institute of Technology

_____
Prof. Dr. Gülden GÖKÇEN AKKURT
Head of the Department of
Energy Engineering

_____
Prof. Dr. R. Tuğrul SENGER
Dean of the Graduate School of
Engineering and Sciences

ACKNOWLEDGMENTS

ABSTRACT

EXPERIMENTAL PERFORMANCE INVESTIGATION AND VARIABLE SPEED COMPRESSOR IMPLEMENTATION OF A HOUSEHOLD REFRIGERATOR

The objective of this thesis is to investigate the performance of a household refrigerator in steady state operating conditions and reveal the effect of variable speed compressor implementation on the system performance. This work is based on experimental studies which include energy consumption (EC) tests in accordance with ISO 15502 standard and implementation of a variable speed compressor (VSC) to a household refrigerator. To accomplish these works, the household test refrigerator is instrumented with various sensors and a comprehensive test program is prepared for data acquisition, analysis, and control of the VSC. During the EC tests, the refrigeration cycle performance is tracked simultaneously by real time analyses of each refrigeration cycle component which include calculations of heat transfer from each component, mass flow rate of the refrigerant, and work inlet to the compressor. In this study, three tests of refrigerators utilizing single speed compressor (SSC) with different condenser lengths, and one test of the refrigerator with a VSC are conducted in an air chamber in which the ambient temperature is kept at 25°C and the relative humidity is under 75%. The VSC is controlled by temperature feedbacks of air stream from the freezer and the fresh-food compartments to maintain the required temperatures in those compartments.

ÖZET

EV TİPİ BİR BUZDOLABININ DENEYSEL PERFORMANS ARAŞTIRMASI VE DEĞİŞKEN DEVİRLİ KOMPRESÖR UYGULAMASI

Bu tezin amacı, ev tipi bir buzdolabının performansının kararlı çalışma koşullarında incelenmesi ve değişken devirli kompresör uygulamasının sistem performansı üzerindeki etkilerini açığa çıkarmaktır. Bu çalışma, ISO 15502 standartlarına göre enerji tüketim testlerini ve ev tipi bir buzdolabı üzerinde değişken devirli kompresör uygulamasını içeren deneysel çalışmalar üzerine temellenmiştir. Bu çalışmaları başarıyla yapmak için, ev tipi buzdolabı birçok değişik duyarga ile donatılmış ve veri toplama, analiz ve değişken devirli kompresör kontrolü için kapsamlı bir test programı hazırlanmıştır. Enerji tüketim testleri süresince, ev tipi test buzdolabının soğutma çevrimi performansı, soğutma çevrimini oluşturan tüm bileşenlerin gerçek zamanlı ısı transferi, soğutucu akışkanın kütlesel debisi ve kompresöre giren iş hesaplamalarını içeren analizler ile eş zamanlı olarak takip edilmiştir. Bu çalışmada, tek devirli kompresörle çalışan farklı yoğuşturucu uzunluklarına sahip üç test buzdolabı ve değişken devirli kompresörle çalışan bir buzdolabının testleri, içerisindeki hava sıcaklığı 25°C' de tutulan ve nem oranı %75'in altında olan bir test odasında yapılmıştır. Değişken devirli kompresör, soğutucu ve dondurucu bölmelerden gelen hava akış sıcaklıklarının geri beslemesi ile bu bölümlerdeki gerekli sıcaklıkları sağlamak amacıyla kontrol edilmiştir.

TABLE OF CONTENTS

LIST OF FIGURES

LIST OF TABLES

LIST OF SYMBOLS

AC	Alternative current	
DC	Direct current	
EC	Energy consumption	W, kWh/24h
SSC	Single speed compressor	
VSC	Variable speed compressor	
EEI	Energy efficiency index	
PDC	Power duty cycle	
COP	Coefficient of performance	
P	Pressure	bar
h	Enthalpy	J/kg, kJ/kg
P-h	Logarithmic pressure-enthalpy	
$\dot{Q}_e$	Heat absorption rate by the evaporator	W
$\dot{Q}_c$	Rejected heat rate by the condenser	W
$\dot{W}_{net}$	Net work inlet to the system	W
T	Temperature	K, ^{o}C
$\dot{V}_{air}$	Volume flow rate of the air stream over the evaporator	m^3/s
v	Velocity of the air stream over the evaporator	m/s
A	Total air inlet area to the evaporator	m^2
$\dot{m}_{air}$	Mass flow rate of the air	kg/s
ρ_{air}	Density of the air	kg/m^3
$\dot{m}$	Mass flow rate of the refrigerant	kg/s, kg/h
ρ	Density of the refrigerant	kg/m^3
$\dot{V}$	Volume flow rate of the refrigerant	m^3/s
V_p	Piston displacement volume of the compressor	m^3
N	Revolution of the compressor per minute	rpm
B	Bore diameter of the compressor	m
S	Stroke of the compressor	m
n	Number of pistons of the compressor	
η_v	Volumetric efficiency of the compressor	

V_a	Actual volume of the compressed refrigerant	m³
$\dot{V}_a$	Actual volume flow rate of the refrigerant	m³/s
$\varepsilon\%$	Relative error	
C_p	Specific heat at constant pressure	kJ/kgK, kJ/kg°C

Indices

a	Actual process
c	Condenser
cap	Capillary tube
co or comp	Compressor
e	Evaporator
f	Saturated liquid phase
g	Saturated vapor phase
h	Hot gas tube
i	Inlet
k	Air velocity measurement locations
o	Outlet
sat	Saturated phase
slhx	Suction line heat exchanger
sub	Subcooling
sup	Superheating

CHAPTER 1

INTRODUCTION

The amount of energy consumption (EC) of refrigeration around the world is increasing drastically day by day. Along with the increment of EC, refrigerants' emissions become another problem due to the harmful impact of them on the environment. In respect to these, to prevent negative effects on the environment and the EC, new policies are forcing the refrigeration industry to develop more efficient and environmentally friendly refrigerators. According to the policies associated to refrigeration industry and EC of refrigerating appliances, the manufacturers are obliged to produce the refrigerators based on some standards, such as ISO, JIS, ANSI/AHAM, etc. These standards dictate that refrigerators EC needs to be determined by standard tests procedures and they are classified and labeled in accordance with their EC test results (P. Bansal, 2003).

In refrigeration industry, vapor compression refrigeration cycle is used more than the other refrigeration cycles since they are relatively small, inexpensive, and efficient (Çengel & Boles, 2005). Household refrigerators constitute one of the biggest parts of the refrigeration industry and a great majority of them is based on the vapor compression refrigeration cycle. Hence, enhancements on energy efficiency of these systems become more remarkable than developments of the refrigerators based on the other refrigeration cycles.

Standard test procedures for household refrigerators are far away from determining the performance investigation of each component of a household refrigerator, and also they consume a long time to be implemented due to the long period of achieving steady state operating conditions. Therefore, this conditions forces the industry to develop new and better test systems, which have many capabilities, relative to conventional ones. A great part of enhancements options on the energy efficiency of household refrigerators are based on utilizing variable speed compressors (VSC) due to their adjustable load control mechanisms (Qureshi & Tassou, 1996).

In the scope of this study, to investigate the performance of a household refrigerator utilizing vapor compression refrigeration cycle in steady state conditions, an improved experimental set-up and analysis program are designed, therefore, each

component comprises the refrigeration cycle is able to be analyzed thermodynamically during EC tests according to "ISO 15502: Household Refrigerating Appliances Characteristics and Test Methods". And also, to reduce the EC of the studied household refrigerator, a VSC implementation is examined.

1.1. The Ideal Vapor Compression Refrigeration Cycle

An ideal vapor compression refrigeration cycle is comprised of four main components: compressor, condenser, expansion device, and evaporator, as shown in Figure 1.1.
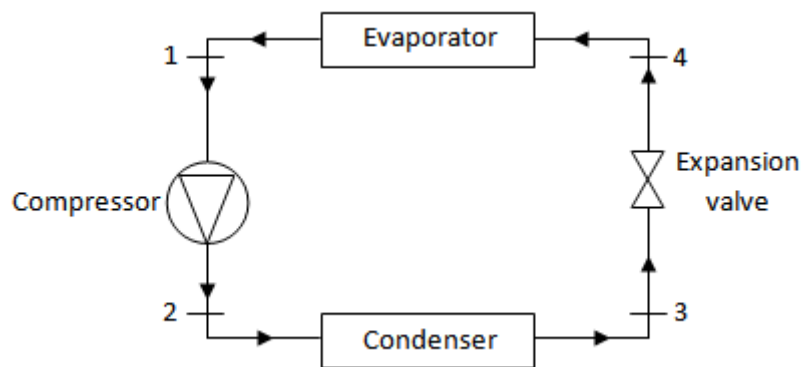
Figure 1.1. An ideal vapor compression refrigeration cycle

For an ideal vapor compression refrigerator, the evaporator contacts with the cold ambient and its temperature is lower than this ambient temperature. The heat is transferred from the cold ambient to the evaporator due to the temperature difference between the evaporator and the cold ambient. Hence, in the evaporator, the refrigerant undergoes phase change from saturated mixture to saturated vapor and it is sucked by the compressor. In the compressor, the refrigerant is compressed and its phase changes from saturated vapor to superheated vapor, therefore, its temperature and pressure increase at the same time. For the ideal vapor compression refrigeration process, the compression process is assumed to be isentropic. The superheated refrigerant is discharged from the compressor through the condenser. The superheated refrigerant whose temperature is higher than the surroundings temperature losses its heat till it becomes saturated liquid in the condenser. The saturated liquid refrigerant enters the expansion device and flows through the evaporator; consequently, the refrigeration

cycle is completed. During this process, the refrigerant's pressure decreases from the condensing pressure to the evaporating pressure by flashing into vapor of a small portion of the liquid. It is assumed that the enthalpy of the refrigerant does not change during this process but the entropy of the refrigerant increases. The reason of the entropy change during the expansion process is the heat transfer which takes place within the refrigerant itself due to internal friction. In ideal refrigeration cycle, it is also assumed that there is no drop in pressure in the lines and across the heat exchangers resulting from the flow of refrigerant through these parts (Dossat, 1961). In Figure 1.2, the logarithmic pressure-enthalpy (P-h) diagram of the ideal refrigeration cycle and all refrigeration cycle performance characteristics are shown.
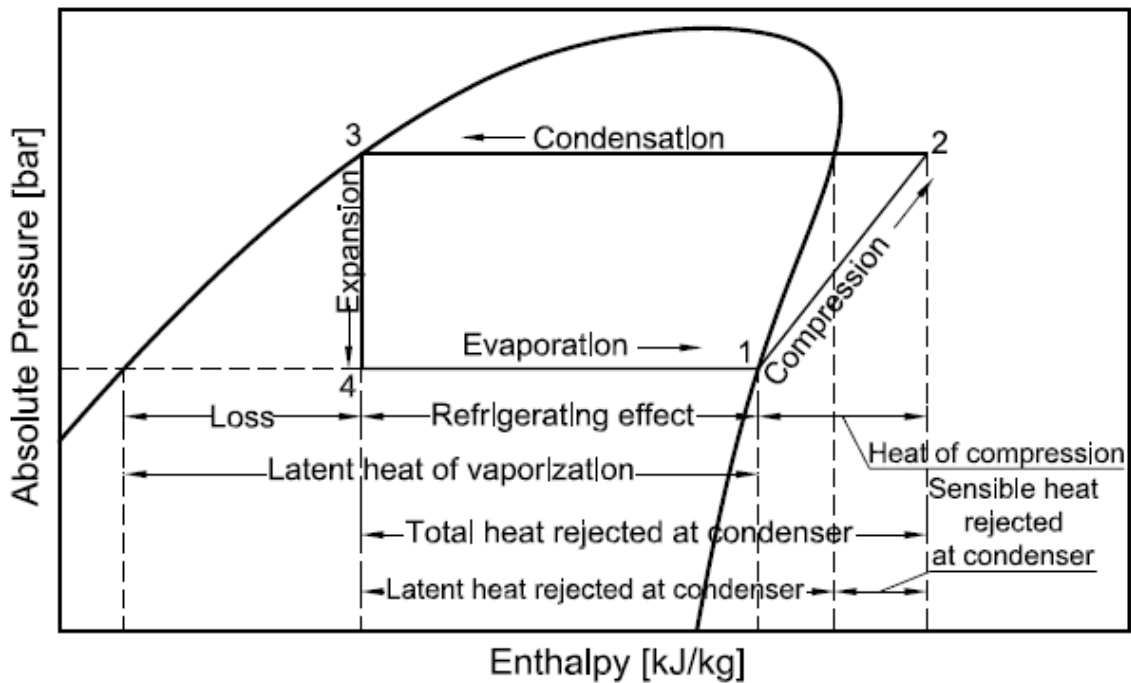
Figure 1.2. Pressure-enthalpy (P-h) diagram of ideal vapor compression refrigeration cycle (Source: Dossat, 1961)

For steady state operating conditions, heat transfer to the evaporator, cooling capacity (refrigerating effect), $\dot{Q}_e$, rejected heat from the condenser, $\dot{Q}_c$, and work inlet to the system, $\dot{W}_{net}$, for the ideal cycle can be expressed as below, respectively.

$$\dot{Q}_e = \dot{m}\Delta h_e = \dot{m}\left(h_1 - h_4\right) \tag{1.1}$$

$$\dot{Q}_c = \dot{m}\Delta h_c = \dot{m}\left(h_2 - h_3\right) \tag{1.2}$$

3

$$\dot{W}_{net} = \dot{m}\Delta h_{comp} = \dot{m}\left(h_2 - h_1\right) \qquad (1.3)$$

where $\dot{m}$ and Δh represent the mass flow rate of the refrigerant and enthalpy change of the refrigerant, respectively. The adiabatic expansion process is defined as

$$h_3 = h_4 = h_{f@3} \qquad (1.4)$$

where $h_{f@3}$ is the saturated liquid enthalpy of the refrigerant for the given temperature and pressure of the condenser outlet. Then the steady energy balance becomes

$$\dot{Q}_e + \dot{W}_{net} = \dot{Q}_c \qquad (1.5)$$

1.2. Actual vapor compression refrigeration cycle

Actual vapor compression refrigeration cycles deviate from the ideal cycle. The assumptions that are made for the ideal cycle are not valid for actual cycles due to the irreversibilities. In actual practice, the refrigerant pressure decreases through the flow line due to the friction, especially through the evaporator and the condenser. In Figure 1.3, comparison of an actual cycle and ideal cycle are shown on a simplified P-h diagram.
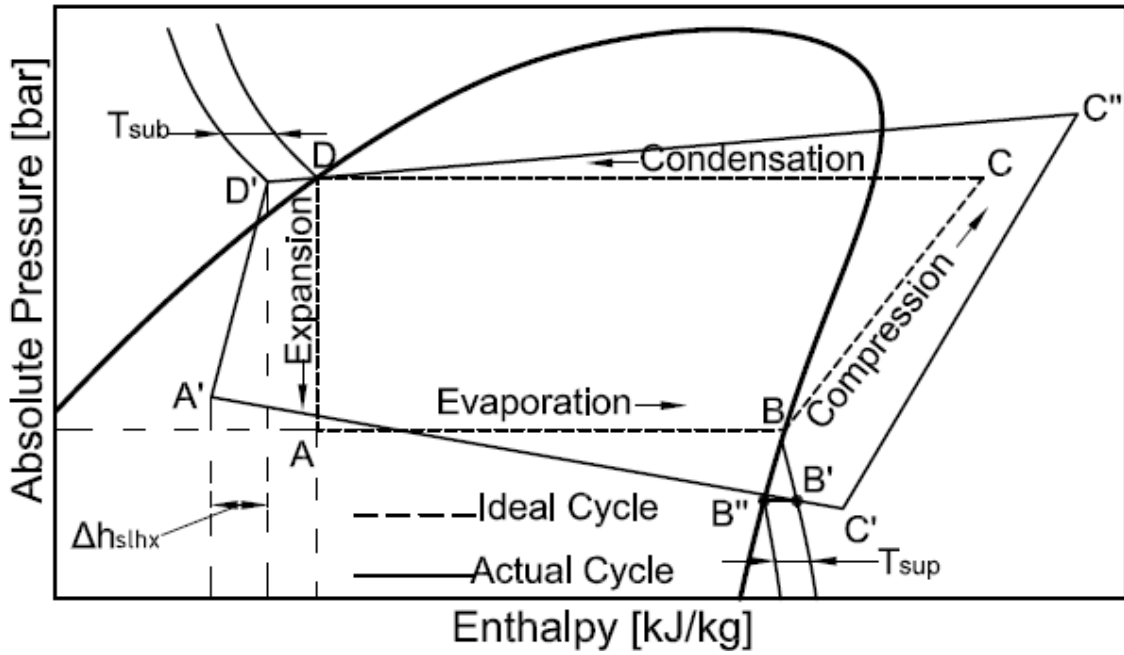
Figure 1.3. Comparison of ideal and actual cycles on P-h diagram

In ideal cycle, the refrigerant is assumed in saturated phase both at the exits of the condenser and the evaporator, however, in actual cycles, this is a rarely encountered situation. After the refrigerant has evaporated completely, it will usually continue to absorb heat and it becomes superheated vapor and this is called as superheating vapor effect and it is illustrated on the P-h diagram between points B" and B'. As a result of this superheating effect, the heat of compression and the exit temperature of the compressor increase for actual cycles. The similar situation is seen at the condenser in the reverse manner. Once the refrigerant phase turn into the saturated liquid in the condenser, it will usually continue to cool down, hence, it becomes subcooled liquid, and the effects of this situation on the entire cycle called as subcooling liquid effect and it is indicated on the P-h diagram between points D and D'.

1.3. Specifications and Refrigeration Cycle of the Test Refrigerator

In the scope of this thesis, a bottom-mounted, double door, and conventional on-off controlled no-frost household refrigerator is investigated experimentally. Thus, in this section, its specifications and refrigeration cycle is covered in a detailed way. The general specifications of the test refrigerator are tabulated in Table 1.1.

Table 1.1. The test refrigerator general specifications

Manufacturer	Indesit Company
Model	Ege Q3 70/30
Total Volume	455 L
Freezer Compartment Volume	145 L
Fresh-food Compartment Volume	310 L
Width	697 mm
Depth	689 mm
Height	1919 mm

The test refrigerator is comprised of one fin-and-tube type cross flow forced convection, aluminum evaporator back positioned of the freezer compartment, one wire-and-tube type cross flow natural convection, steel condenser positioned with a distance of 25 mm to fresh-food compartment back wall, one copper capillary tube as an expansion device with lateral type suction line heat exchanger, and one single speed reciprocating compressor (SSC). The refrigerator is charged with Isobutane (R600a) with the amount of 50 gr. Specifications of the components are given in Table 1.2 and Table 1.3.

Table 1.2. The compressor specifications

Manufacturer	Embraco
Type	Reciprocating
Refrigerant	R600a (Isobutane)
Voltage & Frequency	220-240 V & 50 Hz
Number of pistons	2
Displacement Volume	12.23 cm^3
Speed	3000 rpm
Volumetric Efficiency	78.6%
Isentropic Efficiency	62.9%

To maintain the required cooling during operation periods, a DC fan mounted at the top of the evaporator is utilized. The purpose of the fan is to circulate the air inside the refrigerator through the evaporator and maintain the heat transfer between the refrigerant side and the compartments. The air cools down both compartments by circulation. An air separation mechanism called as "damper" located between the air stream inlet location to the fresh-food compartment and the air stream exit location from the evaporator is used to prevent air to enter the fresh-food compartment when the desired lowest temperature is achieved in this compartment. Hence, the air is only

circulated in the freezer compartment until its temperature reaches the adjusted temperature value for the cooling. The damper location is shown in Figure 1.6.

Table 1.3. Specifications of the evaporator, the condenser, and the expansion device

	Evaporator	Condenser	Expansion Device
Type	Fin-and-Tube	Wire-and-tube	Capillary Tube
Number of Pass	26	26	-
Material	Aluminum	Steel	Copper
Internal Tube Diameter	6.6 mm	3.18 mm	0.71
Tube Thickness	0.7 mm	0.8 mm	0.57
Total Tube Length	13026 mm	19278 mm	3500 mm

Refrigeration cycles of household refrigerators differ from the ideal one. As shown in Figure 1.1, the ideal refrigeration cycle includes only four main components which are compressor, condenser, evaporator, and expansion device, but these components are not sufficient to provide proper functioning in reality. Implementation of a household refrigerator just with these four components includes a risk of suction of saturated liquid-vapor mixture by the compressor. Suction of liquid phase by the compressor is an undesired process because the liquid droplets in the saturated mixture harm the mechanical components of the compressor. Liquid droplets entrance to the compressor leads the compressor's lifespan to decrease. To prevent the liquid phase to enter the compressor, in conventional household refrigerators, an internal counter flow heat exchanger in which heat is transferred from capillary tube to the suction line is utilized, and it is called as capillary tube-suction line heat exchanger (SLHX). The refrigeration cycle of a conventional household refrigerator with SLHX is illustrated in Figure 1.4.
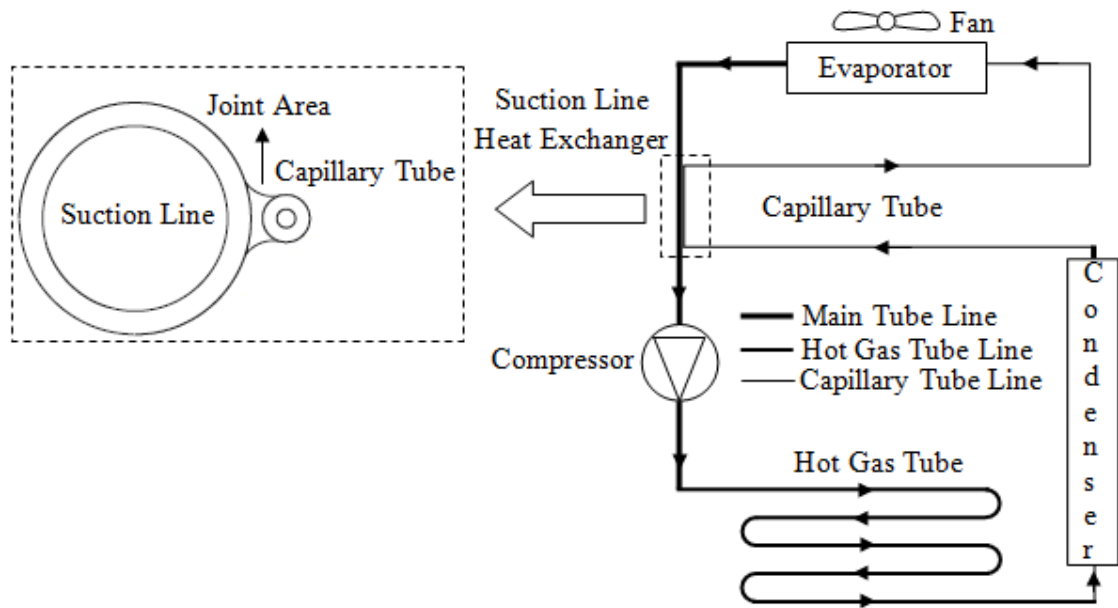
Figure 1.4. Refrigeration cycle of a conventional household refrigerator with SLHX

Utilizing SLHX in the system allows exit of the condenser liquid to be subcooled and suction vapor to be superheated. Therefore, it is ensured that the refrigerant does not enter the compressor in two- or liquid-phase in steady state operating conditions and only enters the compressor as superheated vapor. Another reason of using SLHX, generally, is to increase the cooling capacity by internal heat exchange from the capillary tube to the suction line in practice. On the P-h diagram in Figure 1.5, an actual cycle working with R600a is compared to one in which SLHX is employed. On the diagram, actual cycle without SLHX is identified by points A, B, C, C'', and D, and points A', B', C', C''', and D' identify the one with SLHX. As can be seen from the diagram, the superheating temperature of actual cycle with SLHX is greater than that of actual cycle without SLHX. However, the subcooling temperature of actual cycle with SLHX is lower than that of actual cycle without SLHX.
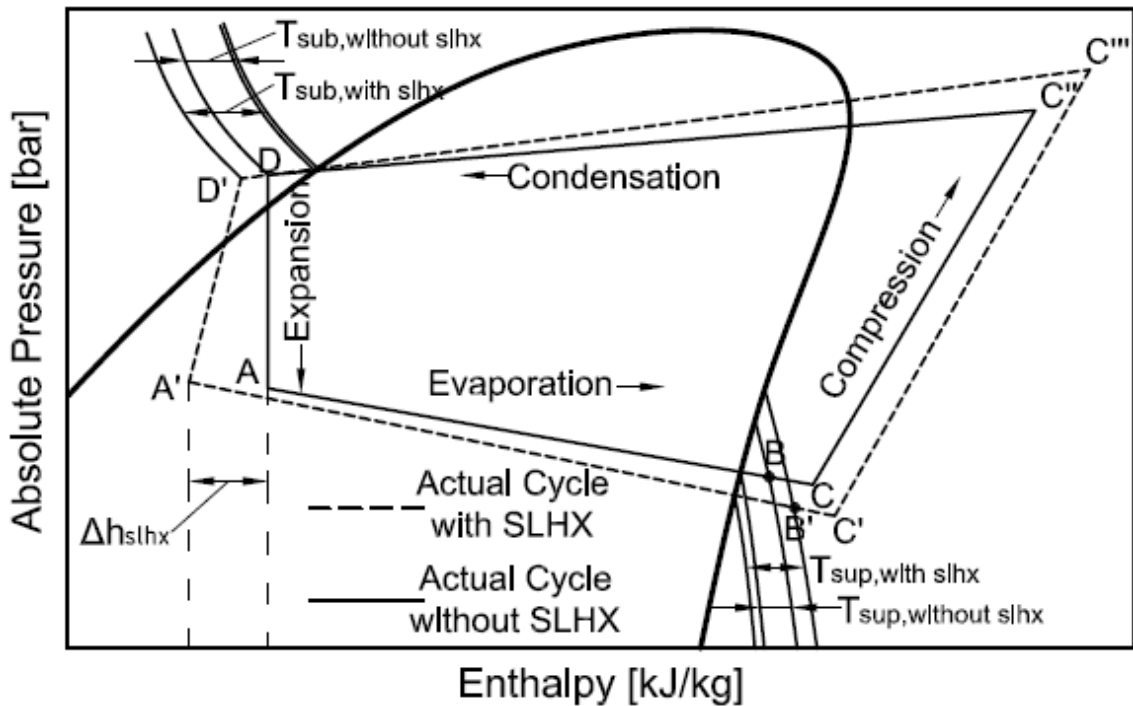
Figure 1.5. Comparison of actual refrigeration cycles without SLHX and with SLHX

Depending upon the refrigerant type and the system, the coefficient of performance (COP) of a refrigeration cycle with SLHX may be either greater than, less than, or the same as that of the cycle without SLHX. The higher superheating temperature at the outlet of the evaporator means the higher power consumption by the compressor and it is a shortcoming. However, the lower subcooling temperature means the higher cooling capacity (Domanski et al., 1994).

The heat transfer occurred in SLHX also affects the condensation and evaporation conditions. The greater heat transfer in SLHX, the lower evaporating temperature and pressure and the higher condensing temperature and pressure are observed. As a rule of thumb in refrigeration, to increase the COP of a refrigeration system, the condensation and the evaporation pressures are needed to be kept close to each other. However, utilizing SLHX may lead to increase the pressure difference between evaporation and condensation. Therefore, to provide the useful cooling by utilizing SLHX, it is necessary to charge the system with an optimal amount of refrigerant.

Along with the other components in the cycle, hot gas tube section is run through the inner frame of the compartment wall in contact with the doors of the refrigerator. It goes through the upper and lower doors' frames from inside the main

9

compartment walls to ensure that the gaskets of the each door would not stick to it due to condensing and freezing moisture.

1.4. Operation Principles of the Test Refrigerator

To prevent spoilage of food by microorganisms, bacterium, enzymes, etc., they have to be kept in proper temperature ranges. Even though every food has their own special conservation, a great portion of this temperature fall into ranges of $+2^{o}$C and $+8^{o}$C for fresh-foods and -18°C and -26°C for perishables such as meat and fish. To maintain the proper refrigeration against to spoilage of foodstuffs, generally, household refrigerators are produced to operate in these temperature ranges.

The test refrigerator's fresh-food and freezer compartments should be able to maintain refrigeration between temperatures of $+2^{o}$C / $+8^{o}$C and -18°C / -26°C, respectively. To achieve the desired temperatures in each compartment, the refrigerator has an end user control panel to define the desired temperature level. The fresh-food and freezer compartments' temperatures are adjustable to temperatures of $+2^{o}$, $+4^{o}$, $+6^{o}$, $+8^{o}$C, and -18°, -22°, -24°, -26°C, respectively. EC tests of the tropical type refrigerators capable of operating ambient temperatures between $+10^{o}$ / $+32^{o}$C are conducted when the freezer and the fresh-food compartments' temperatures are adjusted to -18°C, and $+4^{o}$C, respectively. These temperature set points indicate that the average temperature values inside the compartments are kept at these temperature levels (ISO 15502, 2005). Thus, in this section, the operation of the test refrigerator is explained for only this condition.

For the test refrigerator having a SSC is driven by a conventional on-off control algorithm. Once the compressor starts up, it continues to operate until the freezer and fresh-food compartments reach the desired temperature levels. To keep the average freezer compartment temperature at -18°C, the refrigerator stays on-cycle till the temperature of the freezer reaches -18.5^{o}C and stops; the compressor restarts to operate again when the temperature of it increases to -18°C. In other words, -18° and -18.5^{o}C are the upper and lower temperature control set points. In the same manner, the fresh-food compartment temperature is allowed to fluctuate between $+8^{o}$ and 0°C. To determine whether or not the adjusted temperature levels are reached, two embedded temperature sensors are used for each compartment, one of them is under the fresh-food

compartment internal wall, and the other one is under the freezer compartment internal wall. Both of these sensors detect temperatures of these compartments and send feedback signals to the electronic control card of the refrigerator continuously in order to detect compartments temperatures.
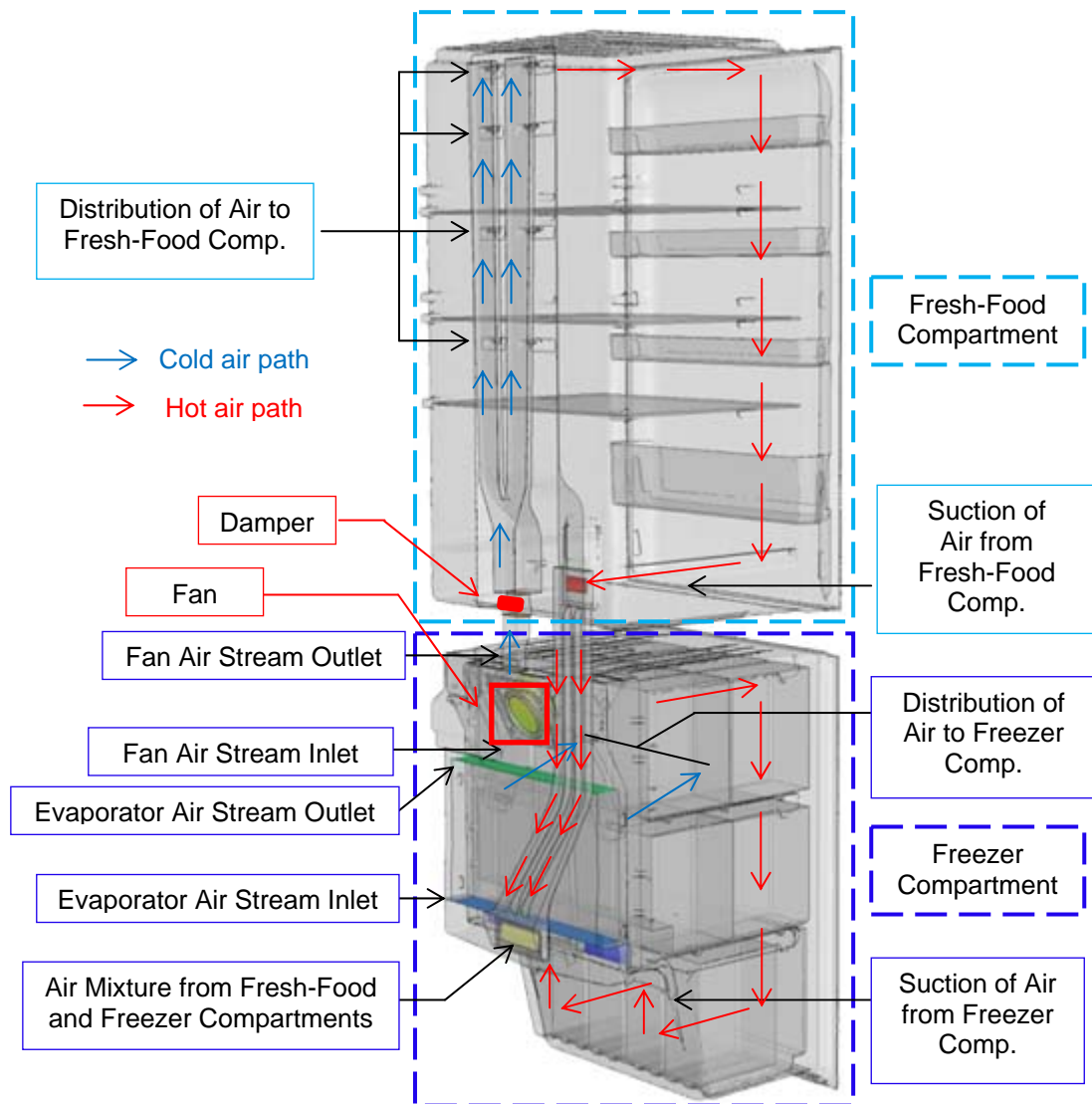
Figure 1.6. Air flow circulation inside the refrigerator

The fresh-food compartment temperature reaches the desired temperature level before the freezer compartment; however, the refrigerator does not stop and it operates continuously until the desired temperature of the freezer compartment is reached. When the fresh-food compartment temperature becomes to 0^oC, the damper is closed to stop air inlet to the fresh-food compartment and it stays closed position until the fresh-food compartment temperature increases to 8^oC and it reopens again. Therefore, the air is sent to the freezer compartment to cool it down to the adjusted temperature level.

According to temperature data from sensors, the compressor is stopped when both compartments reach the adjusted temperature levels which are -18.5°C for the freezer and 0°C for the fresh-food compartments. Damper and fan locations and air flow circulation inside the refrigerator is shown in Figure 1.6.
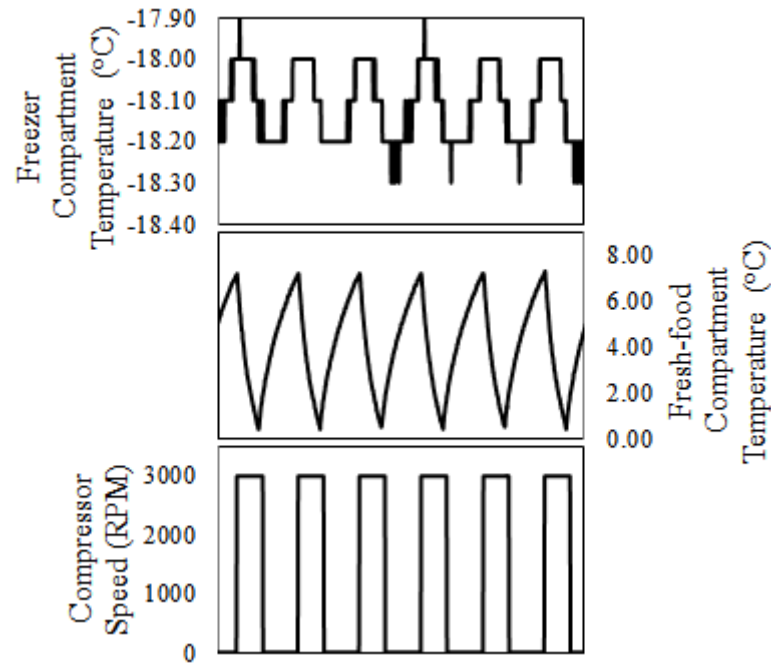
Figure 1.7. Fixed-time on-of control of the household refrigerator

When the refrigerator achieves steady state operation conditions, the off-cycle is driven by the temperature feedback just from the fresh-food compartment. When the temperature becomes +8°C at the fresh-food compartment, the compressor is started to operate. After this time, when the temperature is pulled down to 0°C for fresh-food compartment, the damper is closed and the refrigerator continues to operate for 5 minutes, regardless of the freezer temperature. In this period, air circulates only between the freezer compartment and the evaporator. This type of control of household refrigerators is called as fixed-time control. The fixed-time, in this case, is 5 minutes and it is just valid for the freezer control settings of -18°C. Every temperature control settings' fixed-time value is different and they are determined by a group of tests. It means that after closing of the damper, the fixed-time operation is enough to keep the freezer compartment in desired temperature range. Typical temperatures of the both compartment and the compressor speed are given in Figure 1.7.

The refrigerator operates under defrost cycle once in every 48h, and this cycle lasts about one hour. During the defrost cycle, the ice formation over the evaporator is

melted with the help of an electrical resistance and the liquid water is diverted to the drainage channel. Through the drainage channel, the liquid water is collected outside of the refrigerator in a basin over the compressor and it is evaporated by the compressor waste heat. After defrost cycle ends, the refrigerator stays in off-period for 12 minutes to ensure that the all liquid water is drained from the inside of the refrigerator.

1.5. Energy Classifications of Household Refrigerators

Energy classifications of refrigerating appliances are regulated by many organizations for different countries. In the scope of this thesis, European Commission Directive numbered 2010/30/EU is taken into account for energy labeling of the household refrigerator (European Commission, 2010) and it is explained in this section.
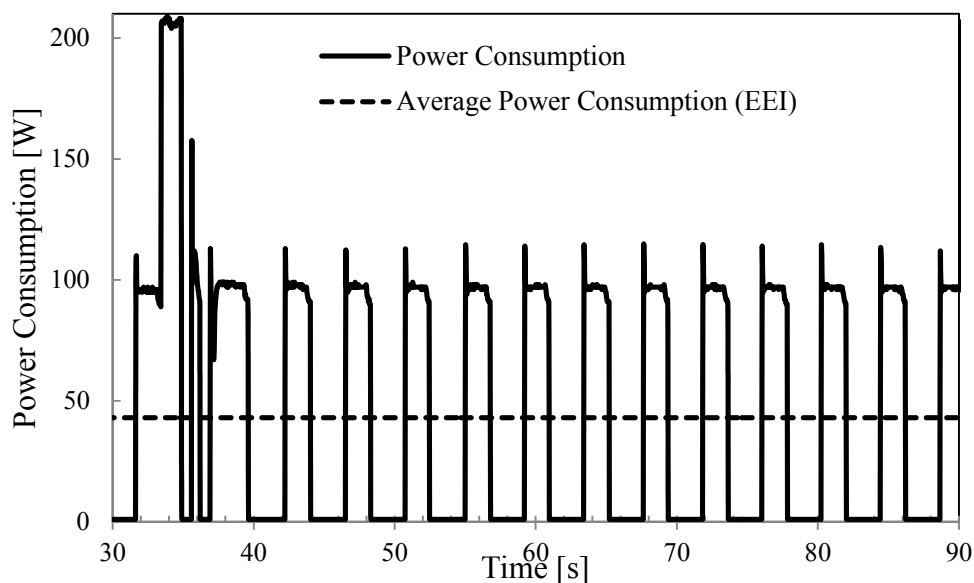
Figure 1.8. Power measurements and EEI representation

The EC of refrigerating appliances according to this regulation is expressed in the form of "kWh/24h", and also known as daily EC. In Figure 1.8, power consumption and total average power consumption in which on and off periods of a household refrigerator are shown. According to the directive, energy classification of refrigerating appliances are determined by the total average power consumption and it is called as "energy efficiency index (EEI)" and it can be simply defined as

$$EEI = \frac{\int_{24h} Power\ consumption\ dt}{Number\ of\ power\ measurement\ points} \qquad (1.6)$$

According to the European Commission Directive 2010/30/EU, energy classifications and color codes based on EEI are given in Table 1.4 below. Refrigerators having lower EEI than 44 W are classified in most efficient classes.

Table 1.4. Energy classifications of household refrigerating appliances

Refrigerating Appliances Energy Classifications, as EEI									
A^{+++}	A^{++}	A^+	A	B	C	D	E	F	G
<22	<33	<44	<55	<75	<95	<110	<125	<150	>150

According to the directive, all refrigerating appliances need to have an energy label which explains the energy class and its color code, annual energy consumption of the appliance, total compartments' and frozen-food storages volumes of the refrigerant, acoustical noise emission. In Figure 1.9, an example energy label of a household refrigerator is indicated.
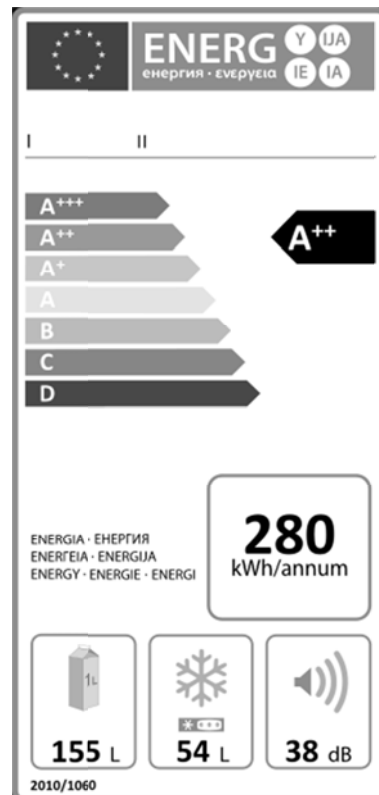
Figure 1.9. An example of the Directive 2010/30/EU energy label of a household refrigerator

CHAPTER 2

LITERATURE SURVEY

Many studies have been performed to investigate and evaluate the performance of refrigerating appliances over the past few decades. In spite of existence of a lot of parameters affecting the performance characteristics of household refrigerators, a great part of studies focused on the effects of refrigerant charge, capillary tubes, capillary tube-suction line heat exchangers and variable speed compressors in the literature. This chapter summarizes the studies associated with these effects on the performance of household refrigerators in the open literature.

2.1. Effects of Refrigerant Charge and Its Distribution

Refrigerant charge and charge distribution of equipment used in refrigeration industry had not had a priority as yet the Montreal's protocol (1987) indicated the destructive effects of some refrigerants on the ozone's layer and the Kyoto's protocol (1997) indicated their contribution to the greenhouse effect (Poggi et al., 2008). From that day forward studies on refrigerant charge reduction and their distribution effect on the performance of refrigerating appliances continue increasingly.

Björk and Palm (2006) presented two studies examining the effects of refrigerant mass charge distribution on the performance of an on-off controlled household refrigerator in which Isobutane (R600a) is used as a refrigerant for transient and steady conditions. They examined that the largest refrigerant charge displacement occurs immediately after a compressor start and stop. During the first half minutes of the on-cycle, it is observed that the evaporator charge decreases sharply and the charge is displaced towards to the condenser. After this period, it is seen that the evaporator refrigerant charge increases and at the end of the on-period the most refrigerant charge is observed in the evaporator. The refrigerant mass charge distribution can be seen in Figure 2.1. Similar to Björk and Palm (2006) studies, Ding et. al. (2009) experimental study on an air-conditioning system uses R410a as a refrigerant, explains that the refrigerant inventory. Contrary to Björk and Palm study, they reported that the

condenser, the evaporator, and the compressor include 50%, 16%, 14% of the entire inventory in the system during on-period, respectively. During the off-period, the refrigerant starts to evaporation in the condenser due to the sharp pressure drop and the great portion of it migrate to the evaporator. As a result of this, the evaporator's pressure and temperature increases and this causes the performance of the refrigerator to reduce. Björk and Palm (2006) reported four types of cycling losses of on-off controlled system which are resulted from liquid suction from the evaporator at start-up, improperly charged heat exchangers during on-period, vapor entering the evaporator through the capillary tube during off-period, and refrigerant vapor pumped through the capillary tube at start-up. They found out that the refrigerant charge distribution causes to reduce the efficiency of the system by 9%. To prevent the adverse effects of refrigerant charge distribution, they suggested some solutions including utilizing a variable speed compressor, decreasing the internal volume of the evaporator, and arranging the refrigerant line in a downward slope.
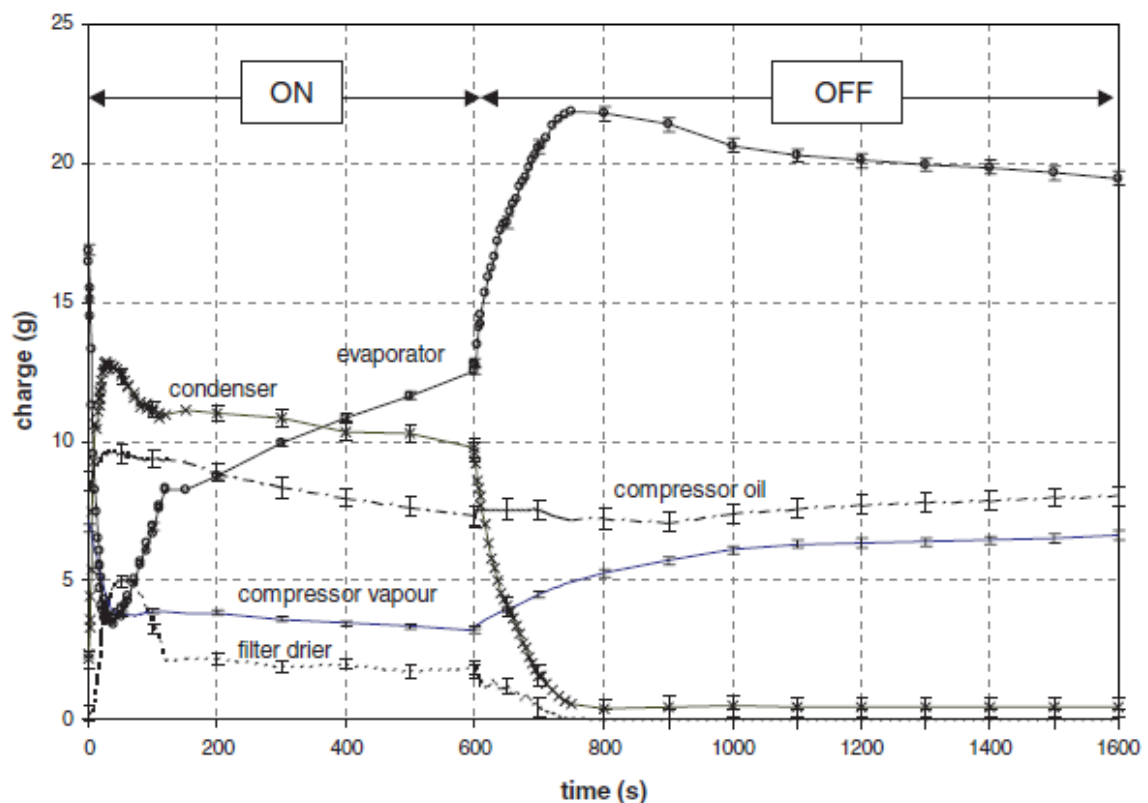
Figure 2.1. Refrigerant charge distribution of a household refrigerator
(Source: Bjork & Palm, 2006)

Ding et. al. (2009) also pointed out that the total energy loss caused by the refrigerant migration of refrigeration system during the start-up and shutdown processes varies between 5-37%.

2.2. Effects of Capillary Tube-Suction Line Heat Exchanger

In vapor compression refrigeration systems, to separate the high and low pressure sides according to load demand, a pressure-reducing device is necessary. Capillary tubes are the most common used devices in small refrigeration appliances which consist of single compressor-single evaporator systems such as household refrigerators, air-conditioning systems, dehumidifiers, etc. Capillary tubes are preferred to thermal expansion valves for these small refrigeration systems due to their low cost and adequate control on some systems (ASHRAE, 2006). Comparing the electronic expansion devices, capillary tube flow characteristics remain constant over the life of the refrigeration system (Greenfield & Dunn, 1994). Capillary tubes helps the compressor starts at a low torque as the pressure across the capillary tube equalize during the off-cycle process. Capillary tubes diameter and length ranges vary from 0.5 to 2 mm and 2 to 6 m, respectively (Liang et al., 2010).

Bolstad and Jordan (1948) described the capillary flow behavior by experimentally. The graph in Figure 2.2 shows their measurement results.
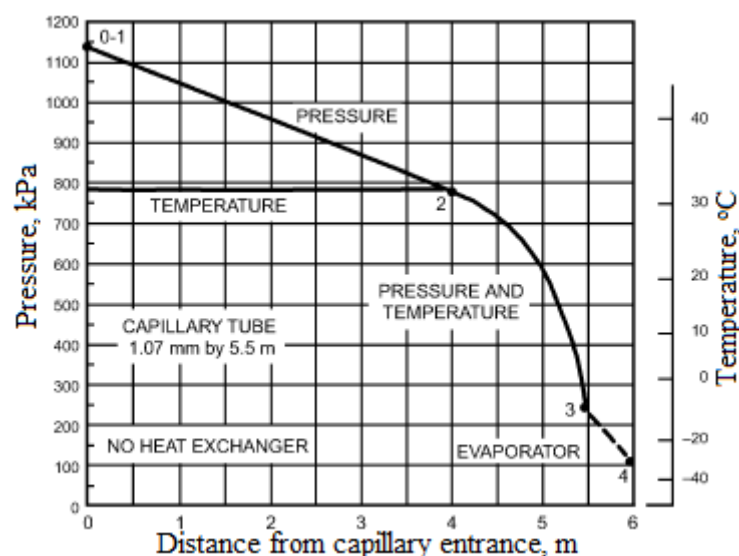
Figure 2.2. Pressure and temperature distribution along a typical capillary tube
(Source: ASHRAE, 2006)

17

According to pressure and temperature measurements shown in Figure 2.2, their results show that at the entrance to the tube, a slight pressure difference occurs, between points 1 and 2, the pressure drop is linear. Bolstad and Jordan (1948) reported that the whole refrigerant is in the liquid phase and the refrigerant starts to undergo phase change at point 2 where a sharp pressure drop is observed at the end of the capillary tube. However, it is reported by many authors that the first bubble generation is not generated at the point where the liquid pressure reaches the saturation pressure at the point 2. From this point, the refrigerant remains in liquid state for some distance along to the capillary tube even after the pressure drops below the saturation pressure and the evaporation of the refrigerant is delayed. This is called as metastable or superheated liquid phenomenon (Kim et al., 2011). According to this phenomenon, the refrigerant stays in liquid state up to a critical pressure, point 3, and its flow rate increases as its pressure decreases up to this critical value, point 3, below this point there is no change in the flow observed, called as choked flow, and it flashes through the evaporator and begins to vaporize at point 4. This phenomenon makes design and investigation of the performance of capillary tubes very difficult (ASHRAE, 2006).

In household refrigerators, generally, two types of capillary tubes are utilized which are adiabatic and non-adiabatic capillary tubes, but the great majority of them includes non-adiabatic capillary tubes in contact with suction line to exchange heat between each other. This built is called as capillary tube-suction line heat exchanger (SLHX).

Hermes et al. (2000) examined the characteristics of R134a flow through adiabatic and non-adiabatic capillary tubes, and they point out that the capillary tube flow is considerably affected by the heat transfer. They reported that for the adiabatic capillary tube the refrigerant enthalpy remains constant through almost the entire length of the capillary tube but at the exit of the tube a small drop in enthalpy is observed due to the flow acceleration. For the case of non-adiabatic capillary tube flow, it is reported that the enthalpy of the refrigerant remains constant along the adiabatic inlet length of the capillary tube and along the heat exchanger length it is reduced due to, mainly, the heat exchange between the capillary tube and the suction line and the kinetic energy change as in the adiabatic case. They showed the comparison of adiabatic and non-adiabatic capillary flow of R134a on a plot as given in Figure 2.3.
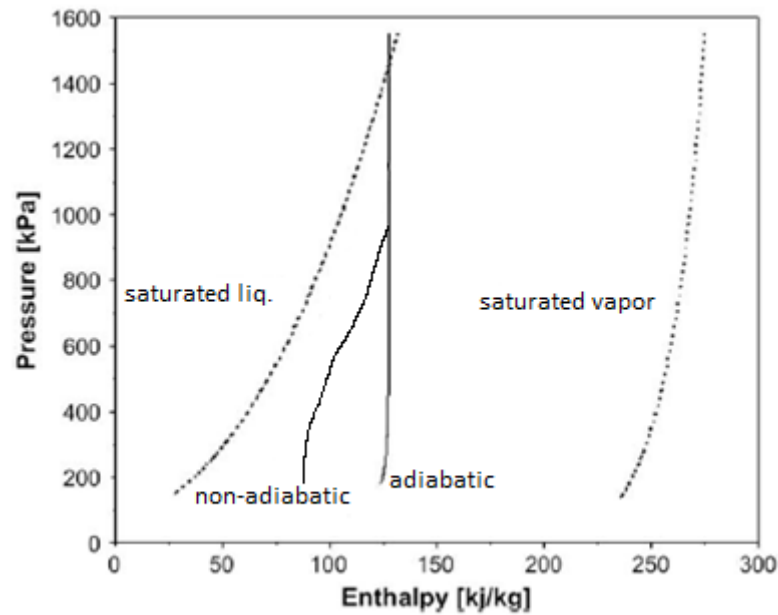
Figure 2.3. Comparison of thermodynamic states of an adiabatic and non-adiabatic
capillary tube flow of R134a (Source: Hermes et al., 2000)

Two types of SLHX configurations can be found in the literature and in practical applications which are the lateral and the concentric configuration, as shown in Figure 2.4. Some part of the capillary tube passes at the axial center of the suction tube in the concentric configuration, while, in the lateral configuration, the capillary tube is soldered or welded to the suction tube. SLHXs are utilized in refrigeration applications for many reasons. Primarily, SLHXs are employed to increase the evaporator capacity and to prevent slugging of the compressor due to the liquid inlet to it (Liu & Bullard, 1997).
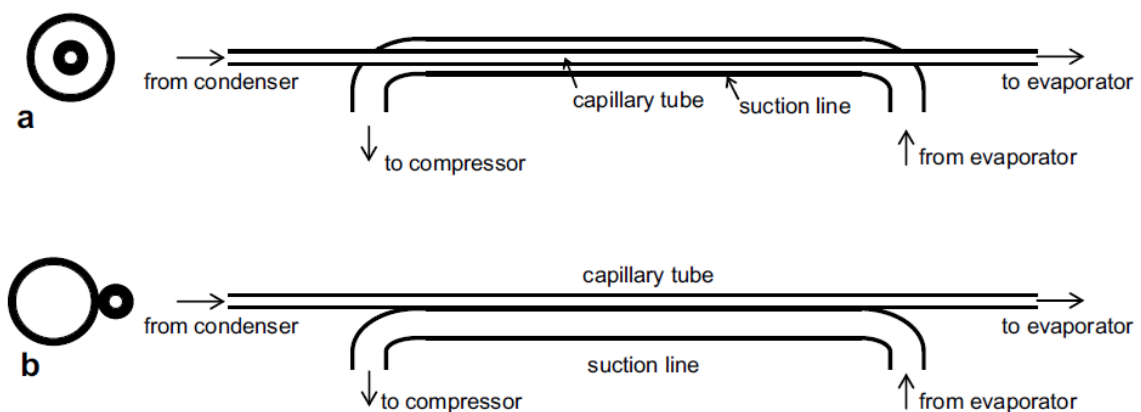
Figure 2.4. Types of SLHXs a) concentric, b) lateral
(Source: Hermes et al., 2008)

Bansal and Xu (2003) performed a parametric study of refrigerant flow to investigate its flow characteristics in SLHXs. Their study shows that high condensing pressurized refrigerant entrance to the evaporator results in high pressure drops. Besides, decreasing of evaporator temperature leads to increase the pressure difference between the inlet and outlet of the capillary tube and also causes increase of mass flow rate of the refrigerant inside capillary tube. The higher mass flow rate causes an earlier flashing point within the adiabatic region and higher quality at the inlet of the heat exchanger region, which leads to a stronger pressure drop effect within the region. As a consequence, they reported that these conditions lead to decrease the performance of the system.

Since the dimensional modeling of two-phase flow has many difficulties, uncertain phenomenon, and requirement of great time to solve these models, authors primarily divert their studies from dimensional modeling to non-dimensional one of refrigerants flow based on adiabatic and non-adiabatic capillary tubes on the last two decays. The studies of non-dimensional analyses are based on both experimental and theoretical works with respect to this concern. The main advantage of this approach is to gather maximum information from a minimum amount of data.

Bittle et al. (1998) developed two generalized dimensionless correlations based on Buckingham-Pi Theorem to predict refrigerant mass flow rate in adiabatic capillary tubes for both subcooled and two-phase flow inlet conditions. The correlations are based on experimental data of R134a, R22, and R410A. It is reported that the mass flow rate of the refrigerant fall within the ±6% and ±13% predictions intervals for subcooled inlet and quality inlet conditions, respectively. The correlations found by Bittle's et al. are suggested by ASHRAE, hence, their model is called as ASHRAE model in some studies. Melo et al. (2002) studied a concentric type SLHX performance of a refrigeration cycle works with Isobutane (R600a) experimentally. Regarding the mass flow rate and the suction line outlet temperature as the performance parameters, they investigated the effects of eight factors which are inlet pressure, subcooling, and suction line inlet temperatures, internal diameters of the capillary tube and the suction line, lengths of the capillary tube, SLHX, and adiabatic inlet. Depending on these parameters they derived two empirical correlations for the mass flow rate of the refrigerant and the suction line outlet temperature; however, these correlations are just valid for concentric type SLHXs. Kim et al. (2003) studied on dimensionless mass flow rate correlations of R22, R290, and R407C based on experimental data. The dimensionless correlation

based on eight Pi-groups which depend on inlet pressure, subcooling degree, geometry, density, friction, bubble growth, vaporization and mass flow rate. They showed that the correlation yields good agreement with experimental data with standard deviation of 5%. Chun-Lu (2005) developed a generalized correlation of refrigerant mass flow rate includes R12, R134a, R22, R290, R407C, R410A, and R600a by use of artificial neural network. It is reported that the mass flow rate is directly proportional to subcooling temperature and condensing temperature. Increasing the subcooling temperature leads the mass flow rate to increase for a constant condensing temperature, in the same manner, as increasing the condensing temperature, the mass flow rate increases for a constant subcooling temperature. They also revealed that the inner diameter is directly proportional to the mass flow rate too. Yang and Wang (2008) also presented a dimensionless mass flow rate correlation of adiabatic capillary tubes based on experimental data of R12, R22, R134a, R290, R600a, R410a. Their correlation predicts the mass flow rate within a range of the experimental data average and standard deviations of -0.83% and 9.02%, respectively. Kim et al. (2011) presented a dimensionless refrigerant mass flow rate correlation for both adiabatic and non-adiabatic capillary tubes and an extensive comparison with other studies associated with dimensionless refrigerant mass flow rate correlations in capillary tubes. Comparing the correlations by Kim et al. and Bittle et al., it is shown that Kim et al. correlations predict the mass flow rate and the suction line outlet temperature more accurately.

2.3. Effects of Variable Speed Compressor

The vapor compression refrigeration cycles with VSC differ from conventional vapor compression refrigeration cycles with SSC in such a way that control of the system capacity at partial load conditions. This is called as capacity control. In refrigeration systems with VSC, the required cooling load is matched by regulating the compressor speed, whereas, those with SSC, regardless of the required cooling load, the same load is provided for different load conditions.

Qureshi and Tassou (1996) presented a review which compares the variable speed capacity control methods in refrigeration systems including on-off, hot gas bypass, evaporator temperature, clearance volume, multiple compressor, cylinder unloading, and variable speed control methods. According to their study, a variable

speed compressor control method is the most energy efficient capacity control method for full and partial load conditions. In Figure 2.5, comparison graph of capacity control methods at half load conditions stated by Qureshi and Tassou (1996) is given and according to this comparison graph, the most energy efficient capacity control method is variable speed capacity control method.
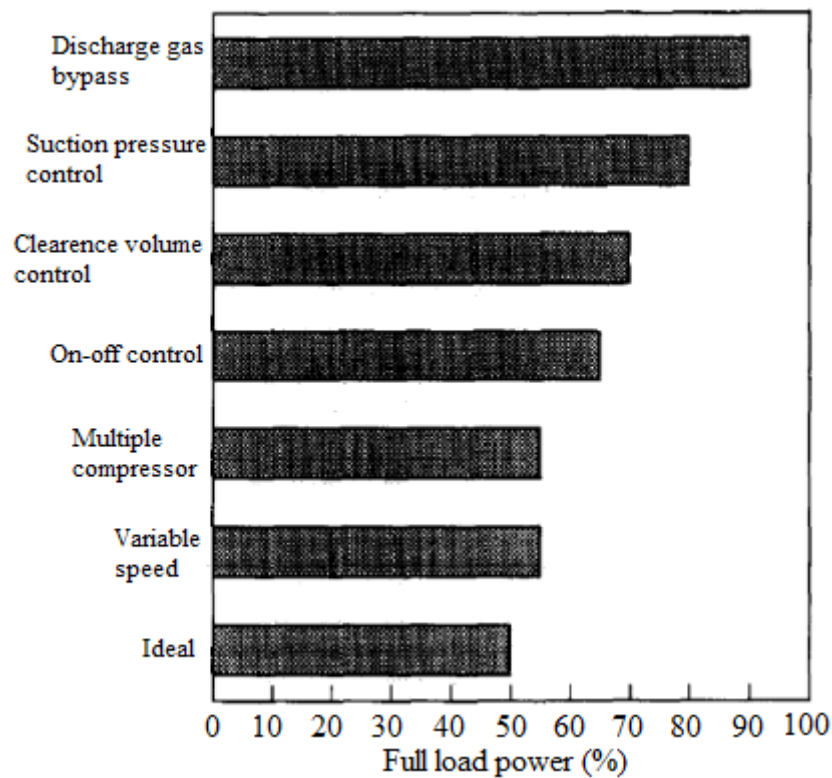
Figure 2.5. Comparison of capacity control methods at half load
(Source: Qureshi & Tassou, 1996)

Variable speed compressor motor control mechanism is classified into two main types: stepwise control and continuously (infinitely) variable control. Stepwise control provides finite number of speeds to match the required cooling loads, whereas, continuously speed control has infinite number of speeds for varied load conditions. Stepwise control method is less costly than continuously variable speed control since they do not require enhanced motor drivers. However, it is less efficient than continuously variable speed control mechanism. Implementation of continuously control mechanism requires enhanced variable speed drives to be designed suitably for applications. By utilizing an unsuitable variable speed drive for a given application, the lubrication of the compressor may not be provided properly and this leads to reduce the compressor life (Dincer & Kanoglu, 2011).

Qureshi and Tassou (1996) reported that a two-speed, stepwise controlled compressor consumes 49% less energy than a SSC does due to the lower friction losses at half speeds and can reduce cyclic losses by 5-7%, compared to on-off controlled compressor. They also examined that variable speed control could achieve a 15% improvement in energy efficiency, compared to a conventional system. Qureshi and Tassou (1996) pointed out some advantages of utilizing a VSC on a refrigeration system are

- Reduction in energy consumption,
- Reduced torque requirements at initial startup,
- Reduction in temperature fluctuations,
- Reduction in required time to achieve desired temperature levels in refrigerator compartments,
- Low noise operation at most loads,
- Fewer on-off cycles,
- Stable humidity control.

Liu and Soedel (1994) examined on a variable speed hermetic compressor that the most efficient operating condition is observed at the designed speeds and frequencies. It is reported that at higher compressor speeds than the designed operating speed, the volumetric efficiency of the variable speed compressor increases since leakages and losses from valves decreases. It is also stated that the increase of compressor speed does not reduce the overall efficiency.

Tassou and Qureshi (1998) presented studies on three different type variable speed compressors. They examined that decreasing the speed of a compressor leads to decrease the volumetric efficiency of it due to leakage taking place between the vanes and the cylinder wall arising from reduced hydrodynamic sealing at lower speeds. It is emphasized that the utilization of a variable speed compressors in warm climates is more cost effective, compared to utilization of it in cold climates due to longer operating hours in cold climates.

Renno et al. (2004) studied on generation of a variable speed reciprocating compressor control algorithm experimentally to reduce the energy consumption and obtain the optimum operating of compressor according to variable cooling loads. Their control algorithm is based on fuzzy control that selects the most appropriate compressor speed with reference to cold storage air temperature feedbacks. In their study, fuzzy

control algorithm and the traditional control, thermostatic control, are compared on a commercial cold storage utilizing R407C as a refrigerant and their results showed that the fuzzy control algorithm provides 13% energy saving.

Li et al. (2004) performed a study on modeling a variable speed compressor based on experimental data. They modeled the compressor by use of map-based method which provides the relation between motor power input, evaporation and condensation temperatures, and mass flow rate of the refrigerant. It is pointed out that the refrigerant mass flow rate is independent of the condensation and evaporation temperatures at a constant frequency. In other words, it is stated that the refrigerant mass flow rate is determined only by the compressor frequency for refrigerating systems utilizing variable speed compressors. They also explained the relationship between the compressor frequency and the COP of the refrigerating system. It is stated that there is an optimal frequency to make COP maximum, which is usually the basic frequency at which the compressor motor is designed to operate.

Chang et al. (2008) compared the effects of using R600a and R134a in a same household refrigerator with brushless DC VSC. They utilized a two speed control algorithm on the VSC and observed the temperature variations inside the cabinets, defrost behavior, and energy consumption of the VSC. They reported that the household refrigerator utilizing R600a with VSC provides 0.59 kWh/24h decrease in energy consumption with an efficient potential of 28.16% based on the household refrigerator with SSC. They also found that the refrigerator with R600a consumes lower energy than the refrigerator with R134a by 13.6%. As comparing with the refrigerants performance on the refrigerators with VSC, it is pointed out that utilization of R600a improves the efficiency by 10 to 15% than that of R134a system.

As increasing the developments in the variable speed compressor technology, the energy consumption of the household refrigerators decreases, however, initial cost of them increases due to the requirement of developed variable speed drives. For a proper variable speed compressor implementation, the variable speed control mechanism should be designed uniquely for application areas and required cooling load variations.

CHAPTER 3

EXPERIMENTAL SETUP

In the scope of this study, to determine the performance of each component in the household refrigerator, an experimental set-up in which temperature and pressure measurements are taken at the inlet and outlet of these components is designed. A volumetric flow meter is utilized on the suction line before the refrigerant enters the compressor. And also, air stream temperatures at inlet and outlet of the evaporator are measured to determine the air side heat transfer in the system. A variable frequency converter is used for driving variable speed compressor at different revolutions per minute to respond different load conditions. To take measurements from these instruments, a data acquisition device and its modules are utilized during the tests. The entire test process is controlled and automatized by a coded software program.

3.1. Temperature Measurements

For temperature measurements, T-type thermocouples are used. Thermocouple specifications are given in Table 3.1. Thermocouples are connected over the tubes of all components inlets and outlets via aluminum tape, whose thermal conductivity is too low, and thin short tie cable. Tie cables and aluminum tapes are used to secure the connection of thermocouples and provide proper contact force. To measure temperature more accurately over the tube walls at the outside of the refrigerator, against the potential disturbance of hot air stream over the thermocouples, they are also covered with cylindrical insulation materials whose thicknesses are at least 15 mm. They are used for temperature measurements over zero degrees of Celsius at condenser and compressor thermocouple connections. For temperature measurements over the evaporator tube, insulation material is not used since they are thick enough to restrict the air stream over the evaporator. In Figure 3.1, example thermocouple connections over the evaporator and the condenser tubes are shown.

Table 3.1. Thermocouple specifications

	Manufacturer	Omega Engineering
	Type	T-type
	Min. Temperature	200°C
	Max. Temperature	300°C
	AWG No	30
	Nominal Size	0.6 mm x 1 mm
	Accuracy	±0.5^{o}C

In addition to temperature measurements of the refrigerant in the cycle, air stream temperature over the evaporator is measured by use of thermocouple array at the inlet and the outlet of the evaporator. Besides, temperatures of air stream inside the fresh-food and freezer compartments, and test packages, which are called as M-packages in ISO 15502, are measured.
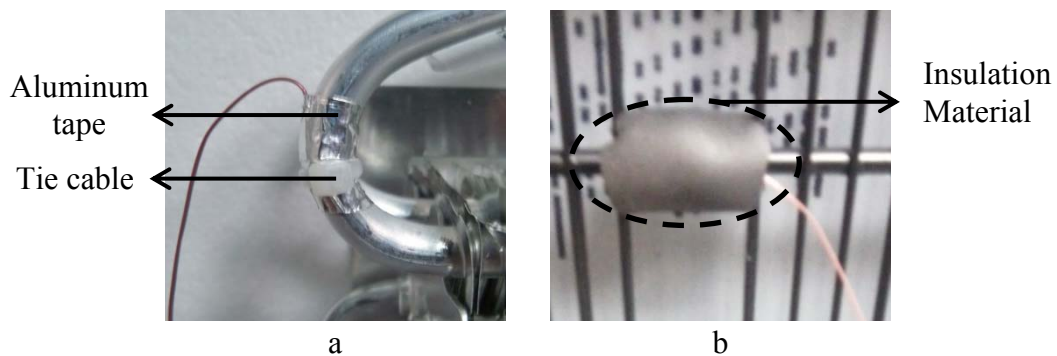
Figure 3.1. Thermocouple connections over tubes of the evaporator (a) and the condenser (b)

To reduce the fluctuations of the air stream temperatures in the fresh-food compartment, thermocouples are connected to cylindrical brass masses. The purpose of using that kind of mass connections at the end of thermocouples is to provide stable temperature measurements due to their high specific heat. Three thermocouples (T1, T2, T3) are located at the geometric centers of three shelves of the fresh-food compartment as shown in Figure 3.2.

During the tests, some test package temperatures in the freezer compartment are also measured according to ISO 15502. The main aim of measuring the temperatures of test packages in the freezer compartment is to observe the temperature fluctuations of them during the tests and make sure that they are in the secure range in accordance with ISO 15502. Figure 3.2 shows test packages storage in the freezer compartment.
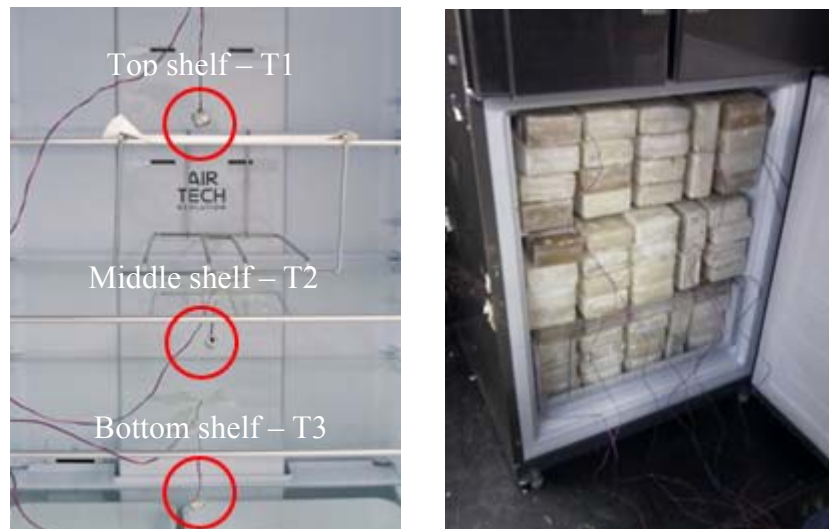
Figure 3.2. Thermocouple connections in the fresh-food and test package storage in the freezer compartments

To measure evaporator air side temperature, six pieces of thermocouples are used. Half of them are utilized at the inlet and the rest are utilized at the outlet. There are three inlet air channels to the evaporator, two of them are belongs to the freezer compartment which are located at left and right sides of the evaporator, and one of them at the middle is belong to the fresh-food compartment. Air stream temperature over the condenser is not measured because the condenser is a cross flow type natural convection heat exchanger which is open to the surroundings. Thermocouple placement for air inlet temperature measurement can be seen in Figure 3.3 below.
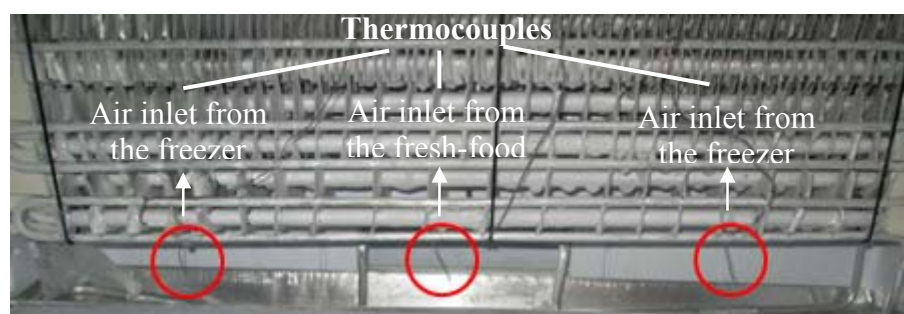
Figure 3.3. Thermocouple array for air stream inlet temperature measurements

All thermocouples distribution on the test refrigerator can be seen in Figure 3.4.
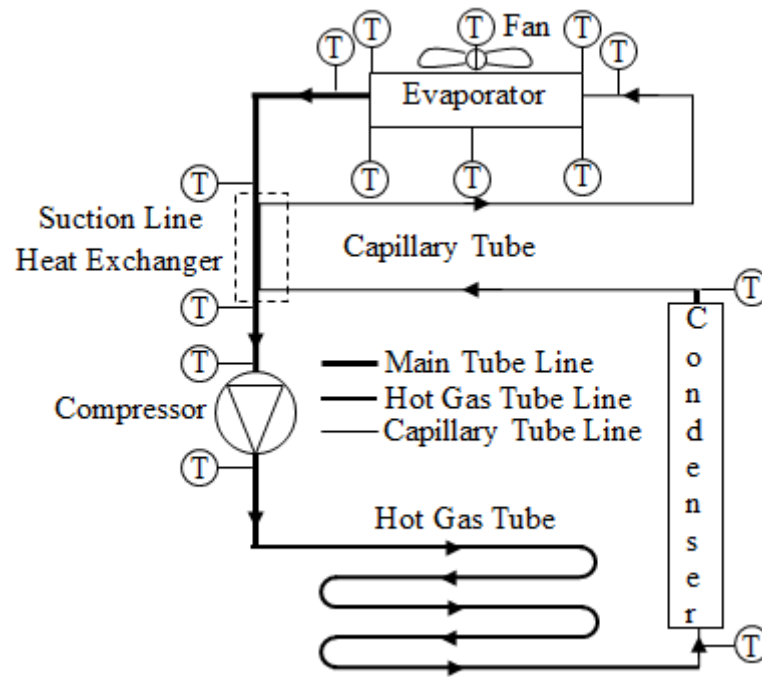
Figure 3.4. Thermocouples locations on the test refrigerator

3.2. Pressure Measurements

On the refrigerator under test, pressures are measured at five different locations which are inlet and outlet of the compressor, outlet of the condenser, inlet and outlet of the evaporator during the tests. Two types of pressure transducers are used on the test refrigerator for high and low pressurized lines of the refrigeration cycle. High pressurized line includes the compressor and the condenser outlets, whereas, low pressurized line includes the compressor inlet, the evaporator inlet and outlet in the cycle. The main reason to utilize two different types of pressure transducer on the test refrigerator is to maintain high precision in pressure measurements during the tests. It should be noted that the pressure transducers for measuring pressures at the inlet and outlet of the evaporator have to be able to measure vacuum since the evaporator operates under vacuum conditions during on-periods. For this reason, Type 1 pressure transducers are used on the evaporator. Pressure transducer utilized in the system and their specifications are shown in Table 3.2.

Type 1 pressure transducers are used for measurements from low pressurized line, whereas, Type 2 pressure transducers are utilized on high pressurized line. Pressure transducers are connected with 1/4" (6.35 mm) copper tube extensions to the system.

Figure 3.5 indicates example pressure transducers connections over the evaporator and the condenser.

Table 3.2. Pressure transducers specifications

	Type 1	Type 2
Manufacturer	Emerson	Emerson
Model	PT5-07M	PT5-18M
Material	Stainless Steel	Stainless Steel
Min. Pressure	-0.8 bar	0 bar
Max. Pressure	7 bar	18 bar
Operation Temperatures	-40°C - +100°C	-40°C - +100°C
Power Input	24 VDC	24 VDC
Output Signal	4-20 mA	4-20 mA
Accuracy	≤±1% FS	≤±1% FS

Analog signal outputs of pressure transducers are transferred to the data acquisition device by their special connection cables. Analog outputs from transducers are converted to digital signals and scaled by coded program.

a   b

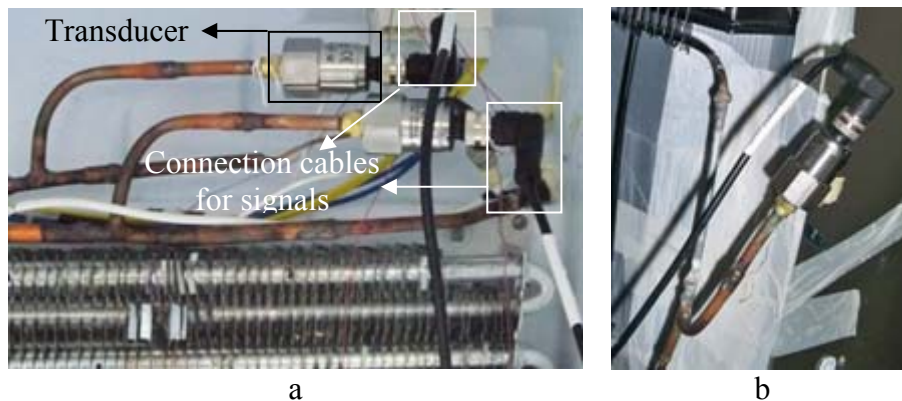Figure 3.5. Pressure transducers connections on a) the evaporator and b) the condenser

3.3. Air Stream Velocity Measurements

For calculations of air side heat transfer, the flow rate of the air stream over the evaporator needs to be determined. Hence, an anemometer is used to measure the air stream velocity over the evaporator. The utilized anemometer specifications are tabulated in Table 3.3.

Table 3.3. Anemometer specifications

	Manufacturer	Omega Engineering
	Model	FMA902R-MA
	Velocity Range	0-5 m/s
	Probe	Remote Probe
	Probe Diameter	6 mm
	Probe Length	305 mm
	Accuracy	2% FS
	Operation Temperatures	$-40^{o}C$ - $+121^{o}C$
	Power Input	15-24 VDC
	Analog Output	4-20 mA

The anemometer enters the measurement area from a hole which is drilled at the right side of the refrigerator cabinet, as shown in Figure 3.6.
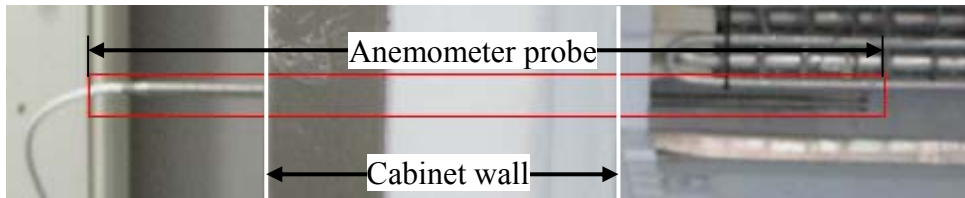
Figure 3.6. Anemometer placement

The air velocity measurements are taken at the inlet of the air stream to the evaporator at which air streams from compartments of the fresh-food and the freezer are mixed. Measurements are taken from points once every 7.20 mm from 33 points along the half of the evaporator inlet. Air stream velocity measurement location and points are shown as small vertical lines in x-direction in Figure 3.7. Four tall vertical lines in the figure separate the air streams entrance areas from compartments of the fresh-food and the freezer. Air stream from the freezer enters the evaporator on the left and the right sides; fresh-food air stream enters the evaporator on the middle area. By sliding the anemometer through the x-axis, which is shown with dashed line, point by point, measurements are taken for the half of the evaporator during the steady state operation of the test refrigerator. The velocity profile for the other half part is assumed as the same as the first half part since the evaporator and the air inlet locations are symmetric.

Figure 3.7. Air stream velocity measurement points

The velocity profile of the air stream over the evaporator for steady state operating conditions is given in Figure 3.8.

Figure 3.8. Velocity profile of air stream over the evaporator

The total volume flow rate of the air stream is calculated by integration of measurements over the air stream inlet area along the evaporator. The total volume flow rate of the air stream, $\dot{V}_{air}$, is expressed as

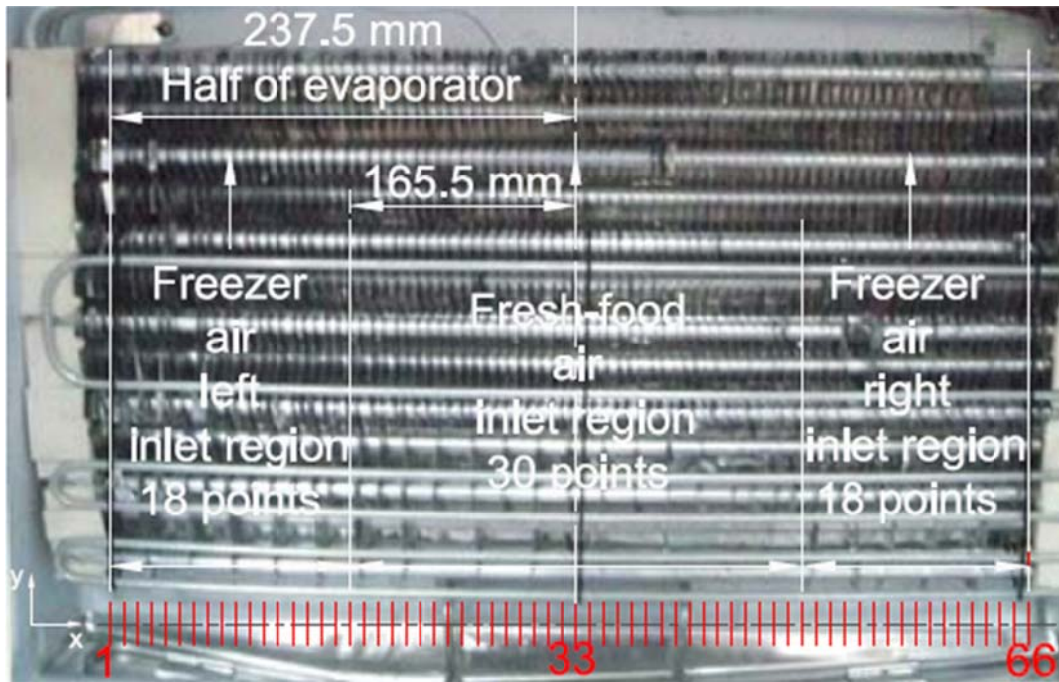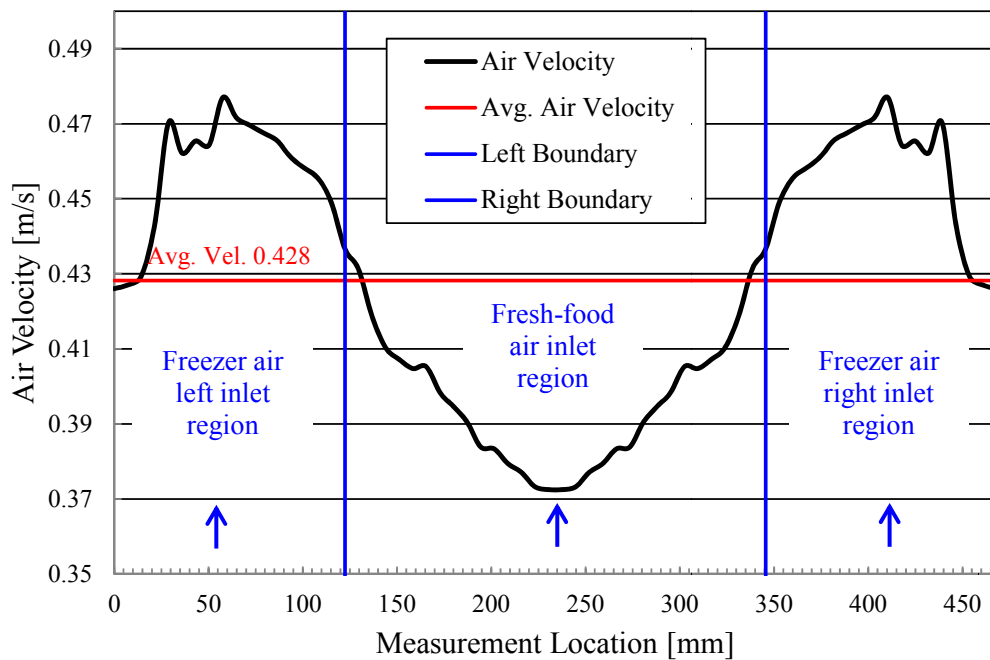$$\dot{V}_{air} = \int_A \bar{v} d\bar{A}$$

(3.1)

where v is the velocity for each point, A is the total air inlet area to the evaporator. Total air inlet area is defined as

$$Total\ Area = A = \sum_{k=1}^{66} a_k = a_1 + a_2 + a_3 + ... + a_{66}$$

(3.2)

where k and a represent the number of velocity measurement points and the unit area of which air velocity measurement is taken at the center, respectively.

The air stream velocity for each point is obtained by taking at least 20 measurements from each point in steady state operating conditions and these measurements average is attained as the air stream velocity for the associated point. For each measurement point, the unit area is the same and it is 0.00036 m². When Eq. (3.1) is written explicitly, it becomes

$$\dot{V}_{air} = \sum_{k=1}^{66} v_k a_k = v_1 a_1 + v_2 a_2 + ... + v_{66} a_{66} = \left(v_1 + v_2 + ... + v_{66} \right) a$$

(3.3)

The volume flow rate of the air stream over the evaporator is shown in Figure 3.9. To calculate the mass flow rate of the air, Eq. (3.4) is applied as below.

$$\dot{m}_{air} = \rho_{air} \dot{V}_{air}$$

(3.4)

It should be noted that the air flow is assumed incompressible, constant density, and the air is taken account into as dry-air since all measurements are taken after the defrost cycle during which almost all moisture in the air is condensed and removed from the refrigerator. The density of dry-air is taken **1.45 kg/m³** by averaging the dry-air

densities at temperatures between -40° and -20°C. Plots of volume flow rate and the mass flow rate of the air can be seen in Figure 3.9 and Figure 3.10, respectively.
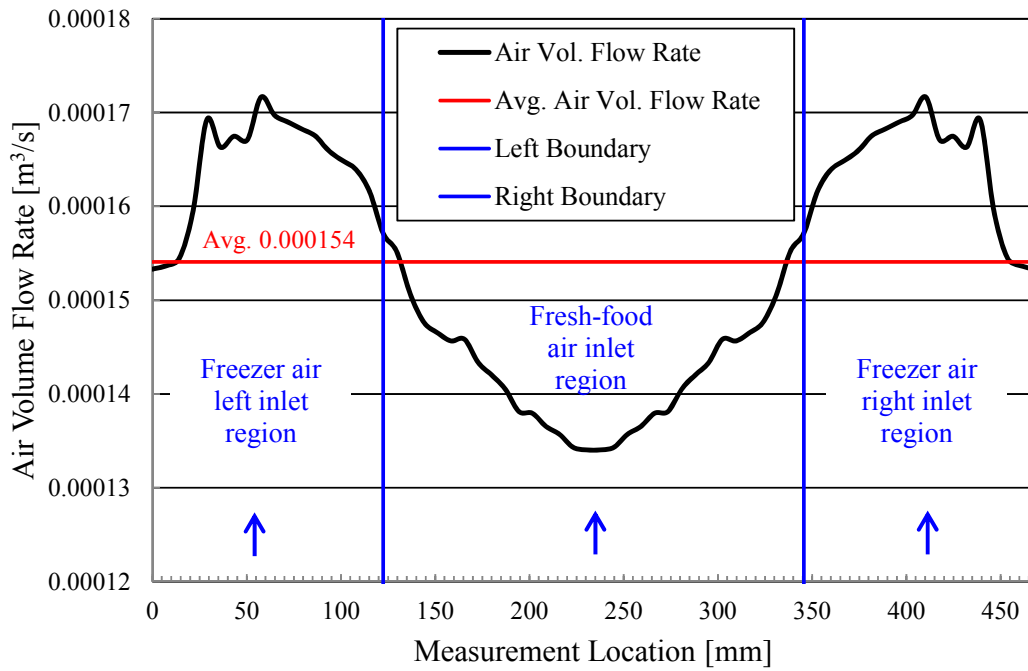
Figure 3.9. Volume flow rate of the air stream over the evaporator
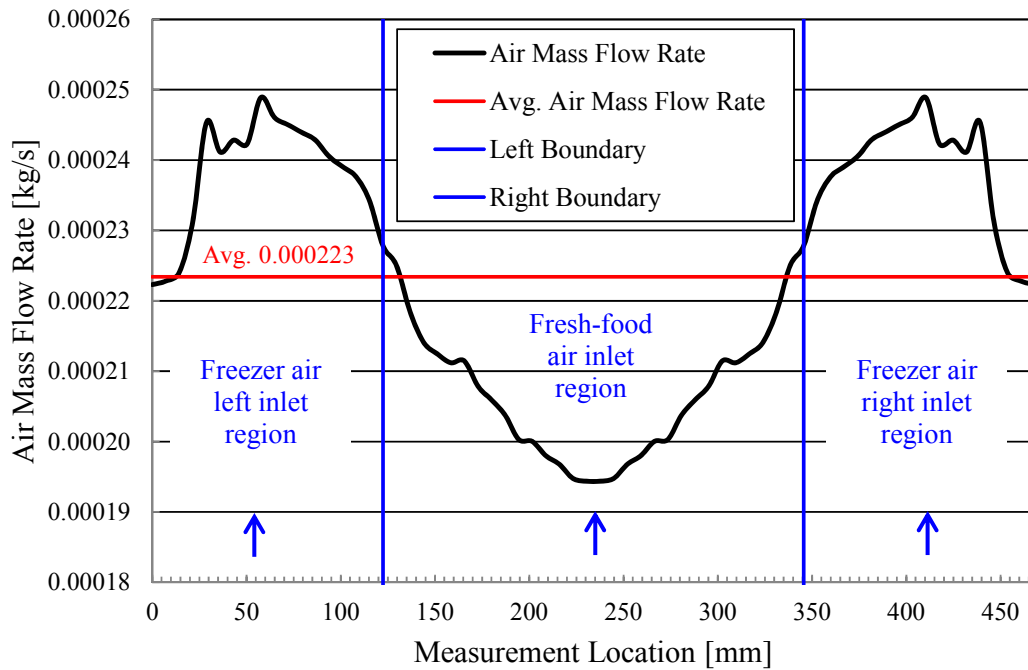
Figure 3.10. Mass flow rate of the air stream over the evaporator

3.4. Refrigerant Mass Flow Rate Measurements

Refrigerant mass flow rate is planned to measure by a thermal based volumetric mass flow meter. The device is located at the inlet of the compressor. Specifications of the mass flow meter are given in Table 3.4.

Table 3.4. Mass flow meter specifications

Manufacturer	New-Flow Tech. Inc.
Model	THF-04-A-1-W-2-1-2
Refrigerant	R600a (Isobutane)
Connections	1/2" NPT Stainless Steel
Min. Operation Pressure	0.1 bar
Max. Operation Pressure	35 bar
Max. Operation Temperature	50°C
Accuracy	0.43% FS
Flow Rate Range	0-50 L/min
Power Input	24 VDC
Analog Output	4-20 mA

The location and connection of the mass flow meter at the inlet of the compressor is given in Figure 3.11.

Figure 3.11. The mass flow meter connection at the inlet of the compressor

During the tests, it is observed that the oil of the compressor creates blockage in the filter which is located before the measurement pipe of the mass flow meter to prevent dust particles to enter to the measurement pipe of the mass flow meter. During

these periods, the mass flow measurement is not available by the mass flow meter. When this problem is encountered during the periods of EC tests, the mass flow rate of the refrigerant is calculated from the knowledge of compressor displacement and volumetric efficiency provided by the compressor manufacturer. Calculations of the refrigerant mass flow rate are explained in section 3.7.2.

All instruments placements are schematized in Figure 3.12.

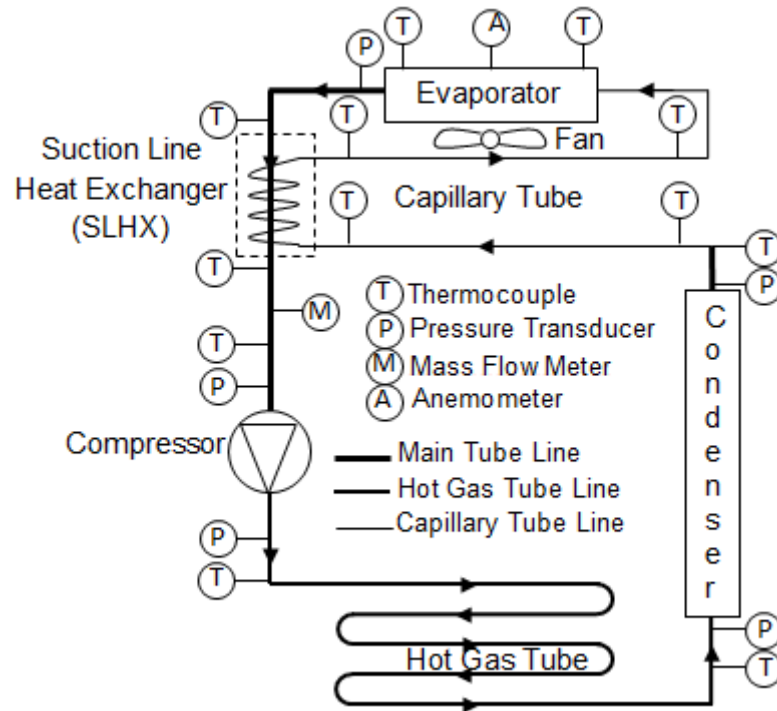Figure 3.12. Instrumentation of experimental set-up

3.5. Variable Frequency Inverter

A variable frequency inverter is used for driving the variable speed AC compressor by varying electrical motor input frequency and voltage. The inverter is capable of driving 3-phase AC motors by varying output frequency range between 50 and 400 Hertz. The specifications of the variable frequency inverter are given in Table 3.5.

Table 3.5. Variable frequency inverter specifications

Manufacturer	Delta Electronics Inc.
Model	VFD-007-L-21-A
Applicable Motor Output	0.2 - 1.5 kW
Rated Frequency	1-400 Hz
Frequency Tolerance	±5%
Output Frequency Resolution	0.1 Hz
Operation Temperature Range	-20°C - 60°C
Cooling	Forced Convection
Analog Input	0-10 V

3.6. Data Acquisition System

To acquire the data from thermocouples, pressure transducers, anemometer, and mass flow meter, a data acquisition system is employed during the performance tests. CompactDaq 9188 chassis from National Instrument (NI) and compatible four data acquisition module with it carry on data acquisition task. These modules are connected to the main chassis (NI 9188) to accomplish their tasks. In this study, two NI 9214 modules for temperature measurements, one NI 9203 analog input module for pressure, air stream velocity, and mass flow rate measurements, and one NI 9263 analog output module for driving the variable speed compressor are employed in the experimental set-up. Specifications of the chassis and each module are given in Table 3.6.

Table 3.6. Data acquisition chassis and modules specifications

Manufacturer	National Instrument
Model	NI cDAQ 9188
Type	Chassis
Number of Slots	8
Resolution	32 bit
Operation Temperature Range	20°C - 55°C
Number of Timers	4
Power Input	15 VDC
Analog Output	4-20 mA

(cont. on next page)

Table 3.6. (cont.)

	Manufacturer	National Instrument
	Model	NI 9214
	Task	Thermocouple
	Number of channels	16
	Resolution	24 bit
	Operation temperature range	-40°C - 70°C
	Accuracy	0.45^{o}C
	Sampling Rate	1088 S/s

	Manufacturer	National Instrument
	Model	NI 9203
	Task	Analog Current Input
	Number of Channels	8
	Resolution	16 bit
	Operation Temperature Range	-40°C - 70°C
	Accuracy	0.049 mA
	Sampling Rate	200 kS/s
	Measurement Range	-20 mA - +20 mA

	Manufacturer	National Instrument
	Model	NI 9263
	Task	Analog Voltage Output
	Number of Channels	4
	Resolution	16 bit
	Operation Temperature Range	-40°C - 70°C
	Accuracy	0.11 V
	Sampling Rate	100 kS/s
	Measurement Range	-10 V - +10 V

3.7. Test Program

A test program based on Labview 9.0.1 is coded for measurements and control of variable speed compressor. The program is capable of operating multitasks simultaneously (parallel processing). To handle with acquiring, analyzing, monitoring, and recording processes, seven subprograms are coded and they are gathered under a main program. For each task, the main program uses seven subprograms. The subprograms and the main program operation hierarchy are given in Figure 3.13.

For each sampling during the tests, firstly, the program acquires data and then converts them to digital signals and scales it. "Initializer" and "Scaling" subprograms are responsible for these tasks. Next, the properties of refrigerant R600a for acquired temperature and pressure are found by "Read R600a Properties" subprogram by means of look-up table method. Once the properties of R600a are found, they are transferred to "Analyze" subprogram for calculations of mass flow rate of the refrigerant, cooling capacity, rejected heat from the condenser, heat transfer in SLHX, rejected heat from the hot gas tube, consumed power, subcooling temperature, superheating temperature, and coefficient of performance of the test refrigerator. "Analyze" subprogram also prepares a P-h diagram for monitoring the cycle behavior during the tests. After, analyses results are monitored in charts and graphs on the front panel of the main program by "Monitor" subprogram. The main program front panel includes four different screens, which are "Setup", "Evap-Cond-Comp", "SLHX-Air-Hot Gas", and "P-h Analysis", mainly aimed to set up the program and monitoring the measurements and analyses results. Finally, measurements and analyzes results are recorded to text files by "Record" subprogram. "Record" subprogram logs both raw measurement data and analyzes results in different text files for post analyzes.
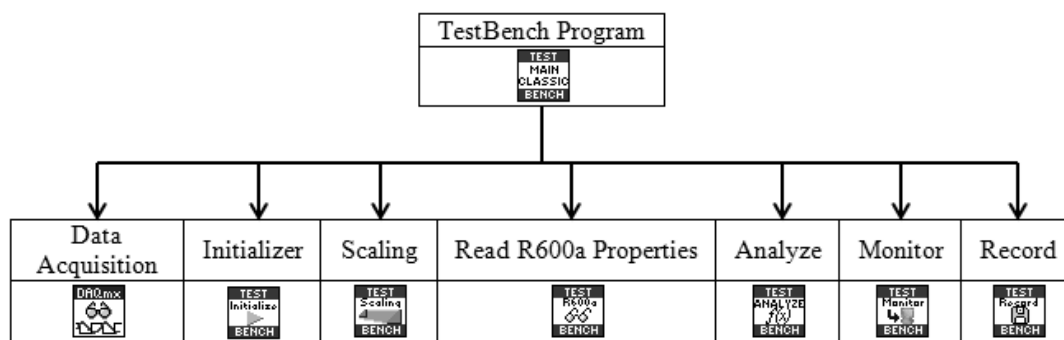
Figure 3.13. Test program operation hierarchy

The "data acquisition (DAQ)" subprogram is responsible for initializing the DAQ devices and adjusting their configuration to adapt the relevant task or tasks. This subprogram has three subroutines which are "AI Temp TC" for temperature measurements configurations, "AI Current" for pressure, air stream velocity, and mass flow rate measurements configurations, and "Analog 1D Waveform NChan Nsample" for acquisition of temperature, pressure, velocity, and mass flow rate data from the test refrigerator.

"AI Temp TC" subroutine detects the thermocouple modules connected to the chassis (NI 9188), and prepares these modules for measurements. Thermocouple channels, temperature unit, expected minimum and maximum values of temperature measurements for auto-calibration, and thermocouple types are adjusted by this subroutine. "AI Current" subroutine detects the analog input modules on the chassis, and configures analog input channels, minimum and maximum values of current measurements for auto-calibration. According to these two subroutines' configurations, "Analog 1D Waveform NChan Nsample" subroutine reads the measurements from thermocouple and analog input current modules. After reading, these measurements are sent to the "Scaling" subprogram to scale of analog current measurements to their physical responses.

"Initializer" program prepares the results for logging text files both of raw and analyzed results. The program creates two text files on the hard disk and writes the columns' titles to both result text files. According to the chosen channels on NI 9214 and NI 9203 for measurements of temperature and pressure, this subprogram detects which channels are in use and prepares control arrays and columns titles for the result text files. The main control cluster of the main program is created by this subprogram.

"Monitoring" subprogram is responsible to prepare the results to monitor on the main program screen in waveform charts. After monitoring all results on the screen, these results are transferred to the record subprogram.

"Record" subprogram simultaneously records the acquired raw data and analyzed results separately in two different text files. Raw data text file includes temperatures and currents data acquired from thermocouples, pressure transducers, anemometer, and the mass flow meter.

The "Read R600a properties" and "Analyze" subprograms are explained in the following sections.

3.7.1. Read R600a Properties Subprogram

Having finished acquiring and scaling processes, temperature and pressure data are sent to "Read R600a properties" subprogram. R600a properties are provided by Refprop v7.0 (Lemmon et al., 2007) as in two tables, one of them includes saturated R600a properties, and the other includes subcooled-superheated R600a properties. This

subprogram includes a subroutine that is capable of finding saturated temperatures and pressures, saturated liquid and vapor densities (df, dg), enthalpies (hf, hg), and entropies (sf, sg) of R600a for a given pressure, and it calculates density, enthalpy, and entropy (d, h, s) of R600a for a given temperature and pressure by means of look-up table method. The flow chart of this subprogram can be found in Figure 3.14. All data are kept in the memory and transferred to "Analyze" subprogram.
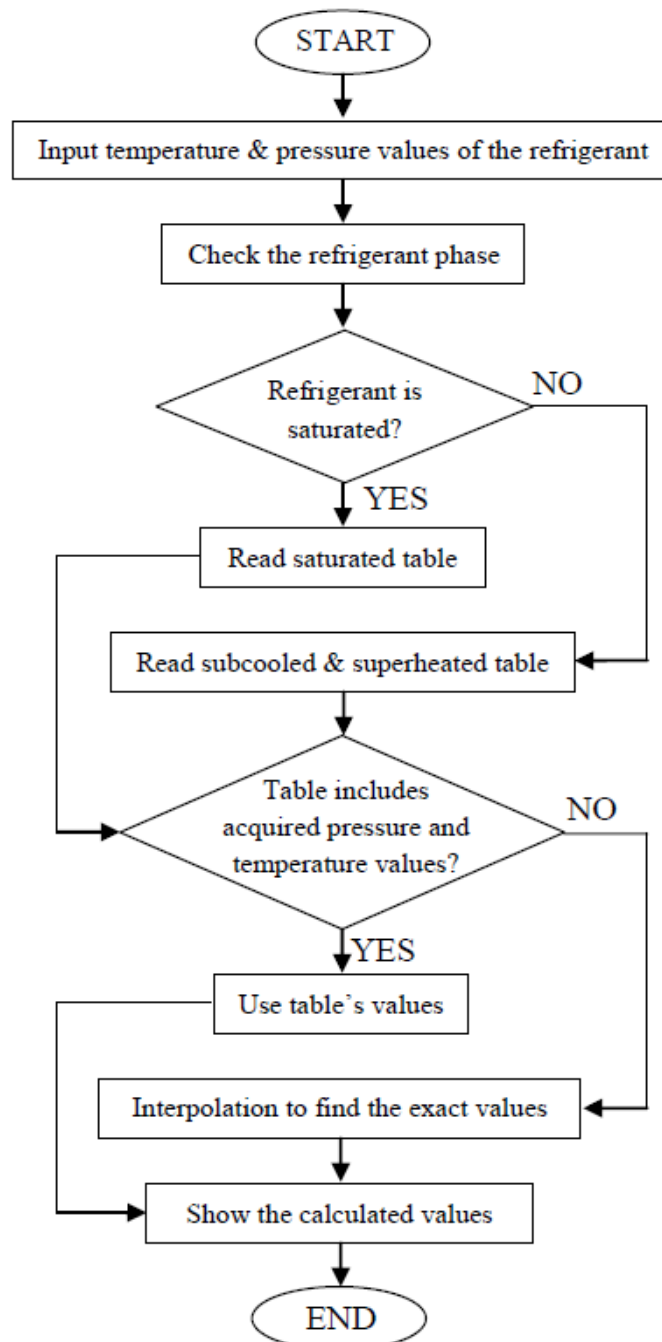

Figure 3.14. Flow chart of "Read R600a properties" subprogram

As noted in the preceding paragraph, the program reads R600a properties from two different tables due to the phase of the refrigerant. For readings from saturated property table, the program searches the refrigerant pressure value in the table and uses corresponding properties to this value and if the table does not include the exact pressure value and its corresponding properties, the program interpolates the nearest lower and greater thermophysical properties and find the exact value. The similar approach is used for readings from subcooled-superheat R600a property table; however, interpolations with property values in this table are dealt with carefully in order to find the exact values due to the refrigerant phase. For instance, when the refrigerant is in the subcooled state for measured pressure and temperature, and the subcooled-superheated table does not include the exact pressure and temperature values, it is possible to do interpolation with the nearest lower value is in superheated state and the nearest greater value is in the subcooled state. This condition leads to calculate the refrigerant property incorrectly and representation of it is given on a P-h diagram below in Figure 3.15.
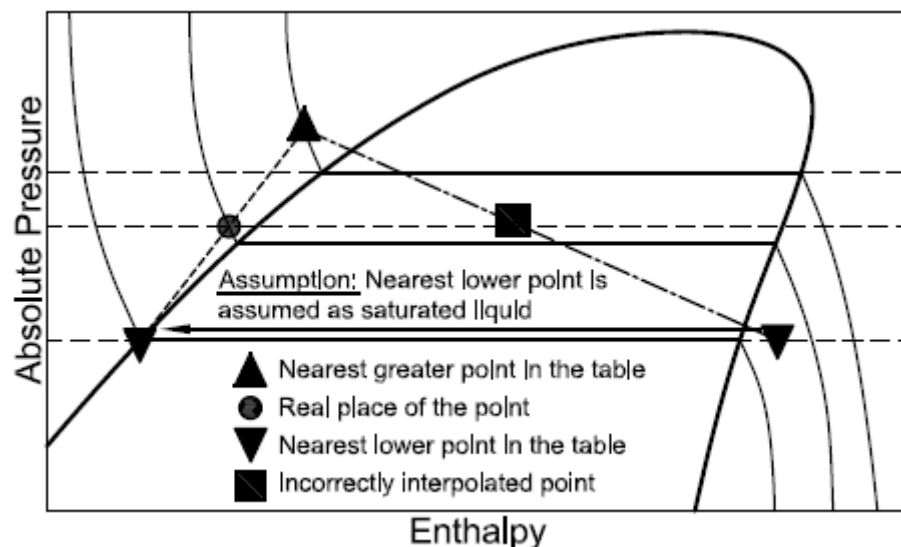

Figure 3.15. Interpolation problem with R600a properties in subcooled phase

It is a rarely situation but, especially, when the pressure and temperature of the refrigerant is close to the saturated state properties, it is possible to come across the nearest lower and greater points' states in different phases. When the refrigerant in subcooled state, it is possible to interpolate the properties of the nearest lower point in superheated phase and the nearest greater point in subcooled phase and similarly, when the refrigerant is in superheated phase, it is possible to interpolate the properties of the nearest lower point in superheated and the nearest greater point is in subcooled phase.

Once these conditions are encountered, to calculate R600a properties properly, for the first condition, while the refrigerant in subcooled phase, the nearest lower point's saturated properties, in the same manner, for the second condition, while the refrigerant in superheated phase, the nearest higher point's saturated properties are used in interpolations to find correct property values. The second condition is schematized in Figure 3.16.
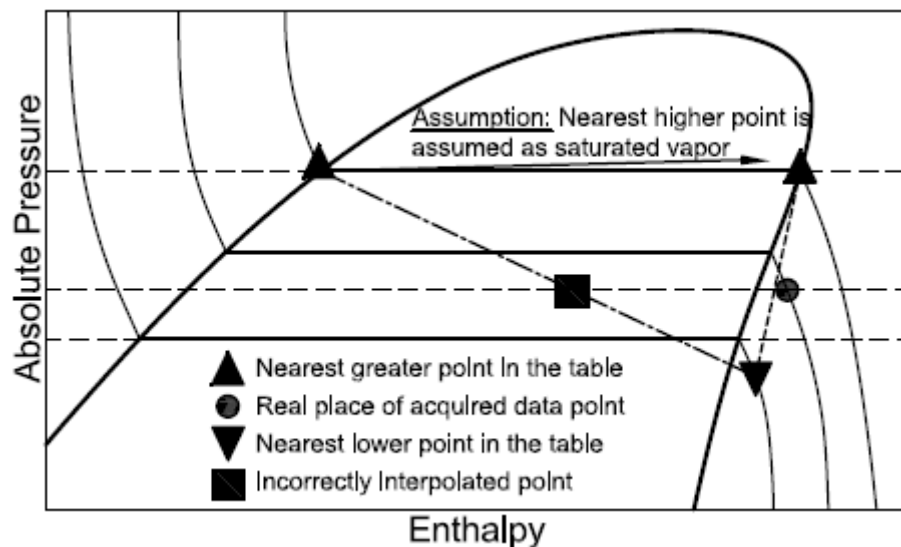

Figure 3.16. Interpolation problem with R600a properties in superheated phase

This approach results are really close to the results of Refprop values and the errors of density, enthalpy, and entropy properties by this approach are calculated. It is found that for the first and second approaches, the maximum relative errors in density, enthalpy, and entropy properties are 0.002%, 0.002%, 0.003%, and 0.02%, 0.001%, 0.02%, respectively, in the pressure range between 0.2 and 17 bar.

3.7.2. Analysis Subprogram

All analyses of the refrigeration cycle are carried out by this subprogram. To observe the refrigeration cycle performance during the tests, the subprogram creates a P-h diagram of the cycle according to analyses. In this section performance parameters and calculations of the refrigeration cycle are explained in a detailed way.

The refrigeration cycle of the experimental set-up is shown on a P-h diagram in Figure 3.18. Main performance characteristics of the cycle are given on the diagram,

which are cooling capacity, compressor work, and rejected heat from the condenser. It is assumed on the diagram that the heat transfer from the capillary tube to the suction line decreases the enthalpy of the refrigerant with the amount of transferred heat at the inlet of the evaporator and it is shown as Δh_{slhx} between points 6 and 1. In this diagram, enthalpy differences between points 2-1, 4-5, and 5-6, respectively, represent the cooling capacity (refrigerating effect), work inlet to the compressor, and rejected heat from the condenser for unit mass of refrigerant. The rejected heat from the hot gas tube is shown between points 5 and 4.
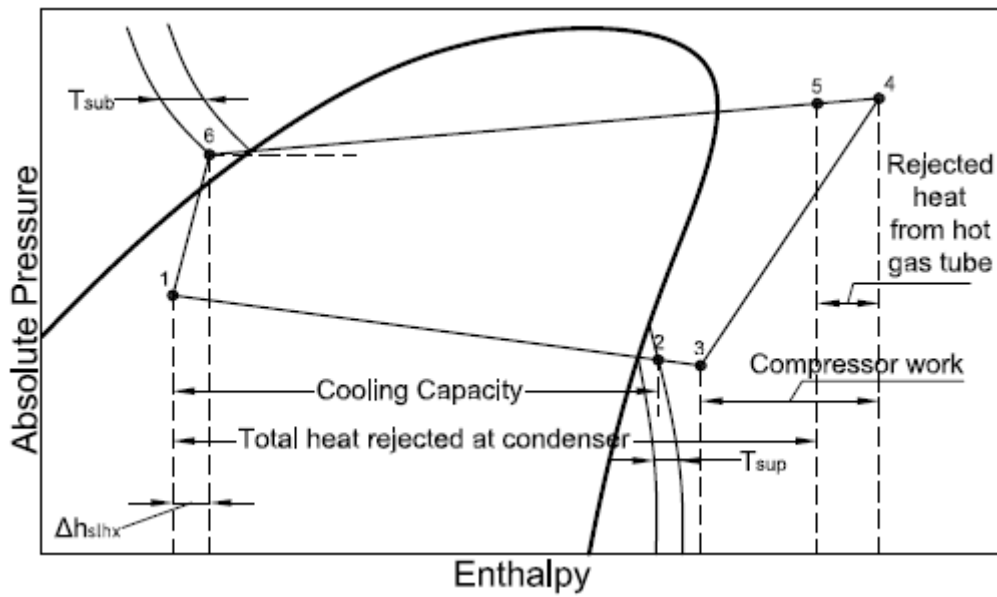

Figure 3.17. Performance characteristics of the household refrigerator on P-h diagram

Regarding the Figure 3.17, the cooling capacity can be written as

$$\dot{Q}_e = \dot{m}\Delta h_e = \dot{m}(h_o - h_i)_e \qquad (3.5)$$

where $\dot{Q}_e$ is the cooling capacity, $\dot{m}$ is the refrigerant mass flow rate, and Δh_e is the enthalpy difference between the evaporator inlet and outlet, subscripts "e", "i", and "o" represent the evaporator, the inlet and the outlet of the component. The net work inlet to the compressor, $\dot{W}$, is

$$\dot{W} = \dot{m}\Delta h_{comp} = \dot{m}(h_o - h_i)_{comp} \qquad (3.6)$$

43

where subscript "comp" represent the compressor. The rejected heat from the condenser between point 5 and 6, $\dot{Q}_c$, is

$$\dot{Q}_c = \dot{m}\Delta h_c = \dot{m}(h_o - h_i)_c \tag{3.7}$$

where subscript "c" represents the condenser.

The rejected heat from the hot gas tube from the surrounding between point 4 and 5, $\dot{Q}_h$, is

$$\dot{Q}_h = \dot{m}\Delta h_h = \dot{m}(h_o - h_i)_h \tag{3.8}$$

where subscript "h" represents the hot gas tube.

In the refrigeration cycle of the experimental set-up, SLHX is utilized and Eq. (1.4) is not valid for actual cycles because the heat transfer rate from capillary tube to the suction line is not as small as in ideal cycle to be neglected. SLHX leads to decrease of enthalpy of the refrigerant by heat transfer between the capillary tube and the suction line during the expansion process. Hence, the expansion process of an actual refrigeration cycle with SLHX is not isenthalpic like in ideal refrigeration cycle. Assuming no heat loss to the surroundings is in SLHX, the energy change in the capillary tube becomes equal to the enthalpy change of the suction line during the expansion process. It yields

$$\Delta h_{cap} \neq 0 \rightarrow \Delta h_{cap} = \Delta h_{slhx} = (h_o - h_i)_{slhx} \tag{3.9}$$

where "slhx" subscript represents the capillary tube-suction line heat exchanger.

Decrease of refrigerant enthalpy in the SLHX also causes to decrease the refrigerant enthalpy at the inlet of the evaporator. Hence, the inlet enthalpy of the evaporator decreases as the change of enthalpy as in SLHX. Hence, it yields the enthalpy of the refrigerant at the inlet of the evaporator

$$(h_i)_e = (h_i)_c - \Delta h_{slhx} \tag{3.10}$$

To find the mass flow rate of the refrigerant during the operation in steady state conditions, following equation is used

$$\dot{m} = \rho \dot{V} \tag{3.11}$$

where ρ is the refrigerant density, and $\dot{V}$ is the volumetric flow rate of the refrigerant. The volumetric flow rate of the refrigerant is calculated with the knowledge of the compressor's piston geometry and displacement. It yields

$$\dot{V}_{comp} = V_p \times \frac{N}{60} = \frac{\pi \times B^2 \times S \times n}{4} \times \frac{N}{60} \tag{3.12}$$

where V_p is the piston displacement volume in m³, B is the bore (the diameter) of the cylinder in m, S is the length of stroke in m, N is the revolution of the crankshaft per minute, and n is the number of pistons.

In ideal cycle, the compression process is an adiabatic process and the compressor is assumed 100% efficient. Unfortunately, in actual refrigeration cycle; this is not the case, the compression process is not adiabatic as in ideal one and it is not 100% efficient due to the irreversibilities. Hence, Eq. (3.12) is not valid for actual cycles. To find the mass flow rate of the refrigerant for actual cycles, volumetric efficiency of the compressor needs to be defined. Due to the mechanical clearance between the piston and the valve plate of the compressor, the suction vapor does not fill the cylinder volume of the compressor completely. Besides, valve and piston leakage, cylinder heating, and wiredrawing affect the volumetric efficiency of the compressor. The volumetric efficiency is defined as

$$\eta_v = \frac{V_a}{V_p} \times 100 \tag{3.13}$$

where η_v is the total volumetric efficiency, V_a is the actual volume of the compressed suction vapor in m³. Hence, Eq. (3.13) yields the actual vapor volume as

$$V_a = \frac{\eta_v V_p}{100} \tag{3.14}$$

Therefore, the volumetric flow rate of the actual cycle becomes in this form

$$\dot{V}_a = \frac{\eta_v V_p}{100} \times \frac{N}{60} = \frac{\eta_v}{100} \times \frac{\pi \times B^2 \times S \times n}{4} \times \frac{N}{60} \tag{3.15}$$

where $\dot{V}_a$ is the volumetric flow rate of the actual cycle in m³/s.

According to the Eqs. from (3.13) to (3.15) and the compressor specifications, which are given in Table 1.2, the volumetric flow rate of the test refrigerator is

$$\dot{V}_a = \frac{78.6}{100} \times \frac{\pi \times 0.026^2 \times 0.0115 \times 2}{4} \times \frac{3000}{60} = 4.79 \times 10^{-4} \text{ m}^3\text{/s} \tag{3.16}$$

During the tests, the density of the refrigerant is calculated depending to the temperature and pressure, hence, the actual mass flow rate of the refrigerant becomes

$$\dot{m}_a = \rho(T,P)\dot{V}_a \tag{3.17}$$

where subscript "a" represents the actual process.

The thermal work inlet to the compressor, $\dot{W}_t$, is

$$\dot{W}_t = \dot{m}_a \Delta h_{comp} = \dot{m}_a (h_o - h_i)_{comp} \tag{3.18}$$

where subscript "comp" represent the compressor. To find the consumed total energy, $\dot{W}$, by the compressor, the mechanical efficiency of it has to be multiplied to the Eq. (3.18), it yields

$$\dot{W} = \eta_m \dot{m}_a \Delta h_{comp} = \eta_m \dot{m}_a (h_o - h_i)_{comp} \tag{3.19}$$

where η_m is the mechanical efficiency of the compressor.

To calculate the overall COP of the refrigeration cycle, Eq. (3.20) below is applied.

$$COP = \frac{\dot{Q}_e}{\dot{W}} \tag{3.20}$$

Applying the conservation of mass principle and the 1st law of Thermodynamics for steady state conditions

$$\dot{m}_i - \dot{m}_o = \Delta\dot{m}_{sys} \rightarrow \Delta\dot{m}_{sys} = 0 \rightarrow \dot{m}_i = \dot{m}_o \qquad (3.21)$$

$$\dot{E}_i - \dot{E}_o = \Delta\dot{E}_{sys} \rightarrow \Delta\dot{E}_{sys} = 0 \rightarrow \dot{E}_i = \dot{E}_o \qquad (3.22)$$

where $\dot{E}$, and subscripts "sys" represent the energy rate and system, respectively. The kinetic and potential energy changes of refrigerants are usually small relative to the work and heat transfer in the system; therefore, these energies can be neglected. The evaporator, the condenser, the hot gas tube, and the capillary tube-suction line heat exchanger do not have any work interaction on the system (Çengel & Boles, 2005). The heat transfer occurs in the capillary tube-suction line heat exchanger is treated as an internal regeneration in the system and its effect is added to the heat transfer of the evaporator (cooling capacity) (Ors, 2006). Regarding the entire system assuming that there are no heat losses from pipe and tubes to the surroundings, energy balance becomes

$$\dot{Q}_e + \dot{W} = \dot{Q}_h + \dot{Q}_c \qquad (3.23)$$

Beyond these calculations, subcooling temperature, T_{sub}, and superheating temperature, $T_{\sup}$, are calculated by this program. They are defined as

$$T_{sub} = \left(T_{sat,o}\right)_c - \left(T_o\right)_c \qquad (3.24)$$

$$T_{\sup} = \left(T_o\right)_e - \left(T_{sat,o}\right)_e \qquad (3.25)$$

where subscripts "sub", "sup", and "sat" represent subcooling, superheating, and saturated, respectively.

All assumptions that are utilized in the calculations of performance of test refrigerators are:

- All heat exchangers tube is thin-walled and the refrigerant temperature is assumed that it is equal to tube wall temperature.

- The condenser inlet pressure is equal to the compressor outlet pressure.
- Expansion process is assumed as totally non-adiabatic, hence, the enthalpy of the refrigerant is reduced from the inlet to the outlet of it
- SLHX pressure is assumed as the same as the evaporator outlet pressure.
- There is no pressure drop in SLHX.
- Once the refrigerant at the exits of the evaporator and the condenser is in two-phase (which is a rarely situation), it is assumed as saturated vapor at the exit of the evaporator and as saturated liquid at the exit of the condenser.
- The air is assumed incompressible and totally dry-air in heat transfer calculations of air side, and also specific heat of it is assumed constant.

The "Analysis" subprogram is responsible for all calculations shown above and according to these calculations; it prepares an online P-h diagram to observe the cycle performance. The experimental set-up analysis interface of the software is shown in Figure 3.18.
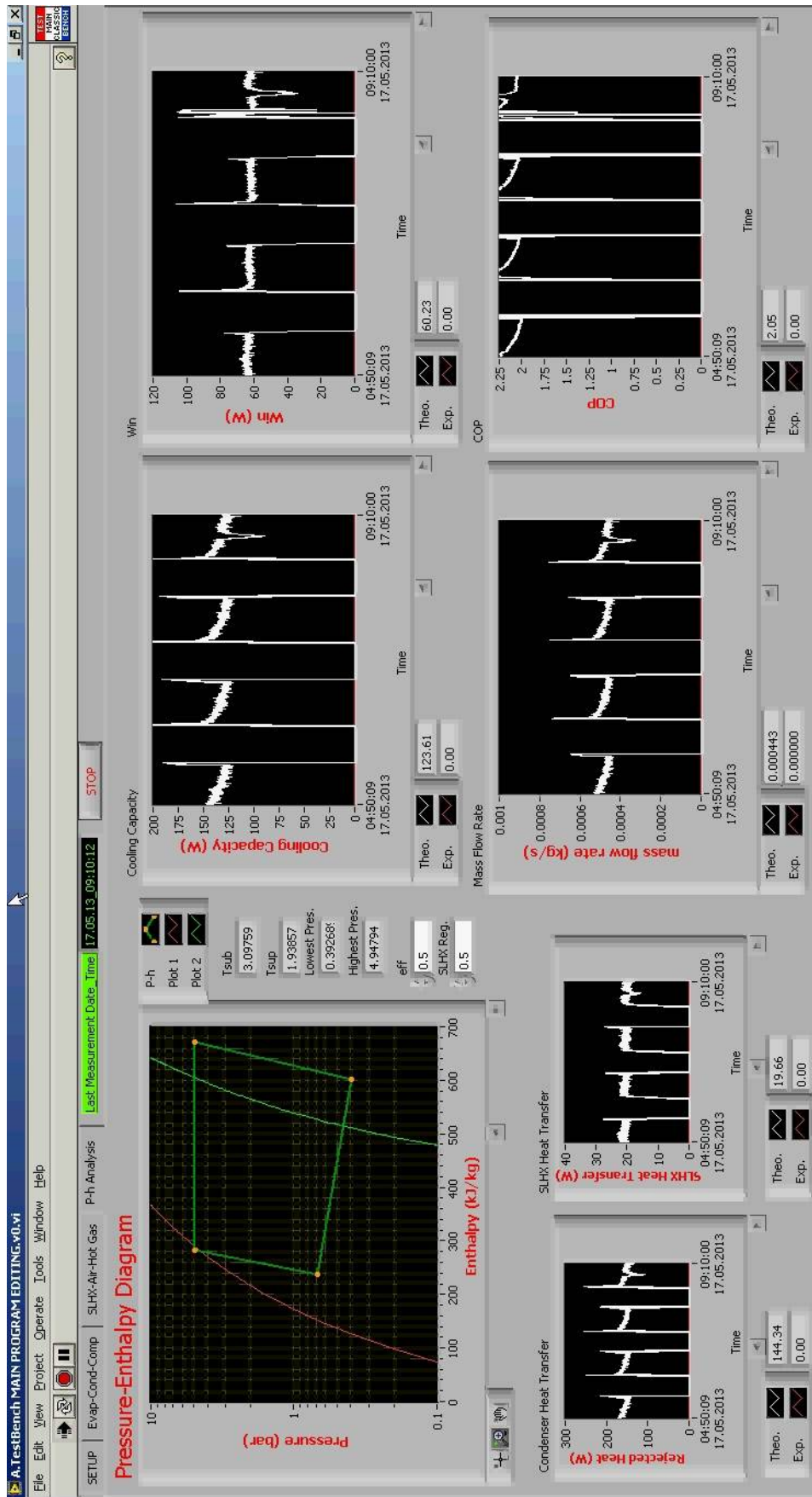
Figure 3.18. Test program analysis interface

49

3.8. Test Procedure

In the scope of this study, EC tests are conducted in accordance with ISO 15502. Energy consumed by the test refrigerator is calculated over a period of 24h. According to ISO 15502, the test refrigerator studied in this thesis is an extended temperature, "SN", type and these type refrigerators energy consumptions tests must be carried out under the condition of ambient whose temperature is 25°C and relative humidity is less than 75%. The ambient temperatures must be kept constant within $\pm$ 0.5 K both during the tests and during the periods required for obtaining for steady state operating conditions. To maintain the required ambient conditions for energy consumption tests, an air chamber in which the temperature and the humidity are adjusted automatically and kept ambient conditions stationary.

The refrigerating appliance should be placed on a wooden solid-top platform painted by black and open for free air circulation under the platform. The bottom of the platform must be at least 0.05 m higher than that of the test room floor and the distance must not exceed 0.3 m. The refrigeration appliance should be surrounded by three vertical partition made of wood, 16 to 30 mm thick, to limit the air circulation around the refrigerating appliance as shown in Figure 3.19 below. The air circulation of the test room should not interfere with the air circulation created by the test refrigerator.
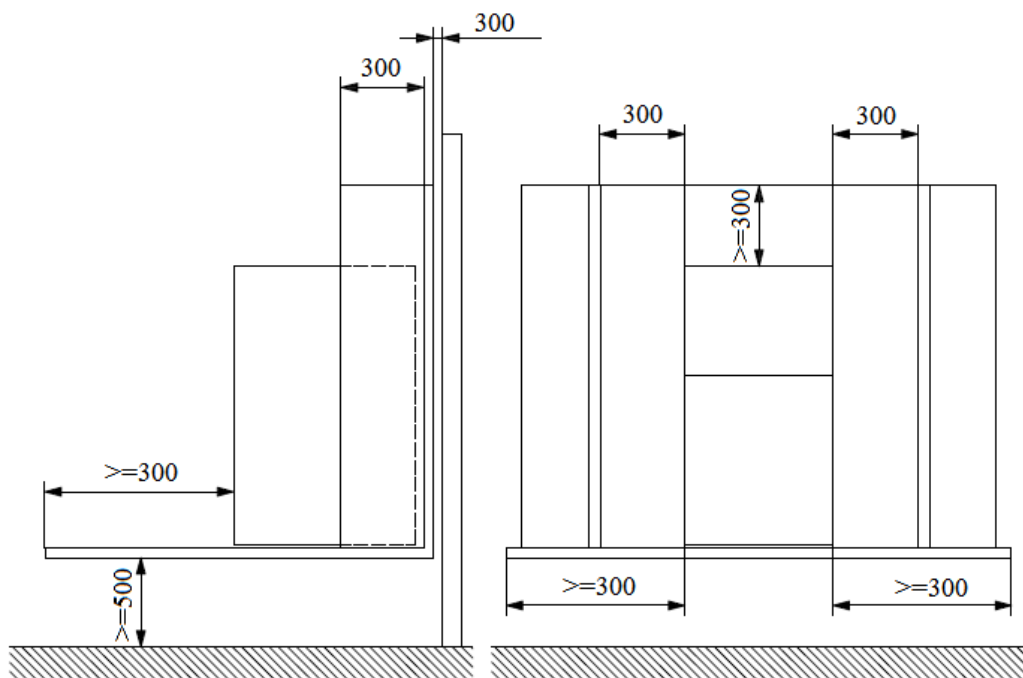

Figure 3.19. Test refrigerator placement in test room (dimensions are in mm)

The fresh-food compartment is empty and the freezer compartment of the test refrigerator is filled with rectangular prism shaped test packages which are used as load in the freezer compartment of the test refrigerator during EC test. Test packages thermal characteristics should correspond to thermal characteristics of lean beef. The suggested content of the tests packages by ISO 15502 is given in Table 3.7. Some of those packages are equipped with thermocouples contacting the test package material directly at the geometrical centers of them to measure the temperature. These test packages equipped with thermocouples are also called as M-packages.

Table 3.7. Test package content and its properties
(Source: ISO 15502, 2005)

CONTENT		PROPERTIES	
Oxyethylmethylcellulose	230 gr	Density	940 kg/m^3
Water	764.2 gr	Specific Heat (Cp)	2000 J/kgK
Sodium Chloride	5 gr	Conductivity	45 W/mK
6-Cloro-m-cresol	0.8 gr	Freezing Temperature	-1°C

The loading plan of test packages in the freezer compartment is given in Figure 3.20. It should be noted that test packages have to be in contact with inner walls of the freezer and entire volume of the freezer needs to be filled with them. A column of test packages in one shelf must not contact with the neighboring test packages' column in order to ensure that the air circulation inside the freezer is not restricted. The storage plan of test and M-packages are shown in Figure 3.20. In the figure, M-packages are shown in red and numbered.

In the fresh-food compartment, air temperature measurements are taken from four different points by thermocouples of which are inserted in solid brass cylinders having a mass of 25 gr.± 5% and a minimum both diameter and height of 15.2 mm in accordance with ISO 15502. Three of them are located at the centers of each shelf and the other one is placed at the center of the crisper which is used for preservation of vegetables in household refrigerators. Thermocouples' placements in the fresh-food compartment are shown in Figure 3.2.

The refrigerator under test is set to keep the required temperatures of which the fresh-food and the freezer compartments to 4° and -18°C, respectively. During the test,

the power consumption and the temperature measurement are measured by data acquisition system. Measurements are taken once in every 60 seconds and recorded to determine the energy consumption of the refrigerator under the test. Along with the EC test, all measurements of each refrigerator's components are recorded in the scope of this thesis.
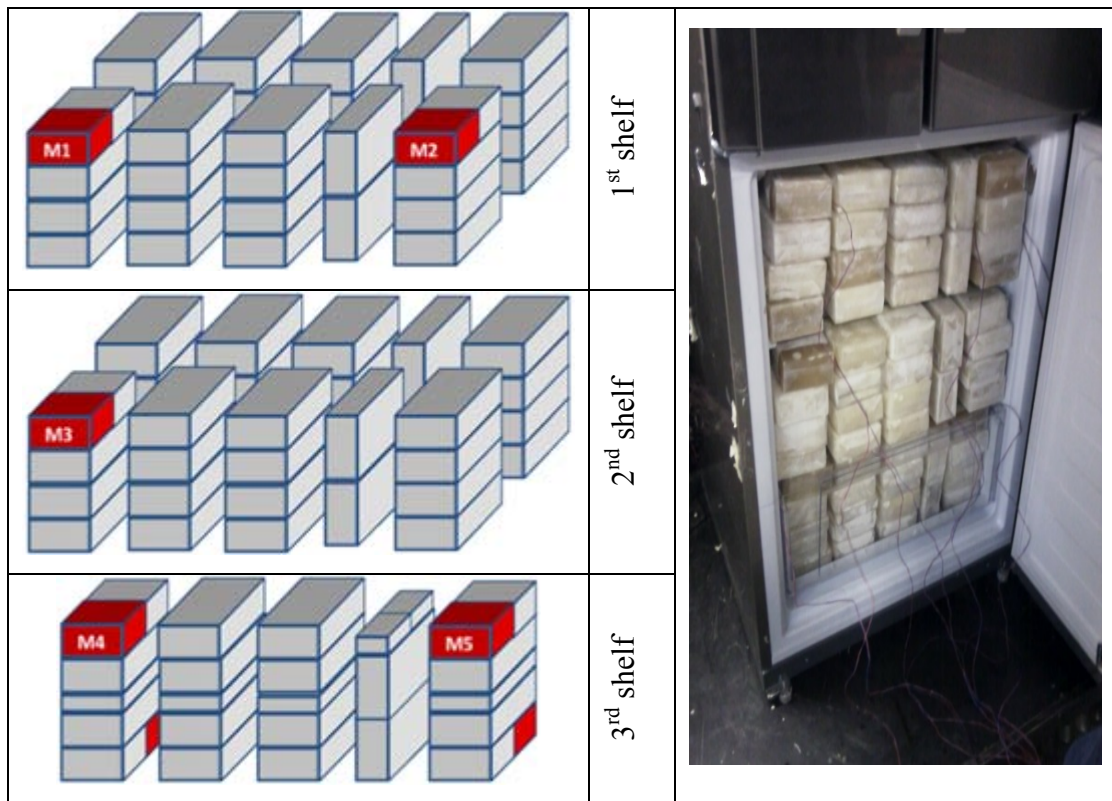

Figure 3.20. The storage plan of the test refrigerator

The EC test continues until the refrigerator under test reaches the steady state operating conditions. To determine the EC of the refrigerator, the power measurements between two defrost cycles are integrated over the time in which the first defrost cycle is included, but the second one is not. In Figure 3.21, the EC test time interval is shown on a graph. Evaporator inlet and M1 M-package's temperature and power consumption are plotted on the graph.
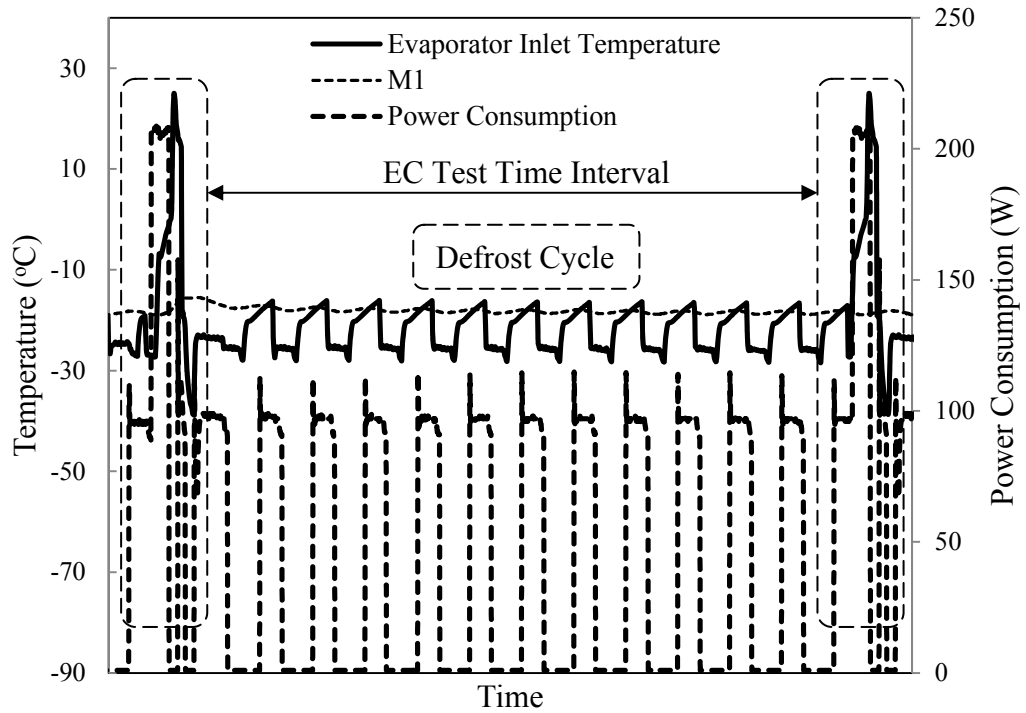
Figure 3.21. EC test measurement time interval

EC is calculated by integrating the power consumption over the EC test time interval for 24h which gives the EC of the refrigerator in kWh/24h.

$$Daily\ EC = \frac{Total\ Power\ Consumption\ \text{x}\ On\ Time\ \text{x}\ 24\ hours}{Total\ Operation\ Time}\text{(kWh/24h)} \qquad (3.26)$$

where the "power" term refers to the total power which is consumed by the test refrigerator during the energy consumption test interval 24 hours, in Joule, "on time" indicates the elapsed time in on cycles, in seconds, and "total operation time" indicates the elapsed time in which on and off cycles times are included, in seconds. The "power" term is equal to the area under the power consumption graph which is shown by hatched area in Figure 3.22, and can be expressed as

$$Total\ Power\ Consumption = \int_{t1}^{t2} Power\ Consumption\ dt \qquad (3.27)$$

where t_1 is the energy consumption test start time and t_2 is the EC test end time.
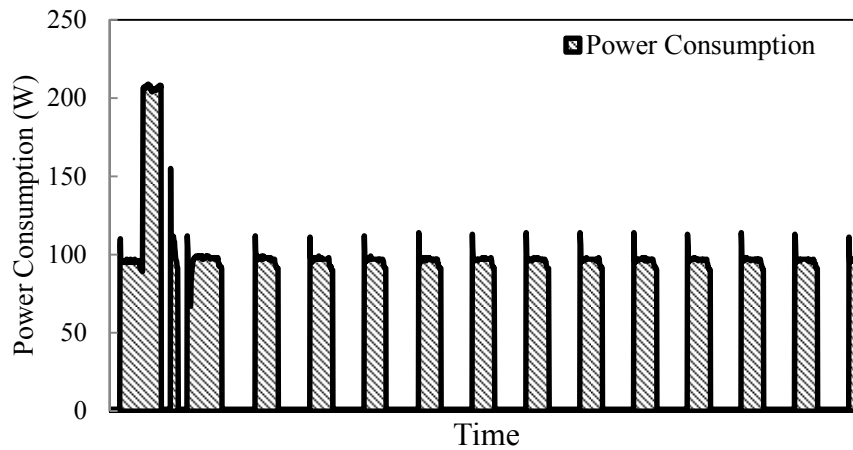
Figure 3.22. The area under the power consumption graph gives the power in Joule

To reveal the effects of the condenser length on the performance of the household refrigerator two additional tests were conducted on the test refrigerator. Two same types of condensers having different lengths were assembled to the test refrigerator sequentially and two tests were performed on the test refrigerator. The first modified condenser length is greater, contrary to this; the second one's length is less than the current one on the test refrigerator. As a modification on the first condenser, two coils are added to the end of the condenser by means of welding, whereas, two coils are removed from the end of the second condenser. Modifications on the condenser can be seen in Figure 3.23. After each modification, the refrigerators recharged with R600a and leak detections are done by both electronic and bubble methods. It should be noticed that for both two tests with modified condensers, the test refrigerator is charged with the same amount of refrigerant, 50 gr.

Modification region of two coils

Figure 3.23. The condenser and modification region

CHAPTER 4

RESULTS AND DISCUSSION

Four EC tests are conducted on the experimental set-up. The first EC test is conducted to obtain a reference point of the current test refrigerator and to validate experimental set-up program, and the rest of the tests are conducted on the same refrigerator with modified condenser's length to reveal the modifications effects on the test refrigerator and on the refrigeration cycle. After these tests are conducted, the on-off compressor is changed with a VSC to investigate VSC effects on the refrigeration cycle and the EC.

4.1. Results of the First EC Test (Reference Point)

The first EC test is conducted on the test refrigerator whose features are given in Chapter 1. Power consumption is measured by the air chamber's measurement system. The air stream inlet and outlet temperatures over the evaporator are not able to be measured in the first test.

For a better visualization, the measurements and analysis results for the test refrigerator are given in three on-off cycles which are included by EC test interval below. In all plots, "i" and "o" subscripts represent the inlet and the outlet of each component, respectively.
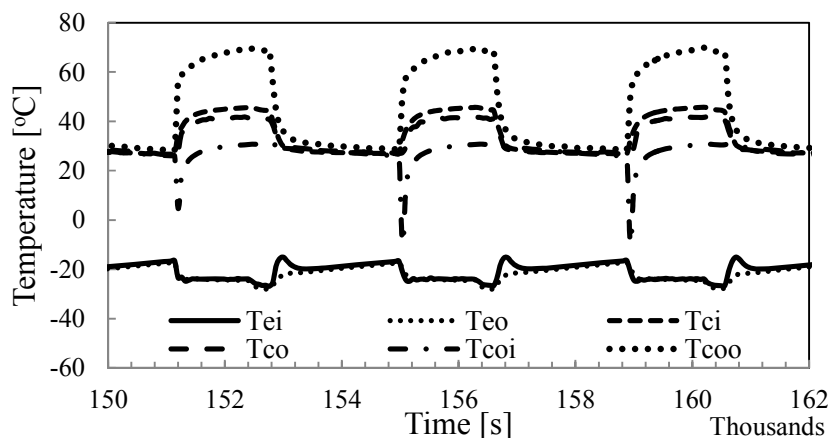
Figure 4.1. Temperature measurements from inlets and outlets of each component
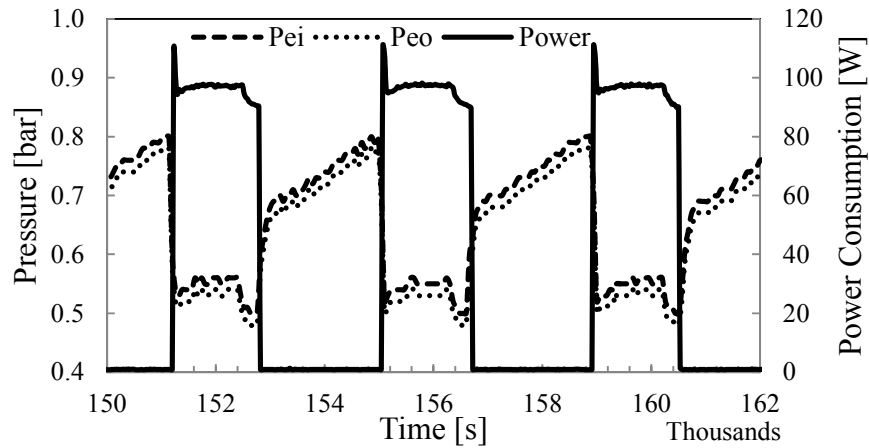
Figure 4.2. Pressure at the inlet and the outlet of the evaporator and power consumption

It is found that the average instantaneous power consumption including only on-cycles is **97 W** and the average total power consumption including both on- and off-periods along the 24h, which is also known as "energy efficiency index, EEI", is **42 W**. According to average total power consumption, as it was mentioned in Chapter 1, the test refrigerator is in A+ energy class. The daily EC of the test refrigerator according to ISO 15502 is calculated by using Eq. (3.26), it yields that the EC of the first refrigerator is **1.03 kWh/24h**. The defrost cycle effect on the EC of the refrigerator is calculated and it is found that defrost cycle increases the EC by **3.8%**.

As it was mentioned in Chapter 3, heat transfer from or to all components of the refrigeration cycle are investigated experimentally. Figures from Figure 4.3 to Figure 4.8 cover the all refrigeration cycle performance characteristics.
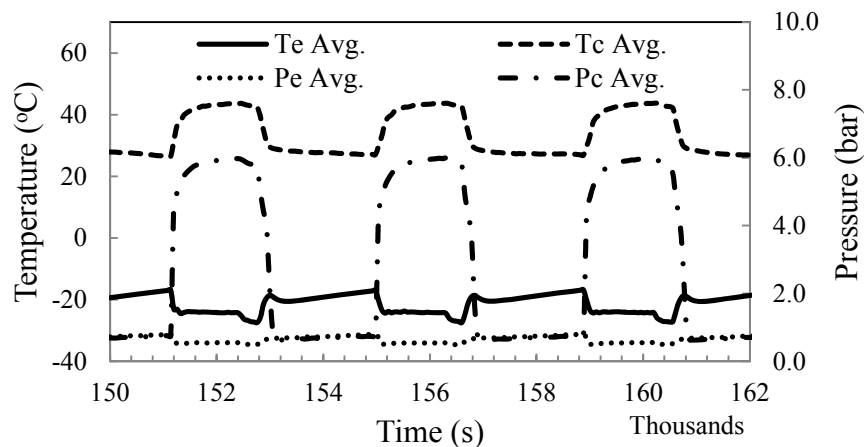
Figure 4.3. Average temperatures and pressures of evaporation and condensation

57

As it is seen in Figure 4.3, the average evaporation and condensation temperatures and pressures are **-24.7°**, **42.3°C**, and **0.53**, **5.78 bar**, respectively.
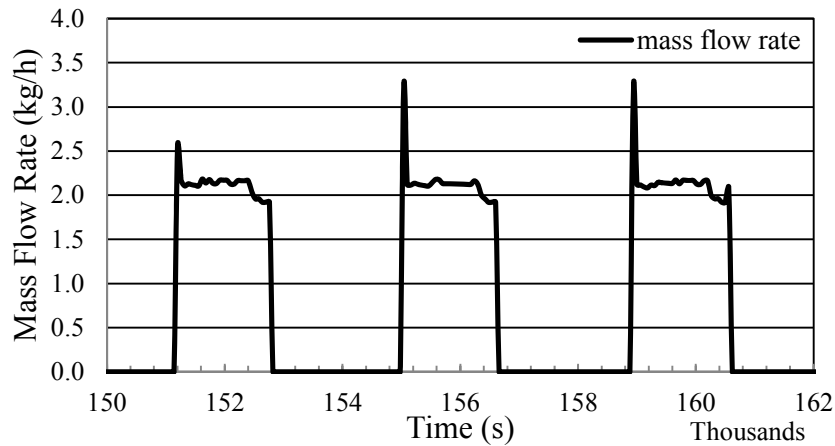

Figure 4.4. Mass flow rate of the refrigerant

As explained in Chapter 3, the mass flow rate of the refrigerant is calculated with the help of displacement volume and volumetric efficiency of the compressor. The average mass flow rate of the R600a is found as **2.10 kg/h**, **5.84×10^{-4} kg/s**.
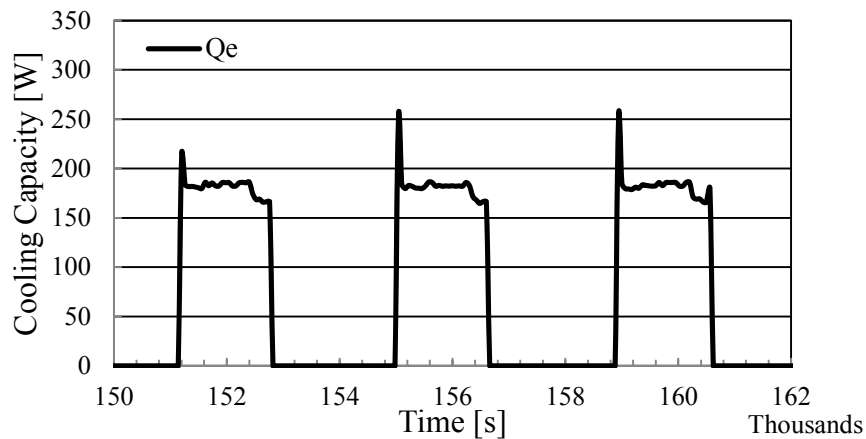

Figure 4.5. Cooling capacity and evaporation temperature and pressure

The cooling capacity of the refrigerator is calculated by Eq. (3.5). The average cooling capacity as shown in Figure 4.5 is **180.14 W**.

The other performance characteristics of the refrigerator, rejected heat transfers from the condenser and the hot gas tube side and the heat transfer of SLHX are given in between Figure 4.6 and Figure 4.8.
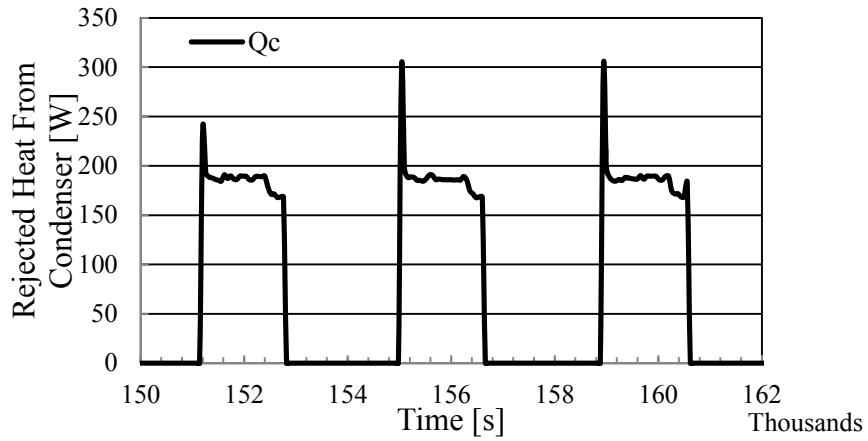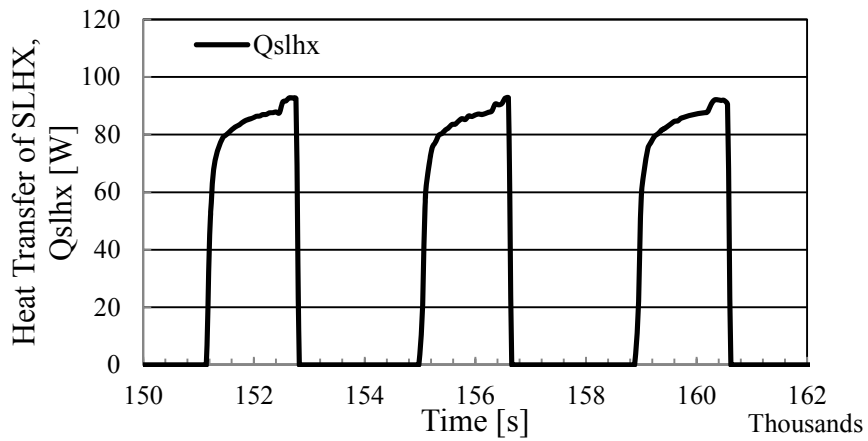
Figure 4.6. Rejected heat from the condenser

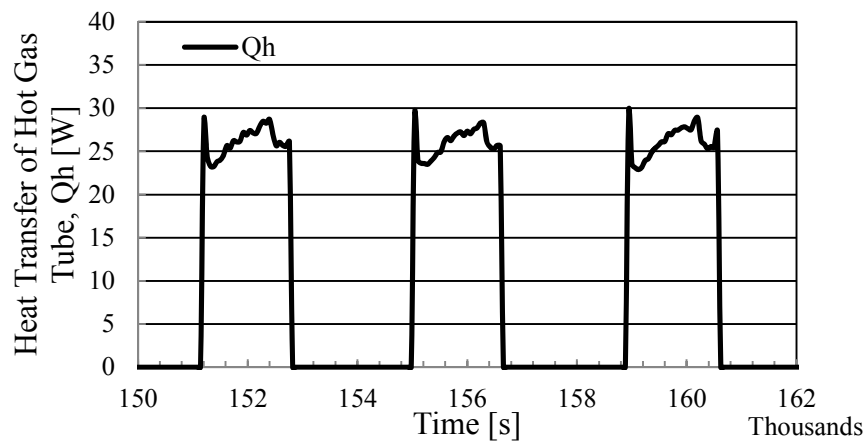Figure 4.7. Heat transfer occurs in capillary tube-suction line heat exchanger (SLHX)

Figure 4.8. Heat transfer from hot gas tube to the surroundings

The measured power consumptions by air chamber (test room) and the calculated one by the test set-up is compared in Figure 4.9. In the figure, thermal power

is calculated by use of Eq. (3.19). It should be noted that the power consumption graph by experimental set-up has an increasing trend at start of the on-cycle. This is resulted from conduction errors of tubes on which temperature measurements are taken. However, as it is seen in the figure below, the results are too close to each other. There are not observed any error in calculated power consumption higher than 10%.
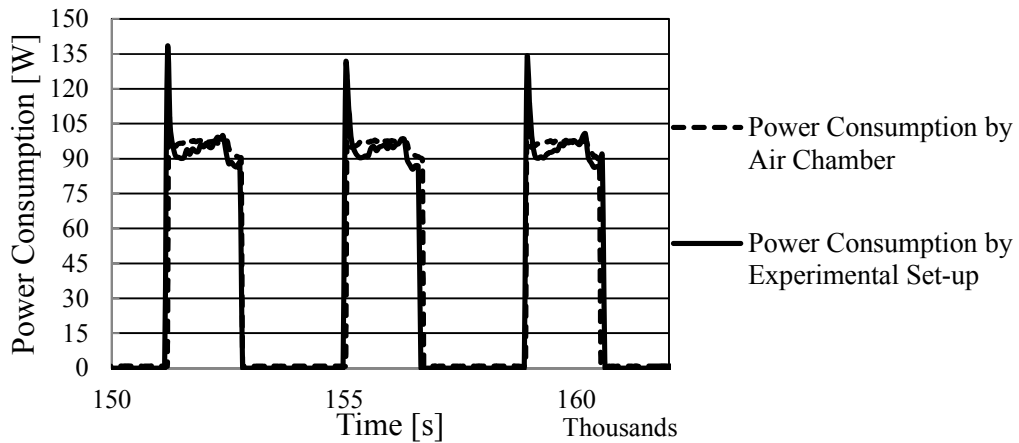

Figure 4.9. Comparison of power consumption calculation with the device measurement

Pressure ratio of condensation to evaporation (Pc/Pe) is an important performance indicator for refrigeration cycles. The lower ratio indicates the higher efficiency due to the lower work inlet to the system relevant to refrigeration cycles having higher pressure ratios. The pressure ratio and the COPs calculated with power consumptions experimentally and theoretically of the refrigeration cycle are given in Figure 4.10.
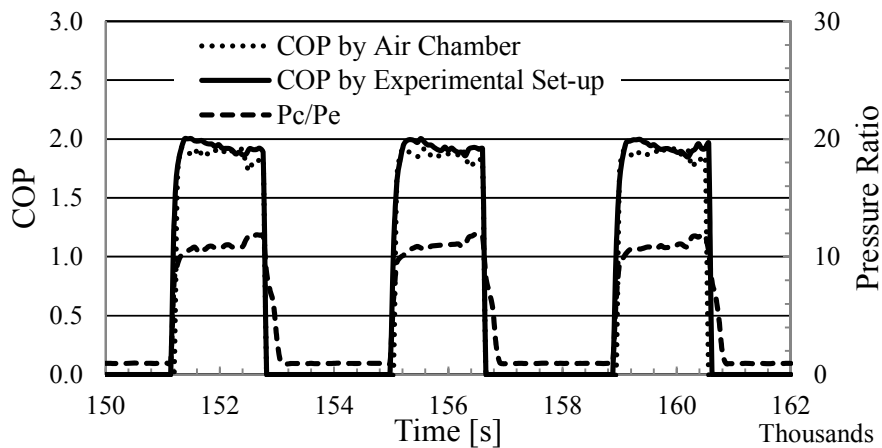

Figure 4.10. Pressure ratio and the COP of the test refrigerator

As mentioned in Chapter 3, both compartments' temperatures are measured during the test. It is observed that the warmest M-package is the M2 and its temperature varies between -15.8° and -20.2°C with the average of -18°C. Average temperature measurements from three shelves and one crisper in the fresh-compartment are, respectively, 6.1°, 4.7°, 6°, and 6.5°C.

To verify the test results and assumptions, first law of thermodynamics, conservation of energy equation is applied to the results and verifications of results are represented by graphs below. It is important to note that in the test, subcooling and superheating temperatures are all greater than zero in steady state operation conditions, which means the refrigerant is in single phase at the outlet of the condenser and that of the evaporator and this condition guarantees the enthalpy calculations are available with the knowledge of temperature and pressure at these locations and makes each component be investigated separately in terms of energy balance. In steady state conditions, energy change of the system must be zero, however, this trend cannot be caught always by experimental set-ups due to the errors of measurements and calculations. In Figure 4.11, the energy balance deviation of experimental results is shown for three on-cycles.
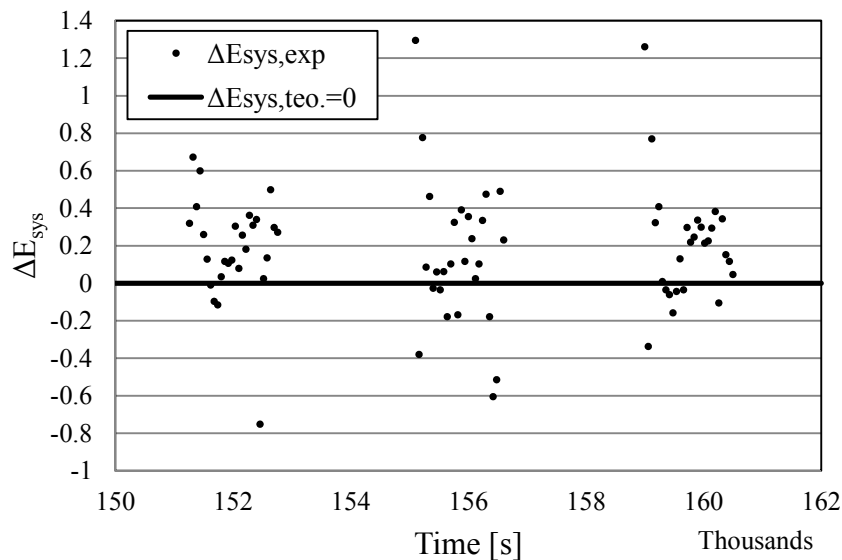

Figure 4.11. Energy balance deviation for the first EC test

Regarding these results shown in Figure 4.11, the maximum deviations are seen in the second and third on cycles and both of them are close to the 1.4 Watt.

Verification of the system may also be represented by relative errors in terms of energy balance. In this case, relative error can be expressed as in Eq. (4.1).

$$\varepsilon\% = \left(\frac{\left| \dot{E}_i - \dot{E}_o \right|}{\dot{E}_i} \right) \times 100 \tag{4.1}$$

Eq. (4.1) is applied to experimental calculated energies at the inlet and the outlet of the control volumes and results are represented by graph in Figure 4.12 for three on-cycles. According to the results, it is seen that the maximum error in calculations of control volume energy is close to the 0.6 %. Regarding these results, it can be said that the experimental set-up values are in consistent range in terms of engineering applications.
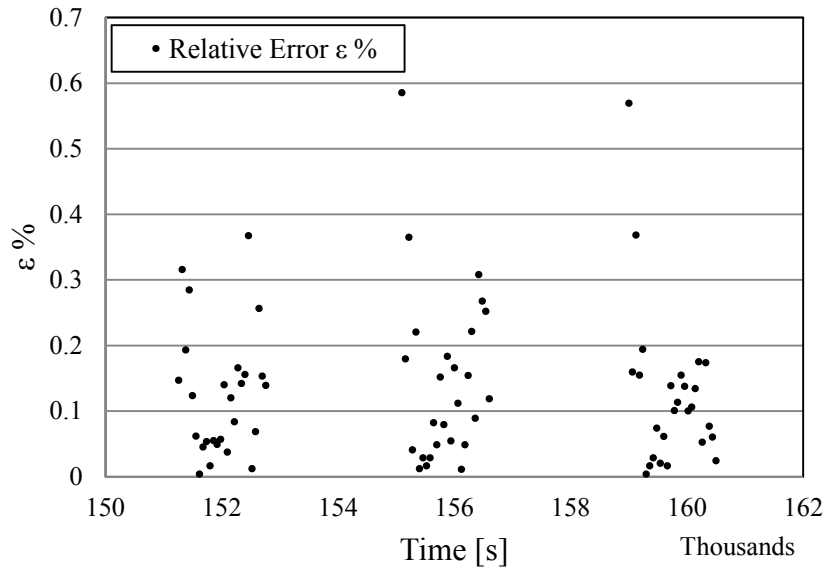

Figure 4.12. Relative errors in energy balance

It can be seen from both Figure 4.11 and Figure 4.12 that the biggest deviations are observed at the startup of the cycles. The main reason of it is the refrigerant maldistribution during off-cycle period and the transition period from off-cycle to on-cycle. When the refrigerator switches from on-cycle to off-cycle, the refrigerant starts to accumulate from high pressurized regions to low pressurized ones until the pressure equalization in the entire system achieved. During this period, the great amount of the refrigerant is collected in the evaporator. Once the system restarts the refrigerant in the evaporator does not start to evaporate immediately and for a while the system works for

evaporating the refrigerant in the evaporator. This causes the evaporator temperature and pressure to decrease sharply below the operation levels. Following this, the required mass flow rate cannot be provided to the system and, as a consequence, cyclic losses occur.

As a second method to verify the refrigerant side calculations, the calculated cooling capacity by the refrigerant side can be compared to air side heat transfer through the evaporator. However, for this test, the air stream temperatures over the evaporator were not able to be measured due to the limited number of channels on the data acquisition system. Comparison of cooling capacities by the refrigerant and the air sides were investigated for the following two EC tests.

The following two tests were conducted to reveal the effects of the condenser length on the household refrigerator performance, as .explained in the previous chapter.

4.2. Results of the Second EC Test – Two Coils Extended Condenser

This test is conducted on the same refrigerator with only one modification on the condenser on it. As the modification, the current condenser is extended with two coils at the end of it. The main aim of this modification is to simulate the subcooling effect on the overall performance of the refrigeration cycle. The same test procedure as in the first test is followed for this test. Additionally, air stream temperatures over the evaporator are measured and cooling capacity of the air side is calculated and compared that of the refrigerant side. The test results are given in figures below for this case too in the same manner as in the reference test results in order to distinguish the greater length effect of the condenser. Three EC tests results are compared in the next section.
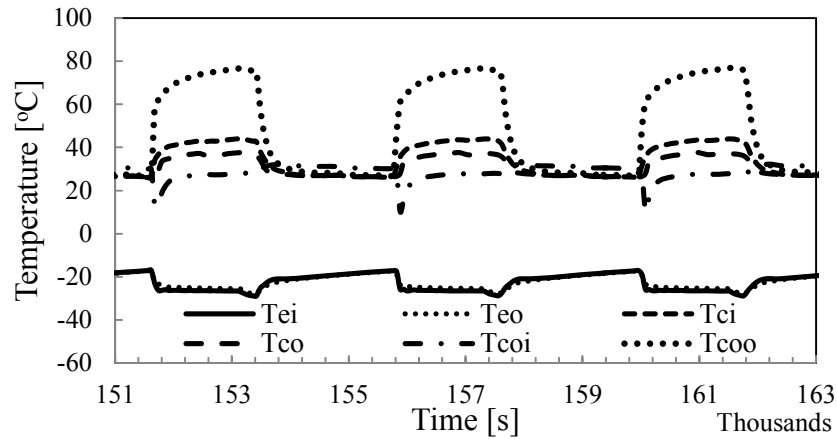
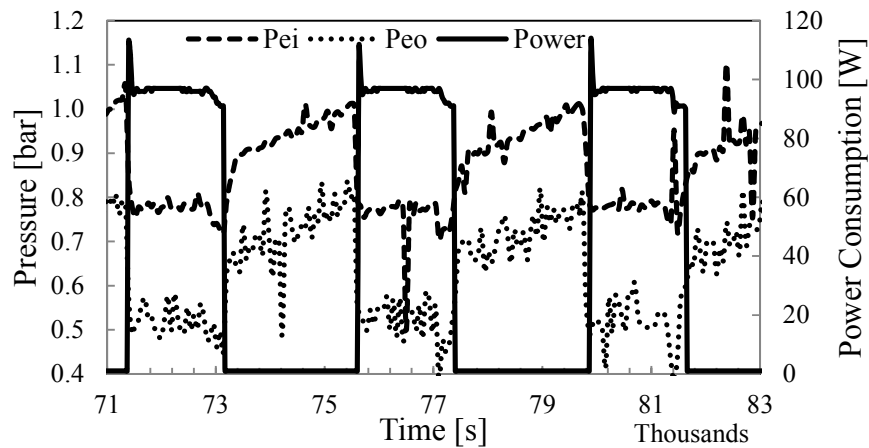Figure 4.13. Temperature measurements of each component for 2nd EC test

Figure 4.14. Pressure measurements of the evaporator and power consumption of 2nd EC test

Comparing with the first EC test, the second one's pressure measurements fluctuations are bigger, especially at the outlet pressure of the evaporator, as it shown in Figure 4.14. This may result from the instability of the modified refrigerator due to the amount of refrigerant charge. Both of the refrigerators use the same amount of refrigerant in their refrigeration cycle which is 50 gr, whereas, this refrigerant charge is optimized for the reference refrigerator, however, there is no optimization process has been done for the modified one.

For this test, the average power consumption of on-cycles and the average total power consumption including both on and off-cycles during the EC test are found as **96.3 W** and **45.52 W**, respectively. Comparing with the first test result, EEI for this test refrigerator is higher and it is classified as A class according to European Union

regulations about energy labeling of household refrigerating appliances. The calculated daily EC is **1.09 kWh/24h**.
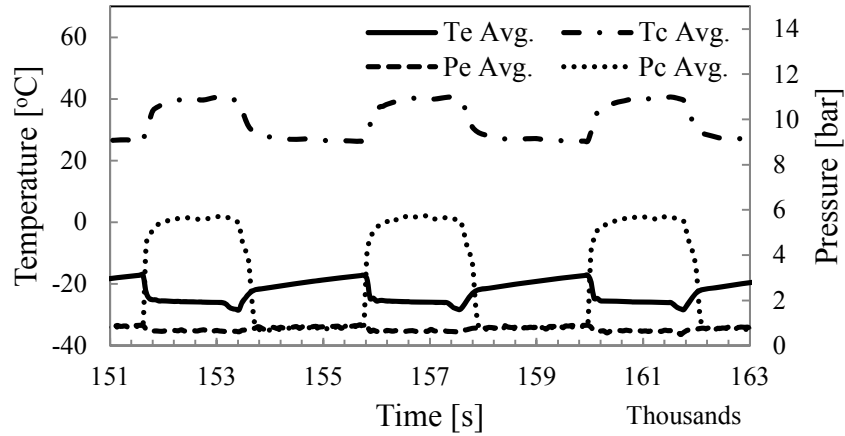

Figure 4.15. Average temperatures and pressures of evaporation and condensation of 2nd EC test

The average condensation and evaporation temperatures and pressures are found as **38.7^{o},-25.9^{o}C**, and **5.43**, **0.65 bar**, respectively. The system equalization pressure of the refrigerator is measured as **0.84 bar** during off-periods.
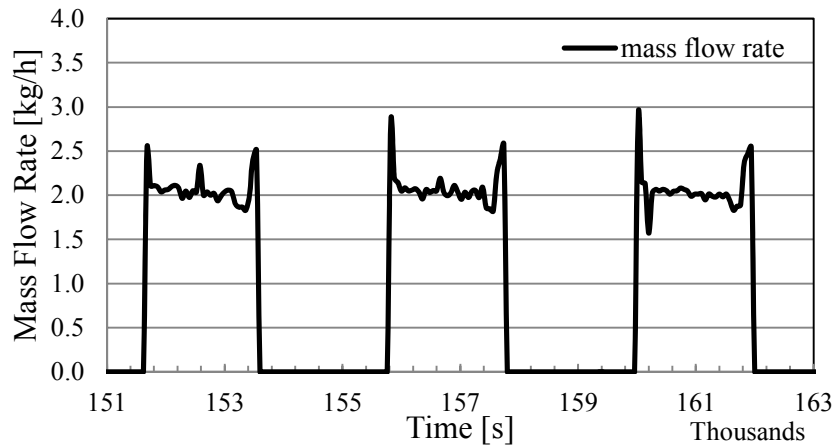

Figure 4.16. Mass flow rate of the refrigerant of 2nd EC test

The average mass flow rate of the refrigerant is calculated and it is found as **2.07 kg/h**, **5.75x10^{-4} kg/s**.

The average cooling capacity of the system is **179.25 W** and the cooling capacity of the refrigerator is shown in Figure 4.17.

The other performance characteristics of the refrigerator, rejected heat transfers from the condenser and the hot gas tube side and the heat transfer of SLHX are given in between Figure 4.18 and Figure 4.20.
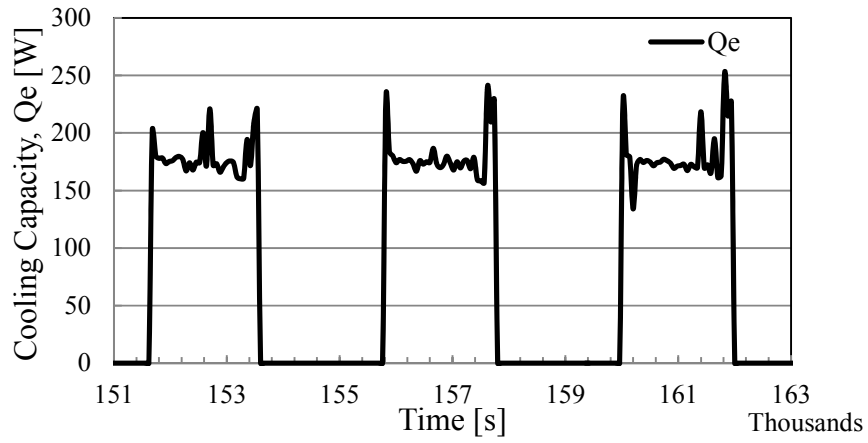
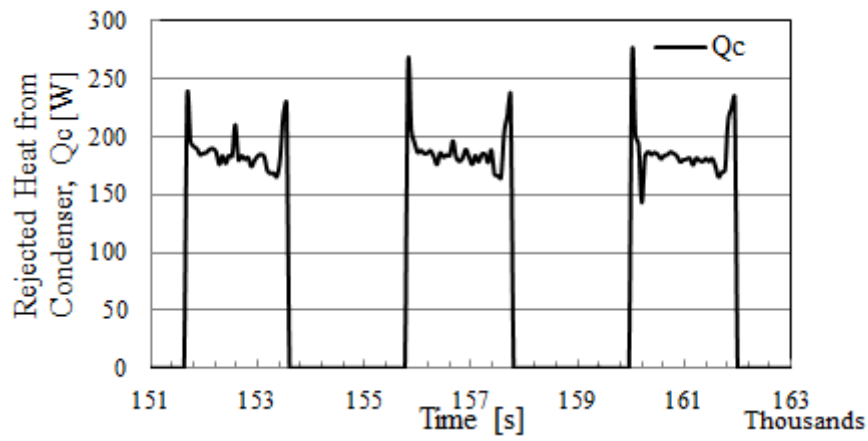Figure 4.17. Cooling capacity of 2nd EC test
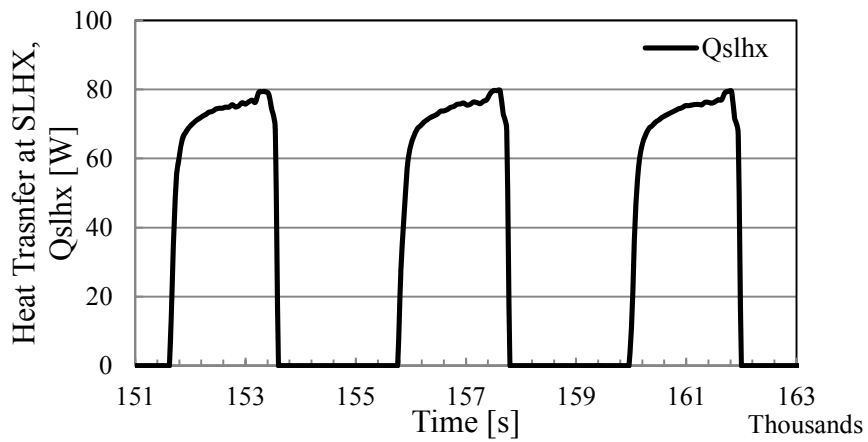

Figure 4.18. Rejected heat from the condenser of 2nd EC test

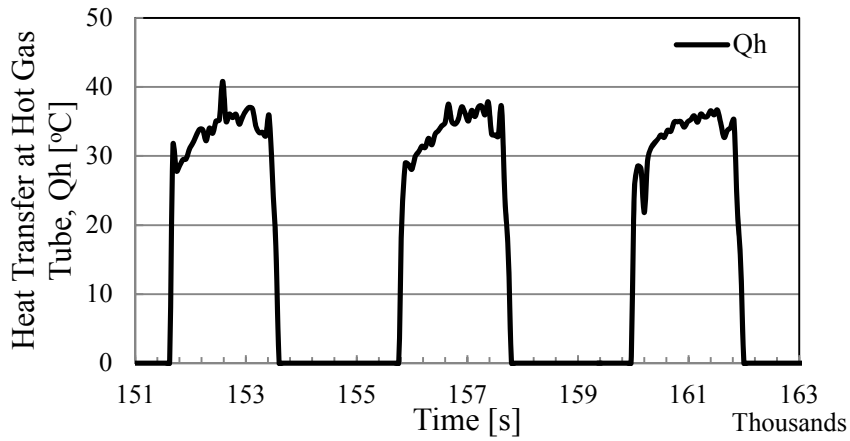Figure 4.19. Heat transfer occurs in SLHX of 2nd EC test

Figure 4.20. Heat transfer from hot gas tube to the surroundings of 2nd EC test
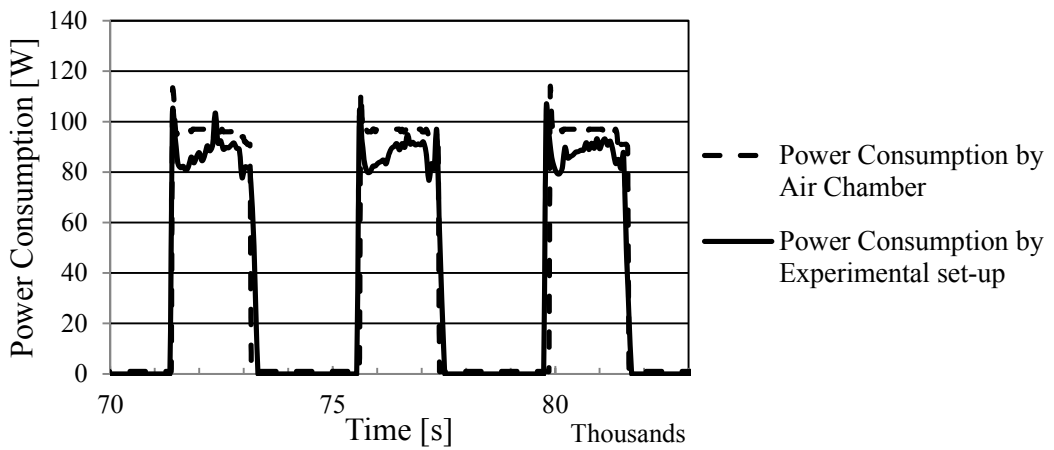

Figure 4.21. Comparison of power consumption calculation with the device measurement of 2nd EC test
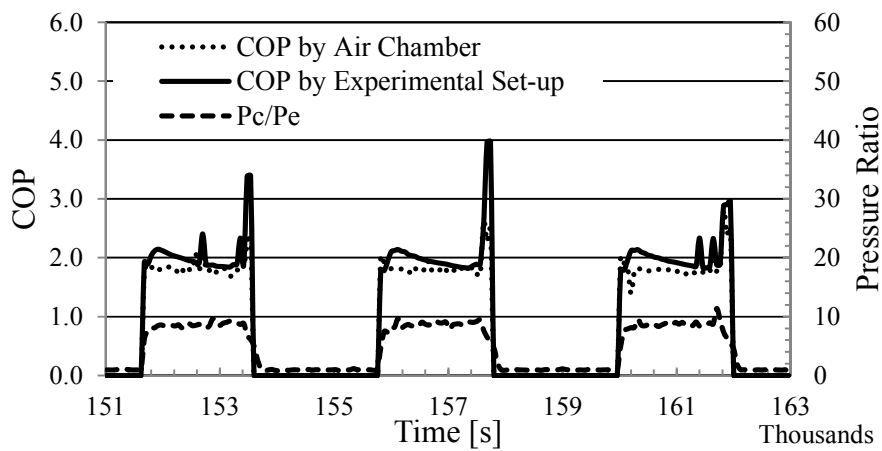

Figure 4.22. Pressure ratio and the COP of the test refrigerator of 2nd EC test
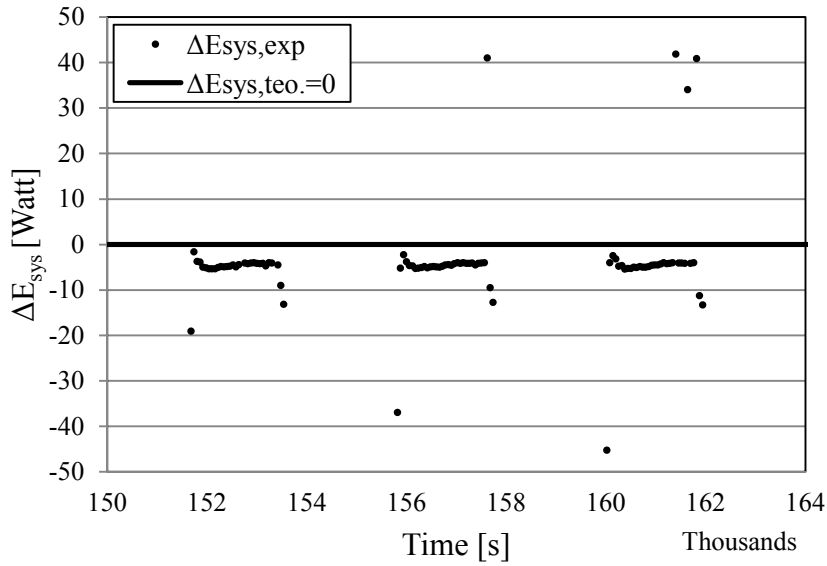
Figure 4.23. Energy balance deviation for the 2nd EC test
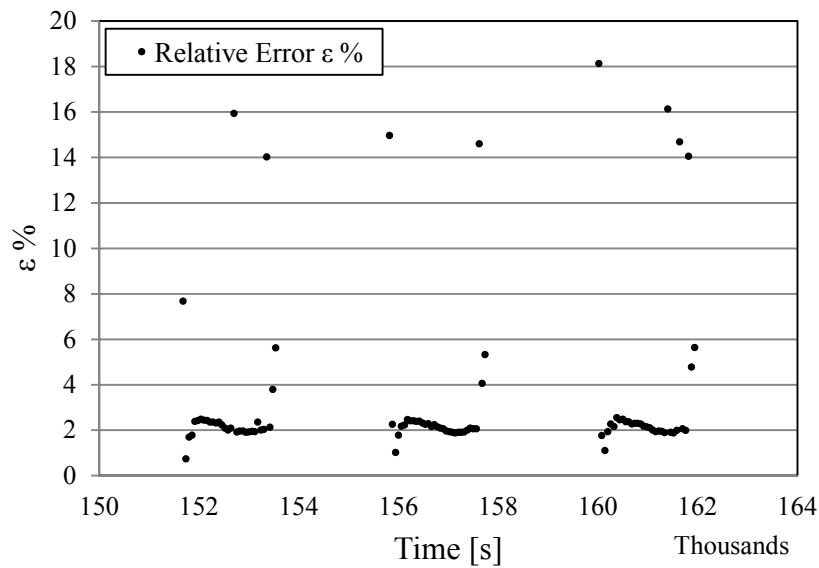

Figure 4.24. Relative errors in energy balance of 2nd EC test

According to the Figure 4.23, the maximum deviation from the energy balance point is seen close to **50 W**. It is important to note that the maximum deviations (outliers) are seen at the start and the end points of on-cycles. The great majority of the calculations are between the **0** and **-10 W** range. As it can be seen in Figure 4.24 again, the maximum relative error is about the **18%** and the main part of results fluctuate around **2%** for the 2nd EC test for the modified test refrigerator having longer condenser length.

Additionally, in this test, the air stream temperatures over the evaporator are measured and comparison of heat transfers by refrigerant and air sides are performed. Both at the air inlet and at the air outlet of the evaporator, temperature measurements are taken with three thermocouples. The air circulated in the freezer compartment enters to the evaporator from the left and right side and leaves the evaporator at the same sides; whereas, the circulated air in the fresh-food compartment enters to the evaporator from the middle side and exits at the middle side again. The air stream temperatures are shown in Figure 4.25. In Figure 4.25, "AI", "AO", "L", "M", and "R" represent the air inlet temperature, the air outlet temperature, left, middle, and right sides thermocouples' locations, respectively.
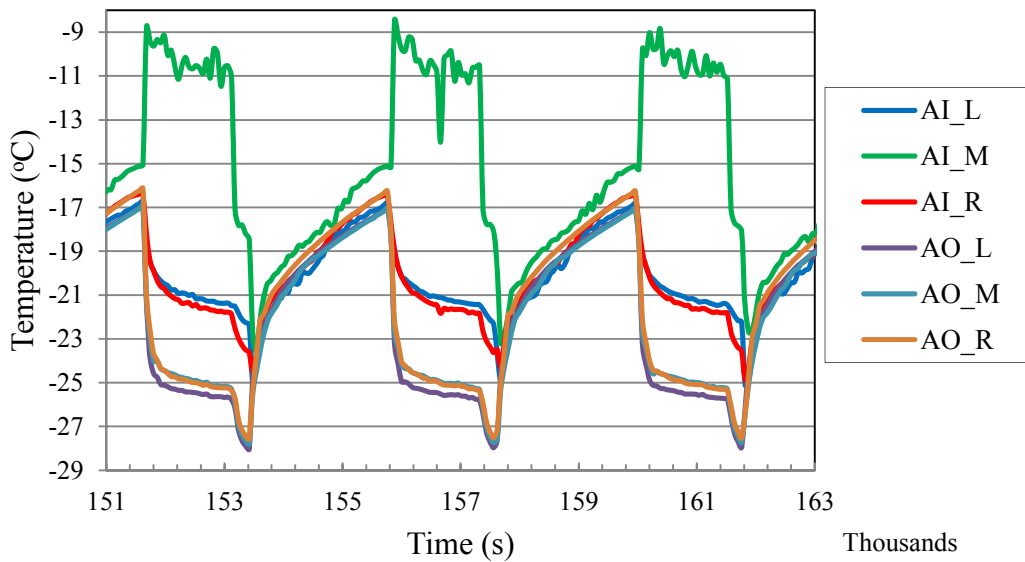

Figure 4.25. Air stream inlet and outlet temperatures over the evaporator of 2nd EC test

The heat transfer from the evaporator to the circulating air inside the entire test refrigerator is calculated and the cooling capacity of air side, $\dot{Q}_{e,air}$, is defined as

$$\dot{Q}_{e,air} = \dot{m}_{air} C_{p,air} \Delta T_{air} \tag{4.2}$$

As mentioned in Chapter 3, the air enters to the evaporator from three regions, and for these three regions temperatures are measured separately. By considering the mass flow rate variation of the air depends on these regions as indicated by Figure 3.10, the Eq. (4.2) can be expressed more explicitly by Eq. (4.3).

$$\dot{Q}_{e,air} = \left(\dot{m}_{air} C_{p,air} \Delta T_{air}\right)_{left} + \left(\dot{m}_{air} C_{p,air} \Delta T_{air}\right)_{middle} + \left(\dot{m}_{air} C_{p,air} \Delta T_{air}\right)_{right} \quad (4.3)$$

Depending on the mass flow rate and temperature variations along with x-axis through the evaporator bottom side as shown in Figure 3.10, Eq. (4.3) turns into

$$\dot{Q}_{e,air} = C_{p,air} \left[\begin{array}{l} \displaystyle\sum_{k=1}^{10} \dot{m}_{k,air}\left(T_{air,i} - T_{air,o}\right)_{left} + \sum_{k=11}^{55} \dot{m}_{k,air}\left(T_{air,i} - T_{air,o}\right)_{middle} + \ldots \\[2em] \ldots + \displaystyle\sum_{k=56}^{65} \dot{m}_{k,air}\left(T_{air,i} - T_{air,o}\right)_{right} \end{array} \right] \quad (4.4)$$

where k, i, o represent the locations points from which air stream velocity measurements are taken and the mass flow rate of air is calculated, inlet, and outlet, respectively. In this equation above, it is assumed that the specific heat of the air does not vary with the temperature change, it is taken as constant.

Comparison of cooling capacities by the refrigerant and the air sides are shown in Figure 4.26. As it is seen in the figure, the cooling capacity of the air side converges almost at the same cooling capacity of the refrigerant side. In Figure 4.26, it is observed that the bigger deviations occur at the end of the each on-cycle which is framed by blue ellipses. It is caused by response times of thermocouple measurements. Thermocouples show that the cycle is on-period even if the compressor stops for a while, however, the fan stops immediately and as an effect of it on the air circulation responses faster than thermocouples when the compressor stops. The relative error in cooling capacities for 38,8% of whole data is higher than 15% and the great majority of them fall in boundaries of ellipses in the figure. All in all, it implies that the calculated refrigerant side cooling capacity is verified with the air side cooling capacity.
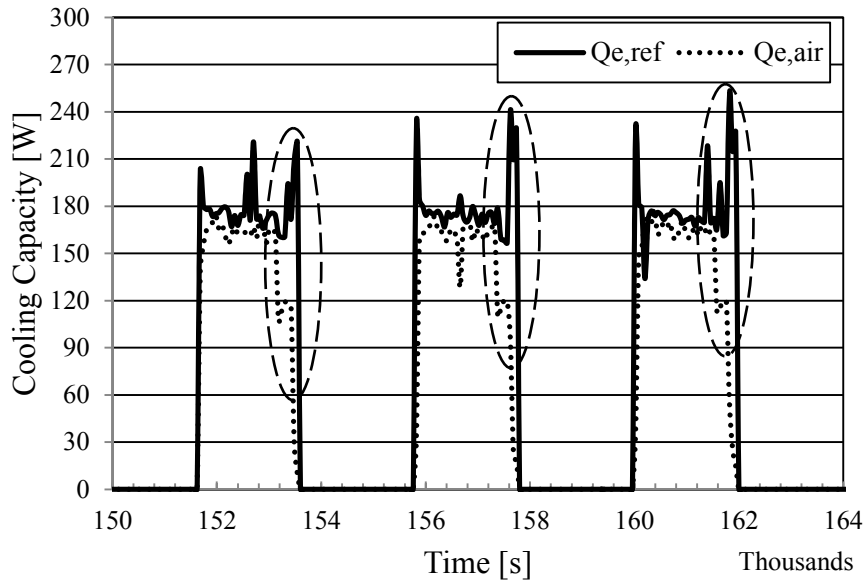
Figure 4.26. Comparison of cooling capacities of the refrigerant and the air sides

4.3. Results of the Third EC Test – Two-Coils Shortened Condenser

This test is conducted on the refrigerator that has a shortened condenser on it. The 2-coils are cut out from the end of the original condenser. The test results are given in figures below for this case too in the same manner as in the reference test results in order to distinguish the smaller length effect of the condenser.
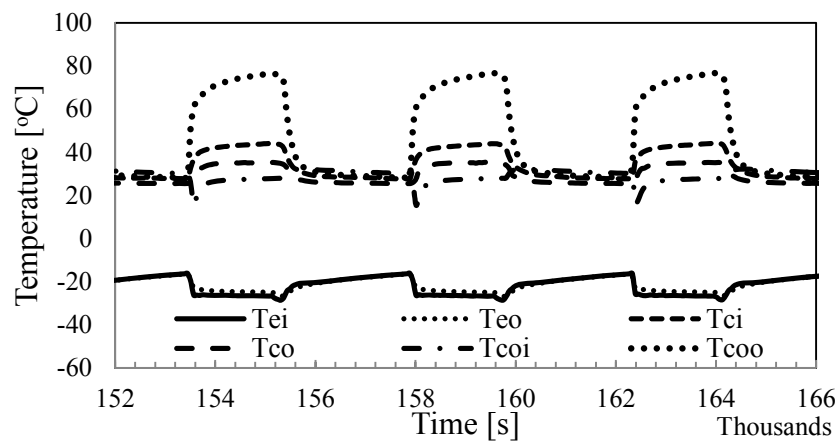

Figure 4.27. Temperature measurements of each component for 3rd EC test
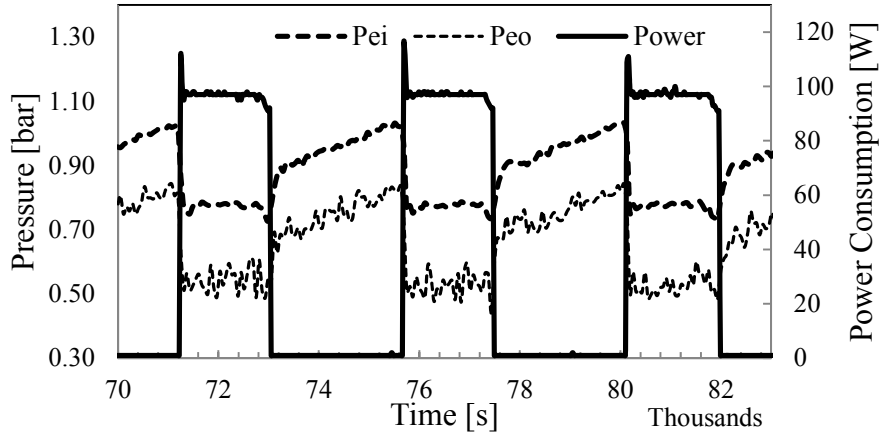
Figure 4.28. Pressure measurements of the evaporator and power consumption of 3rd EC test
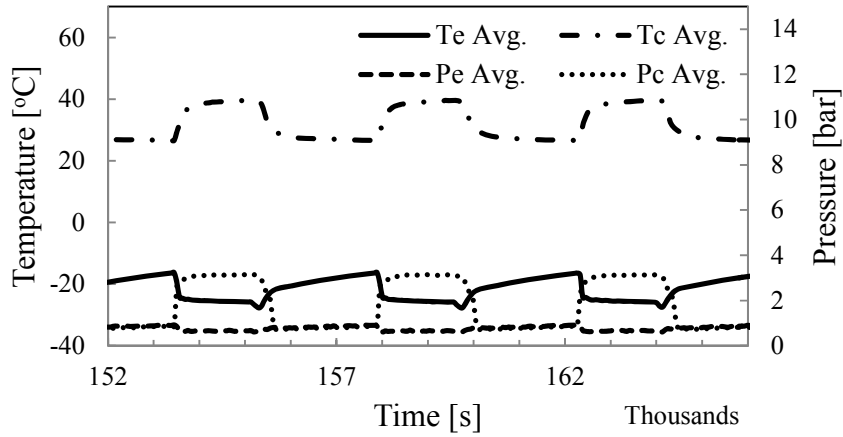

Figure 4.29. Average temperatures and pressures of evaporation and condensation of 2nd EC test

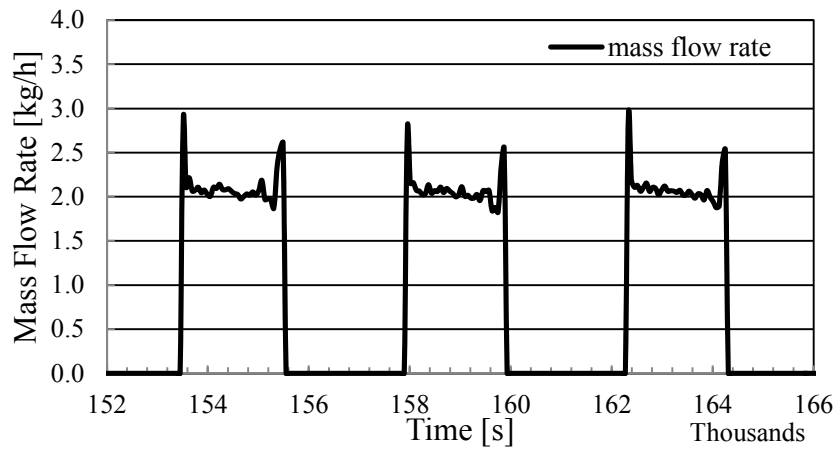Figure 4.30. Mass flow rate of the refrigerant of 3rd EC test
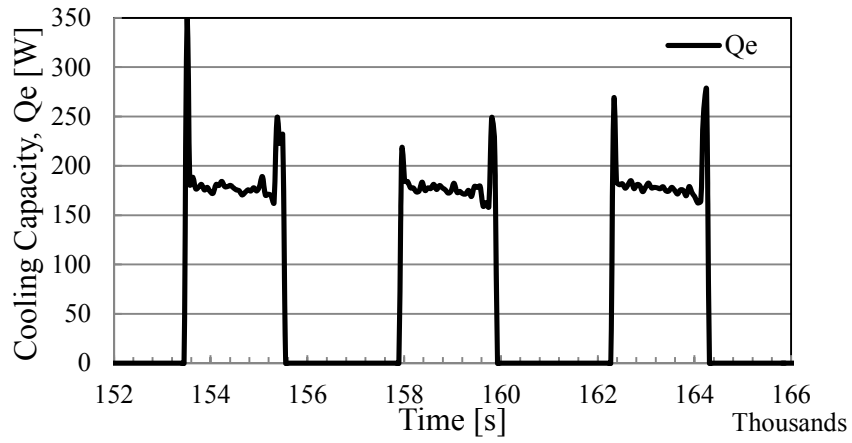
Figure 4.31. Cooling capacity of 3rd EC test

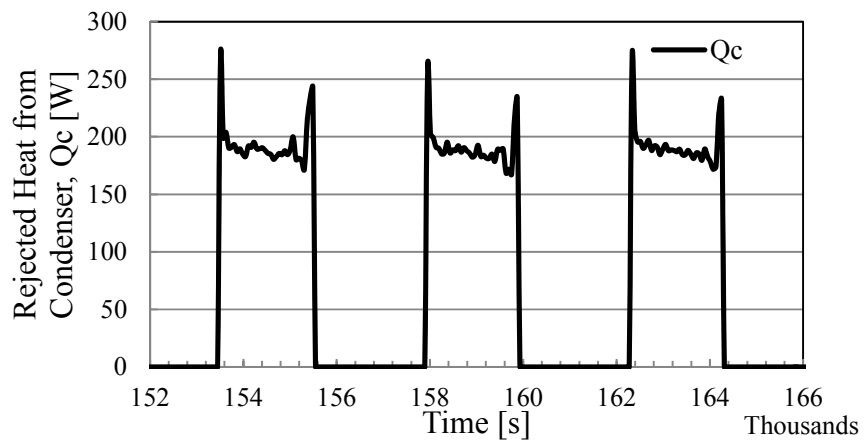Figure 4.32. Rejected heat from the condenser of 3rd EC test
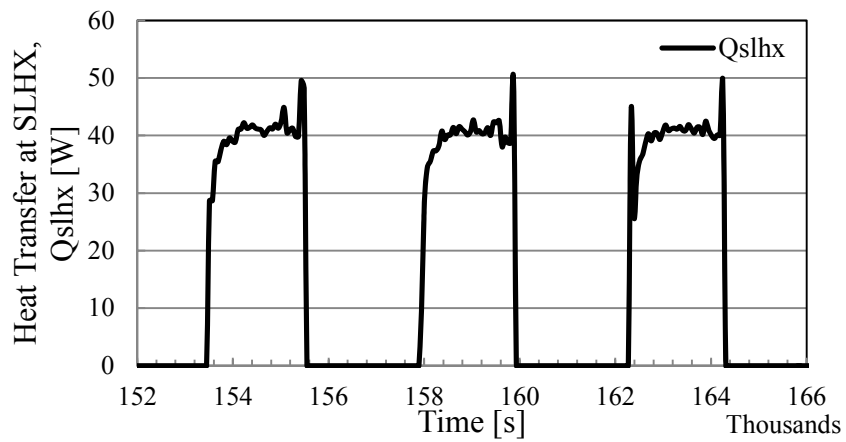
Figure 4.33. Heat transfer occurs in SLHX of 3rd EC test

73
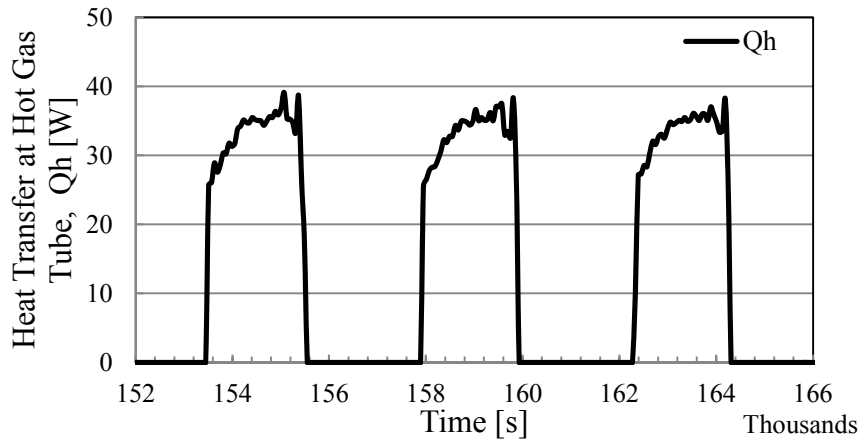
Figure 4.34. Heat transfer from hot gas tube to the surroundings of 3rd EC test
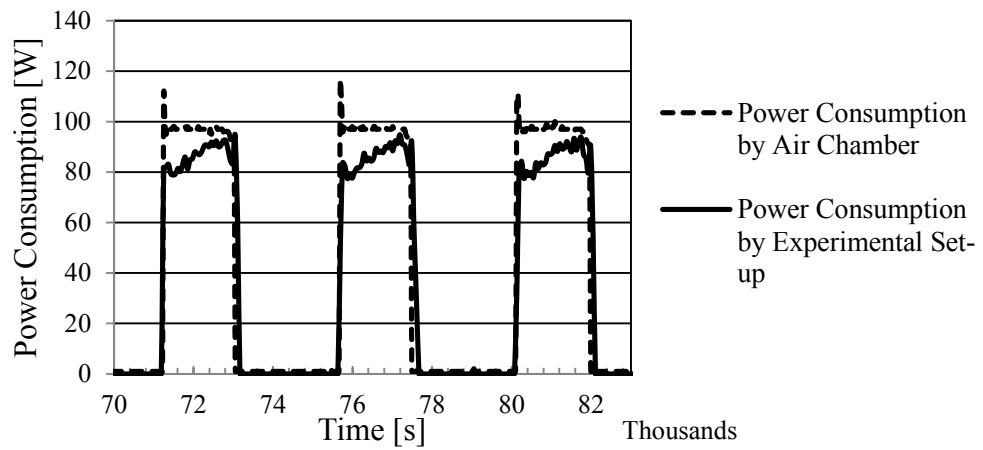
Figure 4.35. Comparison of power consumption calculation with the device measurement of 3rd EC test
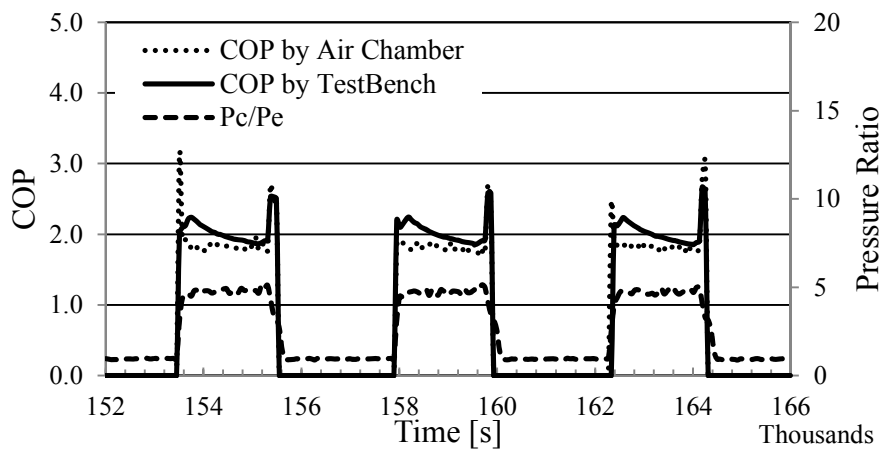
Figure 4.36. Pressure ratio and the COP of the test refrigerator of 3rd EC test
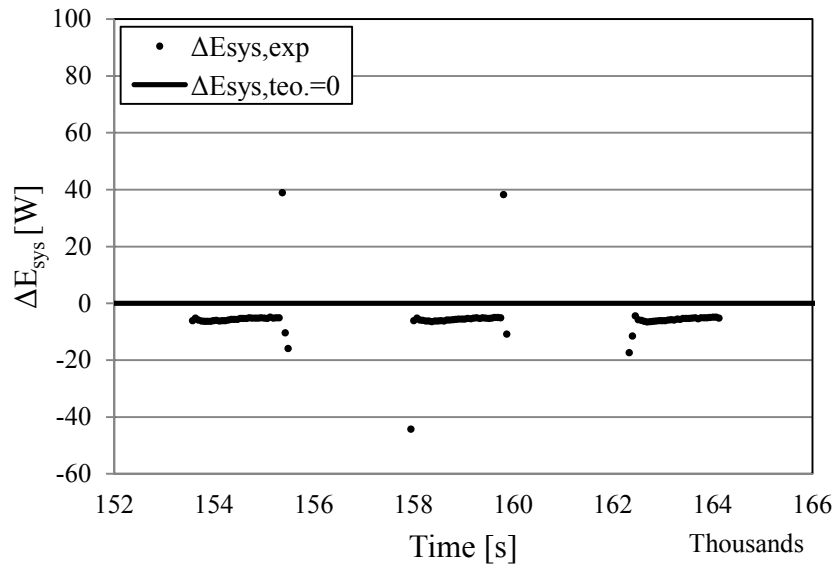
Figure 4.37. Energy balance deviation for the 3rd EC test
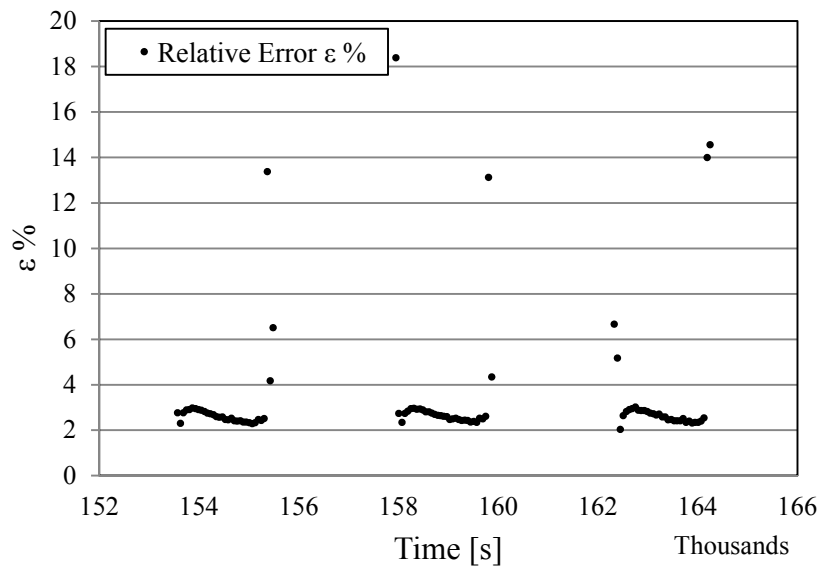
Figure 4.38. Relative errors in energy balance of 3rd EC test

4.4. Condenser Tube Length Effect on the Performance of the Refrigerator

To test the condenser length effect on the performance of the refrigerator, two EC tests are conducted on the refrigerator with two different condenser having different lengths and their results are presented in the preceding sections. Their performance

characteristics are compared with the first EC test results, which is the reference point, in this section.

It is found that the average power consumptions including only on-cycles for three tests are **97**, **96.3**, **96.4 W**, respectively. EEIs for each test are **42**, **45.52**, and **47 W**, respectively, according to these EEIs, they classified as A+, A, and A, respectively. Even though the power consumptions of on-periods are too close to each other, EEIs are different enough to distinguish their energy classes due to the different on-off cycle periods. As it can be seen on Figure 4.39, the on-period of the refrigerator having the smaller condenser is longer than that of the others.
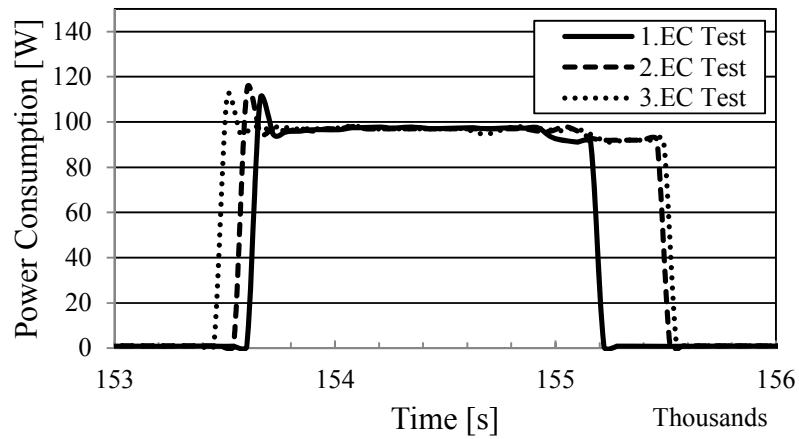

Figure 4.39. Comparison of power consumptions

To compare the on-off cycle time periods, power duty cycle, PDC, approach can be applied to the test results. Power duty cycle is the ratio of the total on-cycle time to the total time interval of EC test. A graphical representation of PDC is given in Figure 4.40. In this figure, 0 and 1 values in power axis represent power on and power off, respectively. It can be written as an equation like below.

$$PDC\% = \frac{Total\ time\ of\ on-cycle\ in\ EC\ test}{Total\ time\ of\ EC\ test} \qquad (4.5)$$

76
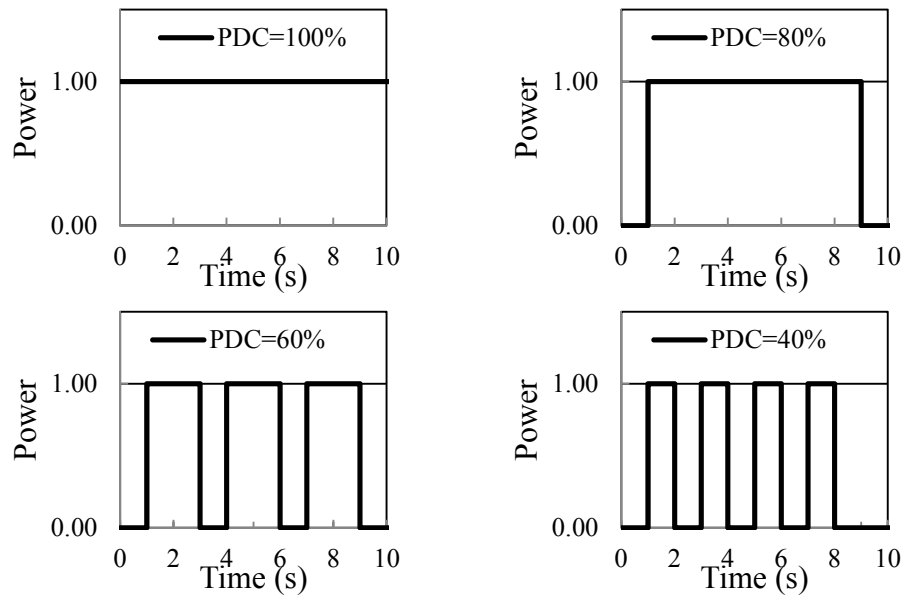
Figure 4.40. Graphical representation of power duty cycle (PDC)

Once the all results of three tests are compared in terms of PDC, it shows that the first, the second, and the third results' PDCs are **42.55%**, **45.54%**, and **45.60%**, respectively. It means that operation time of the third refrigerator takes longer than that of the first and the second refrigerator, which leads the third refrigerator to consume more power.

The cooling capacities of all tests are shown on an on-cycle in Figure 4.41, and it can be said that the refrigerator with condenser having the smaller length has the highest cooling capacity with the average of **186.9 W**, whereas, the first and second tests results show the average cooling capacities are **180.14** and **179.15 W**, respectively.
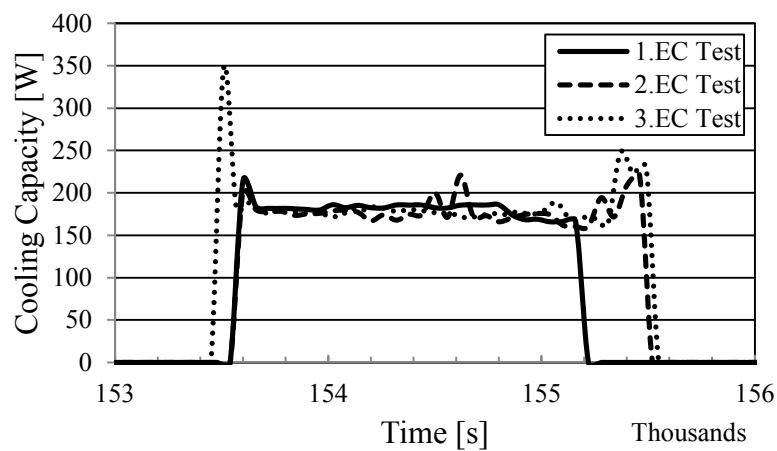
Figure 4.41. Comparison of cooling capacities

The average rejected heats from the condensers for all cases are **184.26**, **186.91**, and **193.92 W**, respectively, and Figure 4.42 shows the comparison of them in a plot. Even though the third refrigerator has the smallest condenser's length, the greater heat transfer from the condenser is seen in this refrigerator due to the longer PDC.
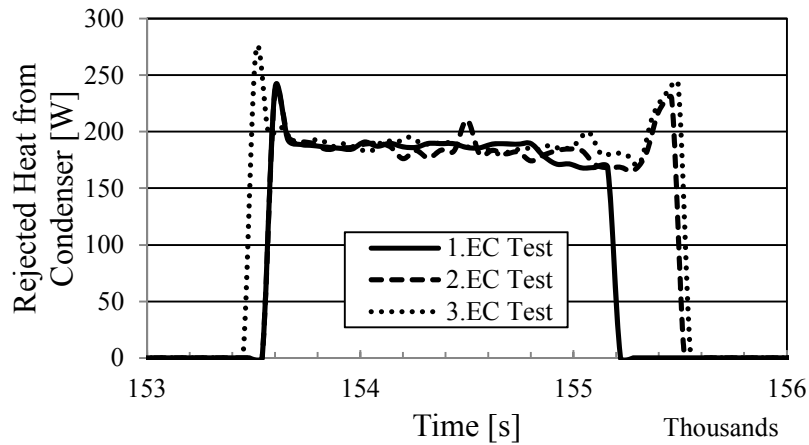
Figure 4.42. Comparison of heat transfers from the condensers

It is observed that the highest heat transfer occurs in the first refrigerator's SLHX. In the first refrigerator, the suction line pressure is lower than others'; therefore, the temperature of the refrigerant is also lower than that of the others. This causes to transfer more heat in the first refrigerator's SLHX. Heat transfer rates of each refrigerator are plotted in Figure 4.43. The average heats transferred in SLHXs are **84.68**, **71.56**, and **40.21 W** for the first, second, and third EC tests, respectively.
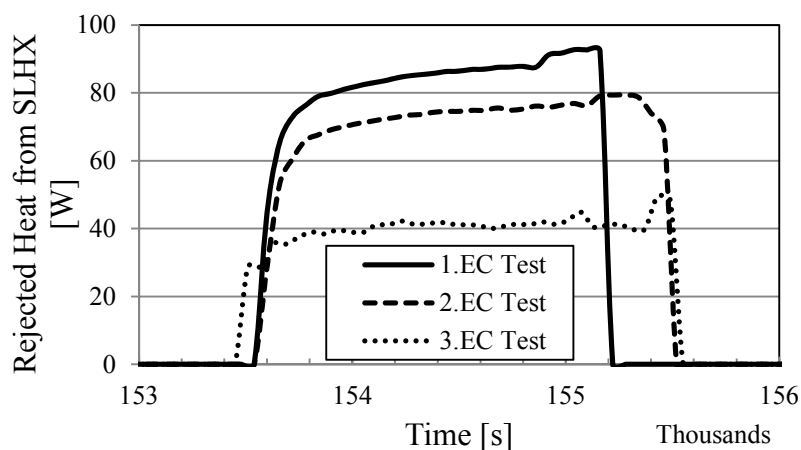
Figure 4.43. Comparison of heat transfer by SLHXs

After the refrigerant is discharged from the compressor, it enters the hot gas tube whose aim is to assure the doors of fresh-food compartment and freezer are closed by means of transferring heat from cabinet's frame to the doors. As it can be seen from Figure 4.44, the first refrigerator's heat transfer from hot gas tube has the lowest amount. Even though the discharge pressure is greater than that of the second and third refrigerator, discharge temperature is lower. This provides the lower heat transfer from the hot gas tube for the first refrigerator. The average heats transferred from hot gas tubes are **26.1**, **33.1**, and **32.8 W** for the first, second, and third EC tests, respectively.
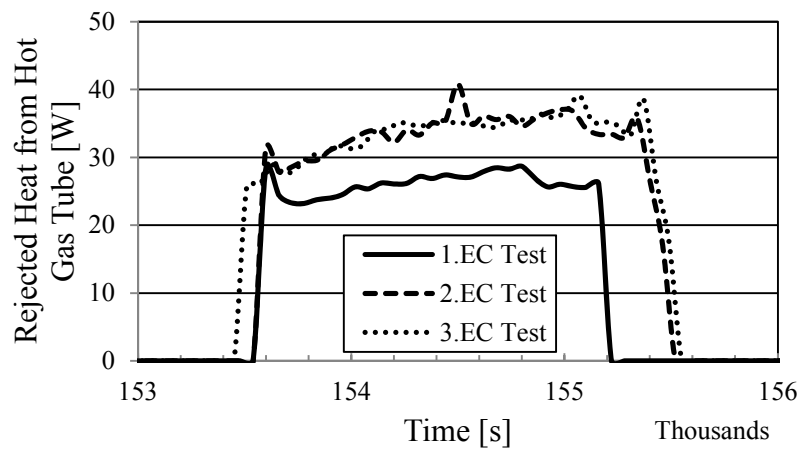
Figure 4.44. Comparison of rejected heat transfers from hot gas tubes

Once one cycle for three tests are shown on a P-h diagram, it can be seen that the first refrigerator's condensation pressure and temperature is greater, evaporation pressure and temperature is lower than that of the refrigerators with modified condensers.
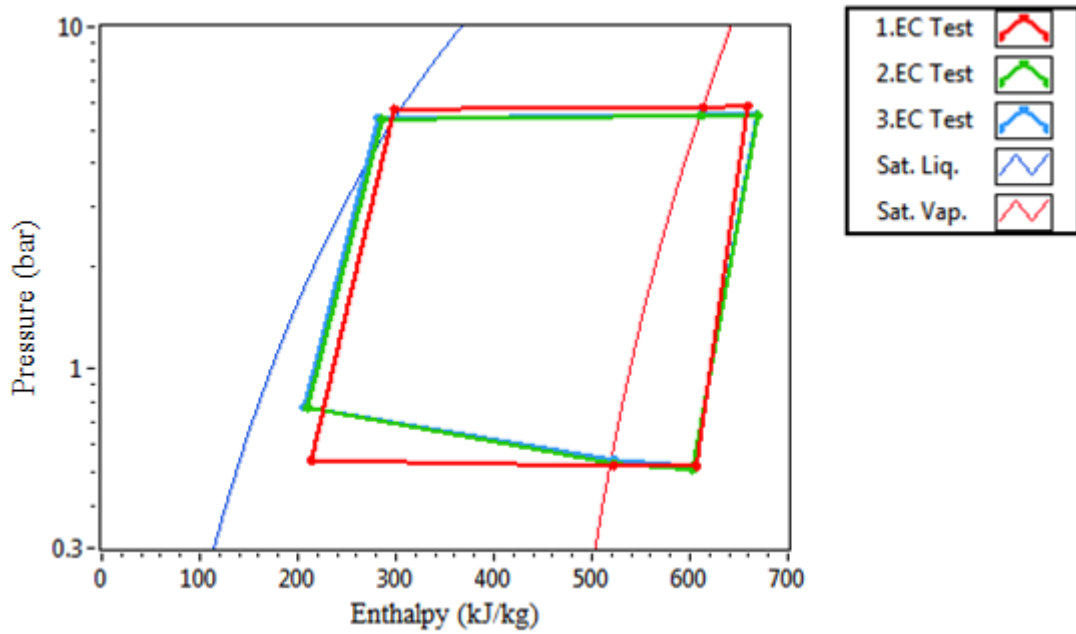
Figure 4.45. Comparison of P-h diagrams

The ratios of condensation pressure to evaporation pressure for all tests are compared and shown in Figure 4.46. The first refrigerator has the greatest pressure ratio which leads fast refrigeration, therefore, its power duty cycle is lowest than the others as shown in Figure 4.39. Average pressure ratios for each test are **10.9**, **8.4**, and **4.6**, respectively.
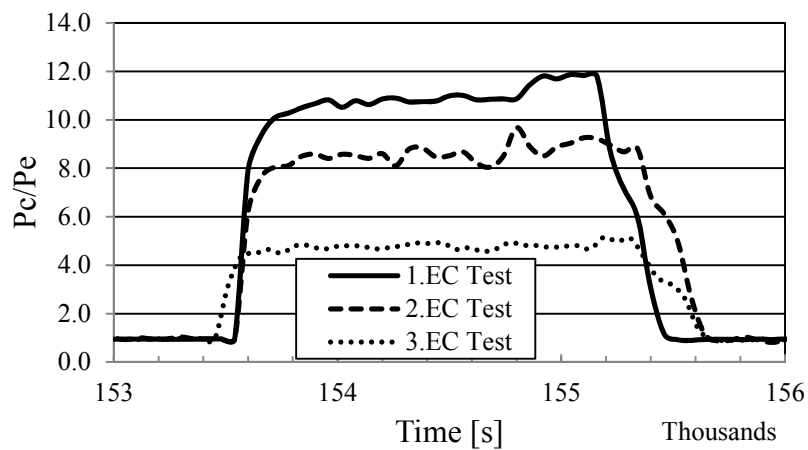
Figure 4.46. Comparison of condensation pressure to evaporation pressure ratios

In Figure 4.47, comparison of subcooling temperatures for all tests is given. The average subcooling temperatures for each tests are **2.52**, **4.65**, and **6.67°C**, respectively.
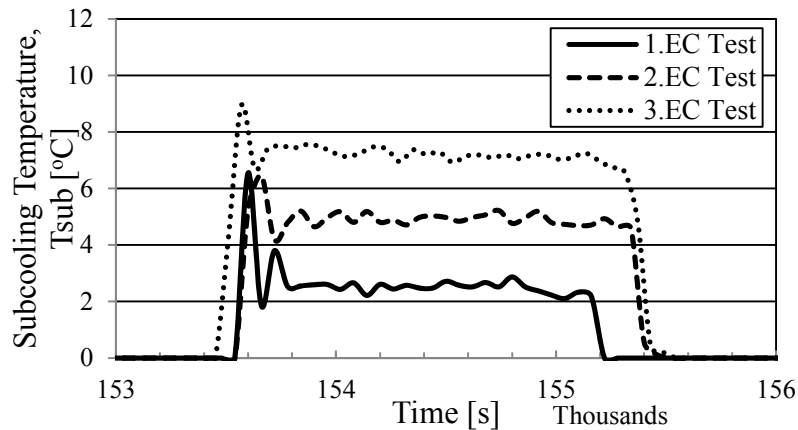
Figure 4.47. Comparisons of subcooling temperatures

A well-known rule of thumb in refrigeration is that keeping condensation and evaporation pressures close to each other leads to increase the performance of the refrigeration cycle. However, according to the EC tests stated by ISO 15502, the important point is to preserve the refrigerated food's temperature in a secure range. According to the results shown in detailed way in this chapter, the first refrigerator pressure ratio is the highest and this leads fast refrigeration, however, the others' ratios are lower than that of the first one provide slow refrigeration and this causes to consume more power.

4.5. Effect of Capillary Tube-Suction Line Heat Exchanger on the Performance of the Refrigerator

For household refrigerators without capillary tube-suction line heat exchangers, the expansion process is occurred in an adiabatic capillary tube. During the expansion process, the amount of heat transfer from or to the refrigerant is too small due to the limited area of the capillary tube. Thus, the expansion process is assumed as an adiabatic process. For those refrigerators, it is not necessarily true but, generally, it is valid that the COP is smaller than that for refrigerators with capillary tube-suction line heat exchanger because the expansion process which occurs in capillary tube is not adiabatic. In the SLHX, the heat is transferred from the refrigerant inside the capillary tube to the refrigerant inside the suction line and the amount of heat transfer is not as small as to be neglected like in refrigerators without SLHX. As a result of this, the cooling capacity of the refrigerator increases as the amount of the heat transferred in the

SLHX, with the assumption of the evaporation and the condensation temperatures and pressures are not change.

For three EC tests, refrigerator has SLHXs in their refrigeration cycle and heat transfer occurs in SLHX is calculated for all of them according to pressure and temperature measurements both at the inlet and at the outlet of the suction line part of SLHX. It is assumed that there is no pressure drop between the inlet and the outlet of the suction line part of the SLHX and its pressure is equal to the outlet pressure of the evaporator for all tests. To determine the effect of SLHX on the refrigerator performance, the current COP and cooling capacity of the reference test refrigerator is compared with that of the refrigerator without SLHX operating in the same conditions.

It can be seen from Figure 4.48 that the increase in cooling capacity in the refrigeration cycle with SLHX leads to increase in COP. It is important to note that for both refrigerators with and without SLHX, the total power consumption is assumed as the same.
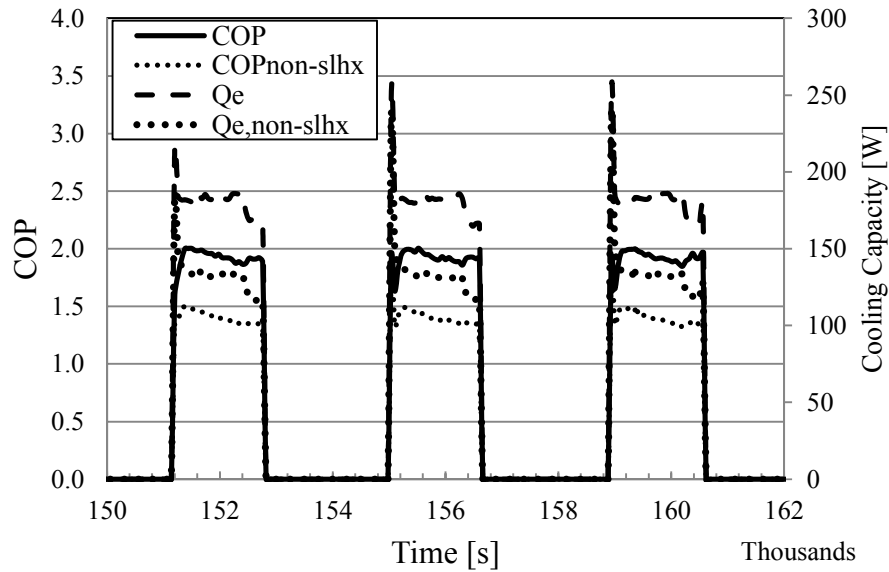

Figure 4.48. SLHX usage effect on COP and cooling capacity of the reference test refrigerator

4.6. Variable Speed Compressor Effect on the EC Test

The last test is conducted on the test refrigerator having a variable speed compressor (VSC). The single speed compressor on the reference test refrigerator is changed with a VSC to investigate the effect of it on the performance and energy

consumption of the test refrigerator. The amount of refrigerant charge is not changed; the refrigeration cycle has as the same amount of refrigerant as in the reference test refrigerator and it is 50 gr of R600a.

The VSC specifications are given in Table 4.1. The variable speed compressor is controlled with the variable frequency driver whose specifications are given in chapter 3.

Table 4.1. The variable speed compressor specifications

Manufacturer	Embraco
Motor Type	3-phase AC
Type	Reciprocating
Refrigerant	R600a (Isobutane)
Voltage & Frequency	230V & 53-143 Hz
Number of pistons	2
Displacement Volume	12.23 cm^3
Speed Range	1600-4500 rpm

The VSC is controlled by temperature feedbacks from the fresh-food and the freezer compartments. The VSC rpm control flowchart and rpm-temperature relations are given in Figure 4.49 and Figure 4.50, respectively. In the flowchart and the graph, T_f and T_{ff}, respectively, represent the fresh-food and the freezer compartment temperatures. T_{ff} is the main control parameter that determines the VSC speed. The VSC is controlled by two-speed stepwise control mechanism. To pull down the compartments' temperatures from ambient temperature level, 25°C, to the desired temperature levels, the compressor is driven at speed of 2000 rpm as shown in Figure 4.50. Once the system reaches the steady state operating conditions, the VSC is driven at speeds of 1600 and 2000 rpms as shown by circles in Figure 4.50. The main reason of driving the VSC at low speeds at high temperatures in the fresh-food compartment is to start the VSC at low torque levels during steady state operation conditions, hence the energy consumption of the VSC is reduced. This is also called as "soft start" control mechanism (Tassou & Qureshi, 1998).

START

Check T_{ff} and T_f

$T_{ff} > 8°C$ — False / True

A=1

A=0

$\Delta T_f = |T_{ff} - (-18)|$

$\Delta T_f > 0.5°C$ — True / False

B=0

B=1

A + B = C

$C \geq 1$? — True / False

OFF-Rpm=0

$T_{ff} > 8°C$ or $\Delta T_f \geq 1°C$ — False / True

D=2000

$5°C < T_{ff} \leq 8°C$ — False / True

D=1600

$0°C < T_{ff} \leq 5°C$ — False / True

D=2000

D=0

ON-Rpm=D
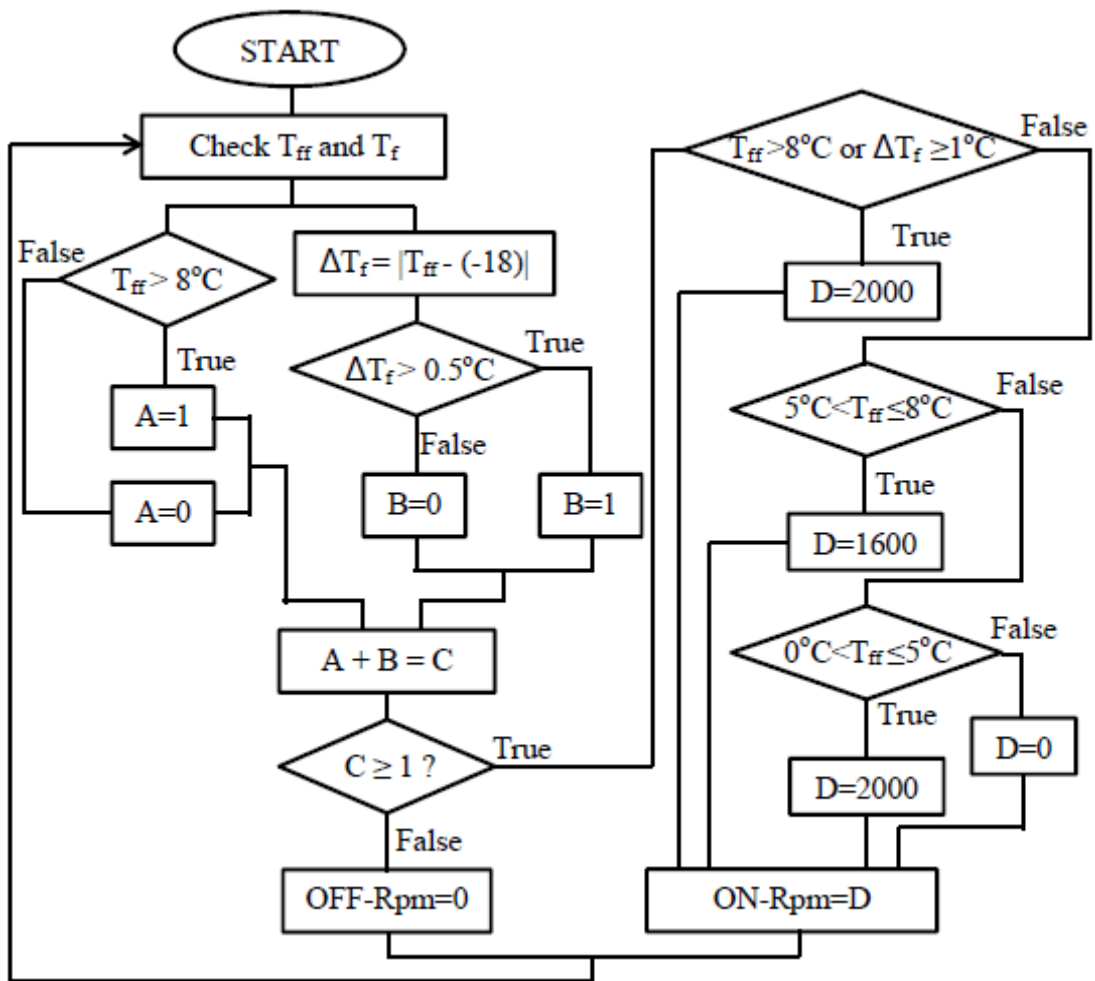
Figure 4.49. Variable speed compressor rpm control flowchart
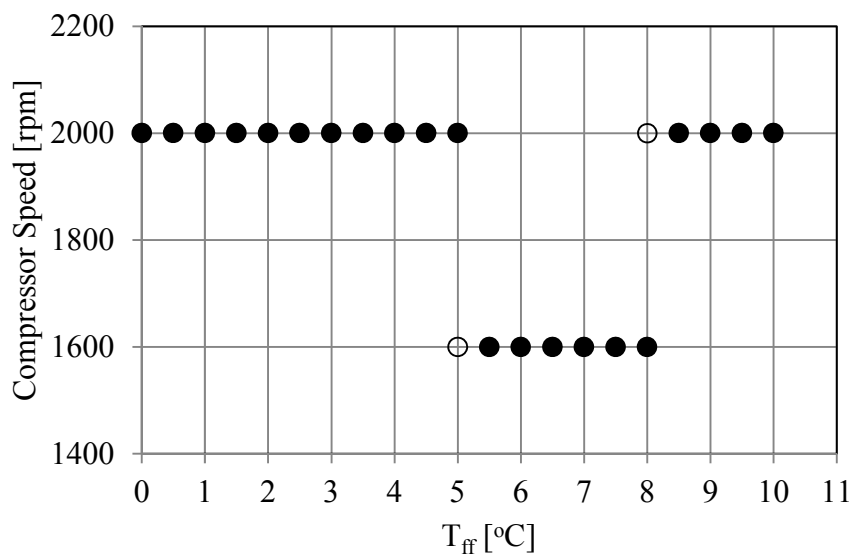
Figure 4.50. The VSC speeds vs. temperature control parameter

According to this control scheme of the VSC, the daily EC and energy efficiency index of the refrigerator having the VSC are found **0.77 kWh/24h** and **32.2 W**, respectively. Compared to the reference test refrigerator having the on-off controlled single speed compressor (SSC), the EC is reduced by **0.26 kWh/24h** with an efficient potential of **25.24%** and the energy class is upgraded from A+ to A++. Regarding the power duty cycles of two test results, PDC of the refrigerator with VSC, **51.7%**, is higher than that of the refrigerator with SSC, 42.6%. It means that the number of on-off cycles of the refrigerator with VSC is lower than that of the refrigerator with SSC, therefore, cyclic losses at on-off time are reduced on the system. Figure 4.51 indicates the comparison of power consumptions of both refrigerators on two on-cycles in steady state operating conditions.

Figure 4.51. Comparison of EC of refrigerators with VSC and SSC

CHAPTER 5

CONCLUSION

Standard energy consumption tests in accordance with ISO 15502 of a commercially available no-frost household refrigerator are performed to investigate the performance of the household refrigerator experimentally and the effect of a variable speed compressor on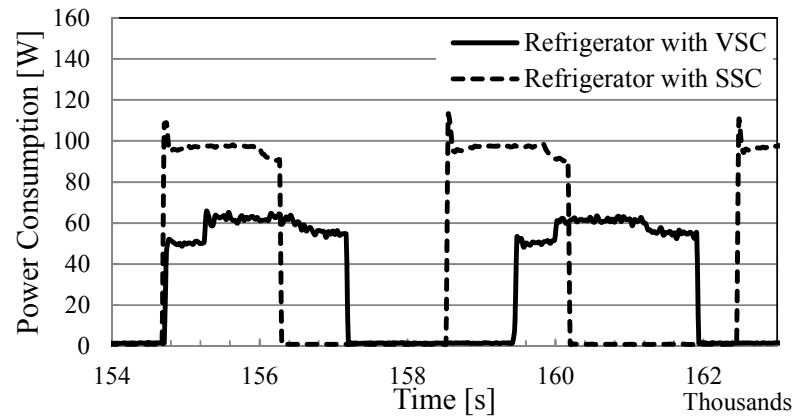 the energy consumption of the system is investigated in the scope of this study. One energy consumption test for the on-off controlled refrigerator without modifications, two tests for the on-off controlled refrigerators with modified condensers, and one test for the variable capacity controlled refrigerator with VSC are conducted to reveal the condenser length and VSC effects on the energy consumption of the current system. To carry out these experiments, a developed experimental set-up capable of acquiring-analyzing data and controlling the VSC simultaneously is designed based on Labview package software. Temperature distributions of the refrigerant and the air circulation and pressure distributions of the refrigerant inside each component are observed and analyzed during the experiments. Comparison of cooling capacities of the refrigerant side and the air side is performed.

It is found that the two coils extended and shortened condenser modifications increase the daily energy consumption of the test refrigerator by 5.96 and 2.41%, respectively. The condenser modifications also caused to increase in the PDC and for refrigerators with two coils extended and shortened condensers, respectively, their values are 45.54 and 45.60%, while the reference test refrigerator's PDC is 42.55%. Comparing the cooling capacities of three refrigerators, it is found that they are almost the same as expected due to the same amount of test packages inside freezer compartment. It is observed that the heat transfer occurs in the SLHX decreases for modified refrigerators. Also, the pressure drop in the evaporator increases due to the modifications. As a result of the condenser modifications, the refrigerator energy class degrades from A+ to A.

The air circulation velocity and temperature over the evaporator are measured and the cooling capacity of the air side is calculated. The cooling capacity of the refrigerant side is compared with the cooling capacity of air side. It is shown that the cooling capacities of both sides are so close at initially and the maximum deviation does

not exceed 15%, but they diverge at the end of each off-cycle. It is thought that the main reason of this divergence is due to restricted air circulation through the fresh-food compartment by the damper mechanism.

A VSC controlled by temperature feedbacks from the fresh-food and freezer compartments is installed to the test refrigerator. The VSC is driven by a variable frequency drive and stepwise control mechanism is applied on the system. The VSC is driven at speeds of 1600 and 2000 rpms to keep the fresh-food and the freezer compartments' temperatures in the desired levels. Implementation of VSC reduces the daily EC of the test refrigerator by 0.26 kWh/24h and its energy class is upgraded from A+ to A++.

Some recommendations about the future works for this study may be presented as:

- Different evaporator, condenser, and capillary tube geometries could be examined for a better understanding of their effects on the refrigerator performance.

- The refrigeration cycle should be utilized with different refrigerants in order to reveal the effects of different refrigerants on the performance.

- Refrigeration cycle modifications should be investigated experimentally and their performance can be discussed in order to determine the best one for a given application.

- Responses of the refrigeration cycle to variable loads should be observed to develop different VSC control algorithms and mechanisms.

- Variable speed fan should be applied instead of single speed fan for the purpose of responding variable loads and its effect on the EC can be studied.

- Variable damper apertures schemes and control algorithms in accordance with variable loads can be examined to enhance the performance of the refrigeration cycle.

- The experimental set-up and the test program could be developed with flow visualization set-ups to investigate the two-phase flow behavior during the operation of the refrigeration cycle.

REFERENCES

Aprea, C., Mastrullo, R., & Renno, C. (2004). Fuzzy control of the compressor speed in a refrigeration plant. *International Journal of Refrigeration, 27*(6), 639-648. doi: 10.1016/J.Ijrefrig.2004.02.004

ASHRAE, (2006). *Handbook - Refrigeration* (SI Edition) . American Society of Heating, Refrigerating and Air-Conditioning Engineers, Inc.

Bansal, P. (2003). Developing new test procedures for domestic refrigerators-harmonisation issues and future R&D needs - A review. *International Journal of Refrigeration, 26*(7), 735-748. doi: 10.1016/s0140-7007(03)00045-8

Bansal, P. K., & Xu, B. (2003). A parametric study of refrigerant flow in non-adiabatic capillary tubes. *Applied Thermal Engineering, 23*(4), 397-408. doi: 10.1016/s1359-4311(02)00208-9

Bittle, R. R., Wolf, D. A., & Pate, M. B. (1998). A Generalized Performance Prediction Method for Adiabatic Capillary Tubes. *HVAC&R Research, 4*(1), 27-44. doi: 10.1080/10789669.1998.10391389

Bjork, E., & Palm, B. (2006). Refrigerant mass charge distribution in a domestic refrigerator, Part I: Transient conditions. *Applied Thermal Engineering, 26*(8-9), 829-837. doi: 10.1016/j.applthermaleng.2005.10.003

Chang, W., Shaut, T., Lin, C., & Lin, K. (2008). *Implementation of inverter-driven household refrigerator/freezer using hydracarbon isobutane for refrigeration.* Paper presented at the International Refrigeration and Air Conditioning Conference, Purdue University, USA.

Choi, J., Kim, Y., & Kim, H. Y. (2003). A generalized correlation for refrigerant mass flow rate through adiabatic capillary tubes. *International Journal of Refrigeration, 26*(8), 881-888. doi: 10.1016/s0140-7007(03)00079-3

Chun-Lu, Z. (2005). Generalized correlation of refrigerant mass flow rate through adiabatic capillary tubes using artificial neural network. *International Journal of Refrigeration, 28*(4), 506-514. doi: 10.1016/j.ijrefrig.2004.11.004

Çengel, Y. A., & Boles, M. A. (2005). *Thermodynamics: An engineering approach.* (5th Ed.). McGraw-Hill Higher Education.

Dincer, I., & Kanoglu, M. (2011). *Refrigeration systems and applications*: John Wiley.

Ding, G., Ma, X., Zhang, P., Han, W., Kasahara, S., & Yamaguchi, T. (2009). Practical methods for measuring refrigerant mass distribution inside refrigeration system. *International Journal of Refrigeration, 32*(2), 327-334. doi: 10.1016/j.ijrefrig.2008.05.002

Domanski, P. A., Didion, D. A., & Doyle, J. P. (1994). Evaluation of suction-line/liquid-line heat exchange in the refrigeration cycle. *International Journal of Refrigeration, 17*(7), 487-493. doi: http://dx.doi.org/10.1016/0140-7007(94)90010-8

Dossat, R. J. (1961). *Principles of refrigeration.* JohnWiley.

European Commission, (2010). Directive 2010/30/EU of the European Parliament and of the Council of 19 May 2010 on the indication by labelling and standard product information of the consumption of energy and other resources be energy-related products. *Official Journal of the European Union.*

Greenfield, K. P., & Dunn, W. E. (1994). Experimental Study of Non-Adiabatic Flow of Refrigerant R-134a in Capillary Tube. *(A. C. a. R. Center, Trans.): University of lllinois at Urbana-Champaign.*

Hermes, C. J. L., Melo, C., Negrao, C. O. R., & Mevazilla, M. M. (2000). *Dynamic simulation of HFC-134a flow through adiabatic and non-adiabatic capillary tubes.* Paper presented at the International Refrigeration and Air Conditioning Conference, Purdue University, USA.

ISO 15502. (2005). *Household refrigerating appliances. Characteristics and test methods.* (Vol. 15502). British Standars Institute.

Kim, L. S., Son, K. D., Sarker, D., Jeong, J., & Lee, S. (2011). An assessment of models for predicting refrigerant characteristics in adiabatic and non-adiabatic capillary tubes. *International Journal of Heat and Mass Transfer, 47*(2), 163-180. doi: 10.1007/s00231-010-0697-0

Lemmon, E. W., Huber, M. L., & McLinden, M. O. (2007). NIST standard reference database 23. *NIST Thermodynamic Properties of Refrigerants and Refrigerant Mixtures Database (REFPROP), Version, 7.*

Liang, N., Shao, S., Xu, H., & Tian, C. (2010). Instability of refrigeration system – A review. *Energy Conversion and Management, 51*(11), 2169-2178. doi: 10.1016/j.enconman.2010.03.010

Liu, Y., & Bullard, C. W. (1997). An Experimental and Theoretical Analysis of Capillary Tube-Suction Line Heat Exchangers (A. C. a. R. Center, Trans.): University of lllinois at Urbana-Champaign.

Liu, Z., & Soedel, W. (1994). *Performance study of a variable speed compressor with special attention to supercharging effect.* Paper presented at the International Compressor Engineering Conference, Purdue University.

Melo, C., Torquato Vieira, L. A., & Pereira, R. H. (2002). Non-adiabatic capillary tube flow with isobutane. *Applied Thermal Engineering, 22*(14), 1661-1672. doi: http://dx.doi.org/10.1016/S1359-4311(02)00072-8

Ors, A. (2006). *Investigation of two performance improvement options for household refrigerators.* (M.S. 1433931), University of Maryland, College Park, United States Retrieved from http://search.proquest.com/docview/305301633?accountid=147333 ProQuest Dissertations & Theses (PQDT) database.

Poggi, F., Macchi-Tejeda, H., Leducq, D., & Bontemps, A. (2008). Refrigerant charge in refrigerating systems and strategies of charge reduction. *International Journal of Refrigeration, 31*(3), 353-370. doi: 10.1016/j.ijrefrig.2007.05.014

Qureshi, T. Q., & Tassou, S. A. (1996). Variable-speed capacity control in refrigeration systems. *Applied Thermal Engineering, 16*(2), 103-113. doi: http://dx.doi.org/10.1016/1359-4311(95)00051-E

Shao, S., Shi, W., Li, X., & Chen, H. (2004). Performance representation of variable-speed compressor for inverter air conditioners based on experimental data. *International Journal of Refrigeration, 27*(8), 805-815. doi: 10.1016/j.ijrefrig.2004.02.008

Tassou, S. A., & Qureshi, T. Q. (1998). Comparative performance evaluation of positive displacement compressors in variable-speed refrigeration applications. *International Journal of Refrigeration, 21*(1), 29-41. doi: 10.1016/s0140-7007(97)00082-0

Yang, L., & Wang, W. (2008). A generalized correlation for the characteristics of adiabatic capillary tubes. *International Journal of Refrigeration, 31*(2), 197-203. doi: http://dx.doi.org/10.1016/j.ijrefrig.2007.06.012